SPECTRAL STATISTICS, RANDOM MATRIX THEORY, AND CLASSIFICATION OF DYNAMICAL SYSTEMS

by

SHASHI C. L. SRIVASTAVA
Radioactive Ion Beam Facility Group,
Variable Energy Cyclotron Centre,
Kolkata-700064, India.

A thesis submitted to the
Board of Studies in Physical Sciences
In partial fulfillment of the requirements
For the degree of

DOCTOR OF PHILOSOPHY

of

HOMI BHABHA NATIONAL INSTITUTE

March, 2013

Homi Bhabha National Institute

Recommendations of the Viva Voce Board

As members of the Viva Voce Board, we recommend that the dissertation prepared by Shashi C. L. Srivastava entitled "Spectral statistics, random matrix theory, and classification of dynamical systems" may be accepted as fulfilling the dissertation requirement for the Degree of Doctor of Philosophy.

P. Barat

Chairman : Prof. P. Barat — **Date :** 12/07/2013

Guide : Dr Sudhir R. Jain — **Date :** 12/7/13

Co-Guide : Prof. Arul Lakshminarayan — **Date :** 12/7/13

Alok Chakrabarti

Member : Prof. Alok Chakraborty — **Date :** 12/7/2013

Member : Dr Jan-e Alam — **Date :** 12/7/2013.

V. Kris. Bhat

Examiner : Prof. V. K. B. Kota — **Date :** 12/7/2013

Final approval and acceptance of this dissertation is contingent upon the candidate's submission of the final copies of the dissertation to HBNI.

I hereby certify that I have read this dissertation prepared under my direction and recommend that it may be accepted as fulfilling the dissertation requirement for the Degree of Doctor of Philosophy.

Dr. Sudhir R. Jain
(Guide)
Bhabha Atomic Research Centre,
Mumbai - 400 085

Prof. Arul Lakshminarayan
(Co-Guide)
Indian Institute of Technology Madras,
Chennai - 600036.

Contents

STATEMENT BY AUTHOR

This dissertation has been submitted in partial fulfillment of requirements for an advanced degree at Homi Bhabha National Institute (HBNI) and is deposited in the Library to be made available to borrowers under rules of the HBNI.

Brief quotation from this dissertation are allowable without special permission, provided that accurate acknowledgement of source is made. Requests for permission for extended quotation from or reproduction of this manuscript in whole or in part may be granted by the Competent Authority of HBNI when in his or her judgement the proposed use of the material is in the interests of scholarship. In all other instances, however, permission must be obtained from the author.

Shashi C. L. Srivastava

DECLARATION

I, hereby declare that the investigation presented in the thesis has been carried out by me. The work is original and has not been submitted earlier as a whole or in part for a degree/diploma at this or any other Institution/University.

Shashi C. L. Srivastava

To my family

ACKNOWLEDGEMENTS

I have been extremely fortunate to have Dr Sudhir R. Jain as my guide. I thank him from depth of my heart for all those little sessions in which I learnt whatever little I know today. As an excellent teacher, he never lost his patience despite me being irritatingly slow at times. I am always amazed of his breadth and depth of knowledge about every aspect of science. The encouragement, support and learning from him have been instrumental to complete the thesis. I can not thank him enough for always making me feel a part of his family during my stay at Mumbai, and I am equally thankful to Alka Madam, Manan and Swarina, Uncle and Aunty for showering their love and affection on me. Now on this very personal note, "Sir, you have shown your faith in me when even I had none. Thank you!"

I have always been in awe of my co-guide Prof. Arul Laksminarayan since PRL days when I was doing my summer internship with him. A person who is at equal ease with the interpretation of entangled mathematical results and proving the (dreaded) mathematical identities and not to forget the computational skills. I admire his knack of clarity and details in every aspect of work. Sir, I express my deep sense of gratitude to you for all the help, encouragement and always making yourself available through mail and chat services. Thank You!

I am very thankful to Prof. Alok Chakrabarty for encouraging me to carry out my research and complete the thesis. Encouragements from him made this duration lot more enjoyable. I also would like to thank my colleagues from RIB group specially Dr Vaishali Naik and Dr Arup Bandyopadhyaya for all the help that has been extended during course of this thesis. I take this opportunity to thank other board members Prof. P. Barat and Prof. Jan-e Alam for their co-operation and encouragement.

When a person as slow as me take the adventure of writing thesis, inadvertently friends had to play a very important role. Specially, Pratap singh Chauhan and Ajeet Kumar , they always have the stock of nice words to encourage me whenever I am down. Thanks Pratap! Thanks Ajeet! Thanks are also due to my dear friends from different arena and age-group like Hemendra Pandey, Dr V. S. Pandit, Jajati Nayak, Anurag Mishra, Animesh Goswami, P.S. Babu, Saurabh

Srivastava, S. V. L. S. Rao, Rajni Pande, Shweta Roy, Piyush Jain, Siddhartha da, Dirtha da, Debashish da, Tapatee di, Prasanta da, Ayan for playing a very important role of continuously reminding me to complete the thesis. Thank you all, the tea time "adda" has been an occasion of several discourses and discussions and proved to be great learning moments too.

It is impossible to thank enough to Sujata, my wife for being with me in all the weather and bearing with me. Believe me whoever knows me will testify that it is not easy. Thank you! I owe a heartfelt thanks to Srishti, my daughter who has been constant source of cheer, happiness and surprises. Thanks are also due to my brothers Monu and Chotu for their love and affection. I would like to thank all the members of my extended family, they always stood with us during times of desperation. I would like to remember my grandfather (late) Sri Sadhu Saran Lal Srivastava, who introduced me to numbers, arithmetic, algebra in a way that seems still fresh in my mind. Finally, I pay my deep sense of reverence to my parents, they are my first teachers, and have always supported me in all my decisions no matter what. It is their blessings that I am here today.

-Shashi.

Publications:

1. **Published:**

   (a) "Random cyclic matrices", Sudhir R. Jain and **Shashi C. L. Srivastava**, Phys Rev E 78, 036213 (2008).

   (b) "Random matrix theory for pseudo-Hermitian systems: Cyclic blocks", Sudhir R. Jain and **Shashi C. L. Srivastava**, Pramana J. Phys. 73, 989 (2009).

   (c) "Biased random walks on a disordered one-dimensional lattice", K. Manikandan, **Shashi C. L. Srivastava**, Sudhir R. Jain. Phys. Lett. A 375, 368 (2011).

   (d) "Random reverse-cyclic matrices and screened harmonic oscillator", **Shashi C. L. Srivastava** and Sudhir R. Jain, Phys Rev E 85, 041143 (2012).

   (e) "Pseudo-Hermitian random matrix theory", **Shashi C. L. Srivastava** and Sudhir R. Jain, Fortschr. Phys., 61, 276 (2013).

   (f) "Record statistics in random vectors and quantum chaos", **Shashi C. L. Srivastava**, Arul Lakshminarayan, Sudhir R. Jain, EPL (Europhysics Letters) 101, 10003 (2013).

2. **Unpublished:**

   (a) "Kolmogorov stochasticity parameter as a measure of quantum chaos", **Shashi C. L. Srivastava** and Sudhir R. Jain, arXiv:1101.5465

SYNOPSIS

Introduction

Development of Random matrix theory (RMT) has been a cornerstone for explaining the fluctuation properties in diverse fields such as in Quantum chaos, Nuclear physics, Number theory, wireless communications, *etc.* In the context of physical systems, whenever the underlying dynamics is complex, or the dimensionality involved is large, it is seen that fluctuation properties are governed by the symmetries respected by the Hamiltonian. This is the key idea behind development and successful application of random matrix theory in Nuclear physics, initiated by Wigner [Wigner 1957], and, Landau and Smorodinsky [Landau 1955]. The invariance enjoyed by the probability measure with respect to symmetry groups is a key to classification of the RMT ensembles, most notably the Dyson's 3 fold model [Dyson 1962a,Dyson 1962b,Dyson 1962c, Dyson 1962d]. These are commonly known as Gaussian (Circular) orthogonal, unitary and symplectic ensembles of Hermitian (Unitary) matrices. Mathematically rigorous analysis of eigenvalue density and spacing distributions were first done by Mehta and Gaudin. The book on Random matrices by Mehta remains a standard reference [Mehta 2004].

At around the same time, Ginibre studied the random matrix theory for non-Hermitian matrices [Ginibre 1965]. Though general joint probability distribution function for Ginibre Unitary ensemble was obtained by Ginibre himself, the Ginibre orthogonal ensemble proved to be the most difficult one. The general results could only be found very recently thanks to the efforts largely by Sommers [Sommers 2008], Akemann [Akemann 2007], among others [Edelman 1997, Kanzieper 2005]. Another class of matrices has become important after the pseudo-Hermitian extension of quantum mechanics [Bender 2002]. These non-Hermitian matrices either have completely real spectra despite being

non-Hermitian or had real and complex conjugate eigenvalues with corresponding unit and zero pseudo-norm eigenfunction. A natural question arose about the statistical distribution of eigenvalues of this class of matrices. The answer though is not known in full detail, but some preliminary steps have been taken by developing the random matrix theory for 2×2 pseudo-Hermitian matrices by Ahmed and Jain [Ahmed 2003b].

The thesis contains a variety of somewhat different topics linked by the common thread of RMT and complex systems. We have presented the random matrix theory of two structured matrices, namely cyclic (pseudo-Symmetric) and reverse cyclic (Symmetric). RMT for cyclic matrices extends our knowledge of RMT of pseudo-Hermitian system while the same for reverse cyclic matrices had brought out effect of reduction of independent parameters on spectral properties of symmetric matrices as well as the connection with exactly solvable model of screened harmonic potential. Going beyond random matrix theory, we have proposed the stochasticity parameter to classify the quantum mechanical dynamical systems based on underlying classical dynamics. To see the integrable-chaos transition in eigenfunctions of standard map, we have studied the record statistics of intensity vectors and presented various analytical and numerical results.

Random cyclic matrices

Cyclic matrices occur in a wide variety of physical situations, including disordered linear atomic chains and the Ising model in two dimensions. For a Gaussian ensemble of random cyclic matrices on the real field, we have studied their spectral fluctuations [Jain 2008b]. The form of a cyclic matrix M is given

in Eq. 1.

$$M = \begin{bmatrix} a_1 & a_2 & ... & a_N \\ a_N & a_1 & ... & a_{N-1} \\ a_{N-1} & a_N & ... & a_{N-2} \\ \vdots & & & \\ a_2 & a_3 & ... & a_1 \end{bmatrix}, \qquad \eta = \begin{bmatrix} 1 & 0 & 0 & ... & 0 & 0 \\ 0 & 0 & 0 & ... & 0 & 1 \\ 0 & 0 & 0 & ... & 1 & 0 \\ \vdots & & & & & \\ 0 & 1 & 0 & ... & 0 & 0 \end{bmatrix}. \tag{1}$$

First we have shown that cyclic matrices are pseudo-symmetric with respect to generalized parity (η in Eq. 1) which in this case is a particular permutation matrix. Utilizing the known eigendecomposition for such matrices *i.e.* $M = F^{\dagger}\Lambda F$, F being the unitary discrete Fourier matrix, we obtained the joint probability distribution function of eigenvalues and the spacing distributions analytically and verified the same numerically. The joint probability distribution of eigenvalues has been obtained and given by (for even N),

$$P(\{E_i\}) = \left(\frac{A}{\pi}\right)^{\frac{N}{2}} \exp\left[- A\left(E_1^2 + E_{\frac{N}{2}+1}^2 + \sum_{i\neq 1,\frac{N}{2}+1}^{N} E_i E_{N+2-i}\right)\right], \tag{2}$$

where E_1 and $E_{\frac{N}{2}+1}$ are the two real eigenvalues, the rest being complex. Here, we note that $E_{N+2-i} = E_i^*$ for $i = 2 \rightarrow N$ except $\frac{N}{2}+1$ when N is even. For odd N, the above result will hold except that there will be only one real eigenvalue, E_1 and the summation in the second term will extend over all i except 1. Due to the presence of complex eigenvalues, they can not be ordered, and hence the Euclidian distance been used for spacing. For small spacings, the level spacing distribution exhibits either a Gaussian ($p_{cc}(s) = \frac{2}{\pi}e^{-\frac{s^2}{\pi}}$) or a linear form. The exact form of the spacing distribution between real and complex eigenvalues is

given by Eq. 3.

$$p_{rc}(s) = \frac{3\sqrt{3}\pi}{16} c^2 s \exp\left(-\frac{3\pi}{16} c^2 s^2\right) I_0\left(\frac{3\pi}{32} c^2 s^2\right) \tag{3}$$

Furthermore, for the general case of two arbitrary complex eigenvalues, leaving out the spacings among real eigenvalues, and, among complex conjugate pairs, we found that the spacing distribution agreed completely with the Wigner distribution for a Poisson process on a plane. A good comparison has been found with numerical data and shown in Fig. 1.

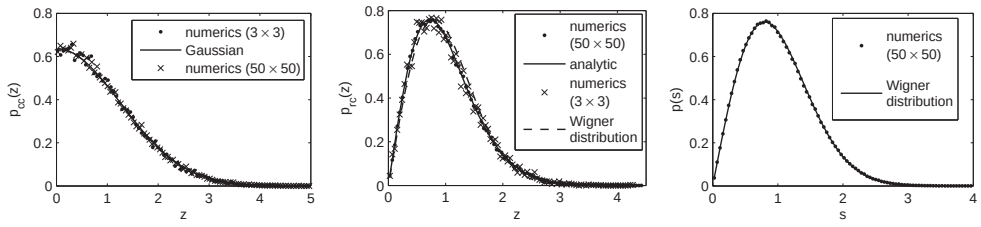

(a) spacing between eigenvalues that are complex conjugate pairs

(b) spacing between a real and a complex eigenvalue, analytic refers Eq. 3

(c) spacing between eigenvalues which are neither real nor complex conjugate pairs

Figure 1: Probability distribution of various spacings are plotted in three graphs and compared with respective analytical results.

Extension of random matrix theory for cyclic block matrices (with individual blocks as cyclic matrix) has been a natural step forward. The form of such block matrices are given by,

$$H = \begin{bmatrix} A_1 & A_2 & \dots & A_n \\ A_n & A_1 & \dots & A_{n-1} \\ \vdots & & & \vdots \\ A_2 & A_3 & \dots & A_1 \end{bmatrix}, \text{ with } A_i = \begin{bmatrix} a_1^i & a_2^i & ... & a_m^i \\ a_m^i & a_1^i & ... & a_{m-1}^i \\ \vdots & & & \\ a_2^i & a_3^i & ... & a_1^i \end{bmatrix} \tag{4}$$

These matrices like cyclic matrices are also examples of pseudo-Hermitian (sym-

metric) matrices. The corresponding η operator is given by,

$$\eta = \begin{bmatrix} \sigma & 0 & \dots & 0 \\ 0 & 0 & \dots & \sigma \\ \vdots & & & \vdots \\ 0 & \sigma & \dots & 0 \end{bmatrix}, \text{ with } \sigma = \begin{bmatrix} 1 & 0 & \dots & 0 \\ 0 & 0 & \dots & 1 \\ \vdots & & & \\ 0 & 1 & \dots & 0 \end{bmatrix}. \tag{5}$$

It is easy to verify then, $H^\dagger = \eta H \eta^{-1}$. We have shown that JPDF for this class of block matrices are given by,

$$P(E_1, E_2, \dots E_N) = \left(\frac{A}{\pi}\right)^{\frac{N}{2}} e^{-A\sum_{i=1}^{N}|E_i|^2}. \tag{6}$$

Here also, like in cyclic matrix case, spacing distributions are found to be Gaussian, Eq. 3, and Wigner spacing distribution for spacings between two real eigenvalues or between two complex conjugate eigenvalues, between real eigenvalues and complex eigenvalues, and between two complex (not conjugate) eigenvalues respectively. A good comparison with numerical data has been found and shown in Fig. 2.

Reverse Random cyclic matrices and random walk

This result was utilized to study the random walk problem on the one-dimensional disordered lattice. From the first treatment of Brownian motion, random walks play a very important role in topics as diverse as polymer physics, to locomotion of bacteria. Systems out of equilibrium are described by a master equation with a non-Hermitian operator, exemplified by the transfer matrix of the random walk problem. Random walk on an ensemble of one-dimensional lattice of N equally spaced sites with periodic boundary conditions can be formulated as a dynamical equation. The transition matrix for biased random walk is an

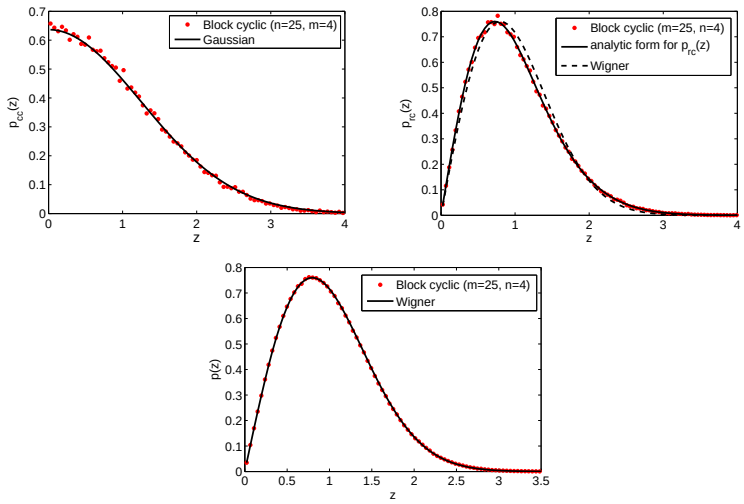

Figure 2: Probability distribution of various spacings are plotted for random cyclic blocks and it is compared with respective analytical results.

example of the cyclic matrix. The transition matrix is given in Eq. 7

$$\mathbf{M} = \begin{bmatrix} (1-w) & pw & 0 & ... & qw \\ qw & (1-w) & pw & ... & 0 \\ 0 & qw & (1-w) & ... & pw \\ ... & & & & \\ pw & 0 & qw & ... & (1-w) \end{bmatrix}, \tag{7}$$

with w as jump probability while q and p as probability for jumping either sides. When jump probability is finite for each lattice point and further taken as random, then to calculate the evolution of the ensemble averaged entropy we have made use of joint probability distribution obtained for random cyclic matrices. In this work, it has been shown that asymptotically the occupation probability goes to uniform distribution as $1/t$, t being the time. The explicit

form is,

$$N\langle\tilde{p}_j(t)(\{\lambda_i\})\rangle_{RMT} \approx \frac{\pi}{4}\frac{e^{-\frac{\pi}{4}}}{\left(-e^{-\pi/4}+\text{Erf}\left[\frac{\sqrt{\pi}}{2}\right]\right)}\left[\frac{2}{3+t}+\frac{\pi}{(t+3)(t+5)}+O\left(\frac{1}{t^3}\right)\right] \tag{8}$$

with $\tilde{p}_j(t) = p_j(t) - 1/N$ where $p_j(t)$ is occupation probability of site j. As the Boltzmann entropy is given by sum of $p_j \log(p_j)$ over all the sites, the asymptotic time dependence for the increase in entropy has been found as $\log(t+3)/(t+3)$ [Manikandan 2011].

Random matrix theory and Exactly solvable models

The other structured matrix for which we have developed the random matrix theory is for the class of reverse cyclic matrices. These are symmetric matrices with very few independent parameters (only N) against the possible number $N(N+1)/2$ [Srivastava 2012]. The explicit form is given as

$$H = \begin{bmatrix} a_1 & a_2 & \dots & a_N \\ a_2 & a_3 & \dots & a_1 \\ \vdots & & \dots & \vdots \\ a_N & a_1 & \dots & a_{N-1} \end{bmatrix}. \tag{9}$$

These class of matrices have an eigenvalue as sum of the row elements, we have referred to it as trivial eigenvalue. Rest of the eigenvalues come as $+/-$ pairs in odd dimensional H. Another trivial eigenvalue occurs in case of even-dimensional matrices and is the alternating sum of row elements. Among other results, this one is also an explicit example of a symmetric matrix which due to additional structure allows to have a density of eigenvalues different than Wigner semi-circle. We have calculated the joint probability distribution function for this class of matrices and shown that it is related to an N-body exactly

solvable model. The form of JPDF for $(2n+1)$ dimensional matrix is given by,

$$P(E_1, E_2, \ldots, E_{2n+1}, \theta_1, \ldots, \theta_{2n}) = \left(\frac{A}{\pi}\right)^{(2n+1)/2} |E_2| \ldots |E_{n+1}| \exp[-A(E_1^2 + 2\sum_{i=2}^{n+1} E_i^2)].$$

We call this well-known model potential as a screened harmonic oscillator. The connection enables us with all the correlations among the particle positions moving in screened harmonic potential, $4A^2x^2 - 1/(4x^2)$. The density of nontrivial eigenvalues of this ensemble is found to be of the Wigner form $(\frac{\pi}{2}E\exp(-\frac{\pi}{4}E^2))$ and possess a hole at origin in contrast to the semi-circle law of the Gaussian orthogonal ensemble of random matrices. An asymptotic result for density have been earlier obtained by Bose and his collaborators [Bose 2009]. Here, the results are exact and valid for all orders. A numerical comparison for density is shown in Fig. 3. Various spacings among the eigenvalues have been

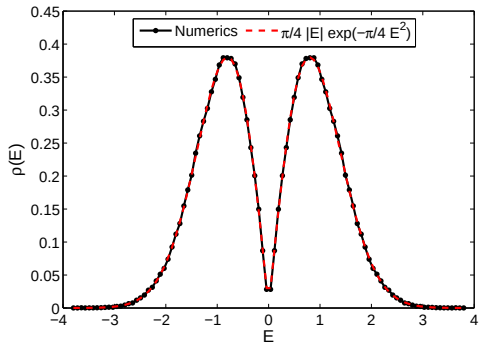

Figure 3: Normalized density of non-trivial eigenvalues for an ensemble of 20000 reverse cyclic matrices of size 15×15 is compared with the analytical form. The density is normalized such that averaged density for positive eigenvalues is $1/2$.

calculated and compared with numerical spacing distribution. They are found to be in good agreement (See Fig. 4).

Stochasticity parameter : a measure of quantum chaos

Classical integrability and chaotic nature of dynamics reflect also in various quantum mechanical quantities. One of such quantity is spacing distribution of

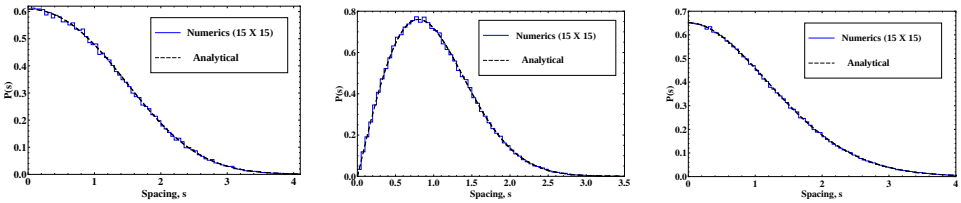

(a) spacing between the trivial eigenvalue and other positive eigenvalues.

(b) spacing between positive-negative pair.

(c) spacing between positive eigenvalues.

Figure 4: Probability distribution of various spacings are plotted for random reverse cyclic matrices of size 15 and it is compared with respective analytical results (not given here). It can be seen that they are in clear agreement.

eigenvalues which in generic chaotic system displays level repulsion while level attraction for integrable systems in small spacing distribution. Random Matrix theory works well at the small and medium scale of spectra, but at large scale two-point correlation saturates in contrast to increasing nature predicted by RMT. If this was not enough, some examples, which later have been known to be examples of Arithmetic chaos, are chaotic but behave as integrable ones as far as spacing distribution *etc.* is concerned [Bolte 1992]. Keeping these in mind, we proposed the Kolmogorov stochasticity parameter, λ (Eq. 10) for energy level spectra to classify quantum systems with corresponding classical dynamics ranging from integrable to chaotic [Srivastava 2011]. Kolmogorov stochasticity parameter has been defined as in (Eq. 10),

$$\lambda_n = \sup_E \frac{|N_n(E) - N_0(E)|}{\sqrt{n}}, \tag{10}$$

with $N_0(E)$ denoting the average, smoothed cumulative density of energy levels while $N_n(E)$ (empirical counting function) represents the number of eigenvalues E_i which are $\leq E$. We studied the probability distribution function (PDF) of λ. Remarkably, the PDF of all the integrable systems studied here is the same and is found to be completely different from the PDF of chaotic systems as is seen

in Fig.5. We also note that λ_n for n energy levels scales as $\lambda_n \sim n^{-\alpha}$ (see Fig.

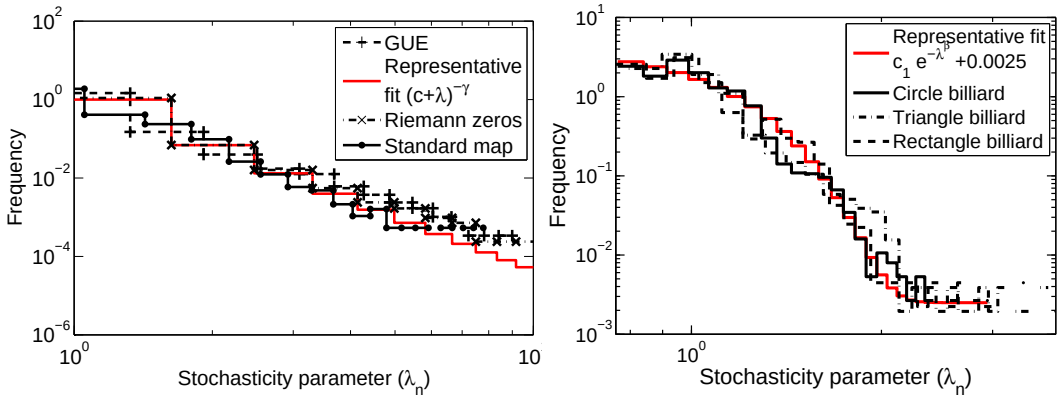

(a) The probability distribution functions of the stochasticity parameter are shown for three integrable billiards, viz. circle (red), rectangle (blue), and equilateral triangle (black). For these billiards, the distributions have been fitted to a functional form, $c_1 \exp(-\lambda^{\beta}))$, with (c_1, β) taking values (4.344, 2.927), (4.163, 3.196), and (4.703, 3.826) for circle, rectangle, and equilateral triangle respectively.

(b) The probability distributions of the stochasticity parameter are shown for standard map, Gaussian Unitary Ensemble (GUE), and Riemann zeros. For these systems, the distributions can be fitted to a functional form, $(c + \lambda)^{-\gamma}$, with (c, γ) taking values (0.1688, 3.632), (0.1932, 4.097), and (0.2103, 4.397) for standard map, GUE, and Riemann zeros respectively.

Figure 5: Probability distribution of λ for two class of systems.

6a). This parameter helps in classifying the dynamical system on the quantum level, based on underlying classical dynamics. This has been summed up in Fig 6b.

Record statistics for eigenfunctions

Now we turn our focus to eigenfunctions of the dynamical systems. It is well known that intensity distribution of a system violating time reversal symmetry follows the Gaussian (Circular) unitary ensemble. The question asked in this thesis is more about the extreme intensities occurring in the eigenfunctions, statistics of their positions and difference between two extreme intensities *etc.* To answer these kind of questions record statistics proves to be a useful tool. For any one dimensional sequence (real) $\{x_t, t = 1, \cdots N\}$, the first element, R_1, of the corresponding records series is x_1 itself and at subsequent indices t

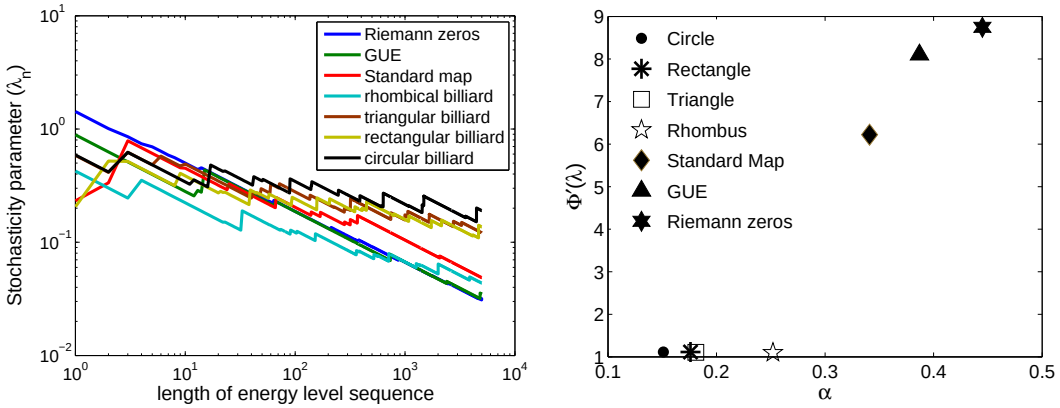

(a) Stochasticity parameter for all the systems considered are displayed here as a function of logarithm of the length of the sequence, $\ln n$. This brings out an interesting observation, λ scales as $n^{-\alpha}$ and leads us to finding the best fitted values for the index, α (R^2 varies from 0.80 for circular billiard to 0.95 for Riemann zeros). As the systems become increasingly stochastic, the value of the index increases.

(b) Two measures of stochasticity, α and $\Phi'(\Lambda)$, are being plotted here against each other. For calculating the PDF at stochasticity parameter for a specific system, we have normalized the distributions. As the index α increases, we see that the $\Phi'(\Lambda)$ undergoes a jump by an order of magnitude.

Figure 6

it will be $R_t = \max(x_t, R_{t-1})$. We first generalized the record statistics of independent and identically distributed variable to a weakly correlated sequence. The correlation in these random vectors has been induced due to normalisation of the sequence. The JPDF of intensities of random vectors is given by,

$$P(x_1, \ldots, x_n) = \Gamma(N)\delta\left(\sum_{i=1}^{N} x_i - 1\right). \tag{11}$$

The probability density that the record is R at time t, is shown to be, $P(R,t) = \sum_{m=1}^{t}(-1)^{m+1}\binom{t}{m}m(N-1)(1-mR)^{N-2}\Theta(1-mR)$. For large N and $t \gg 1$, the t^{th} record has been shown to be Gumbel distributed with shift and scaling parameters as $\log(t)/N$ and $1/N$ (see Fig. 7).

We also have shown that average number of records in complex random

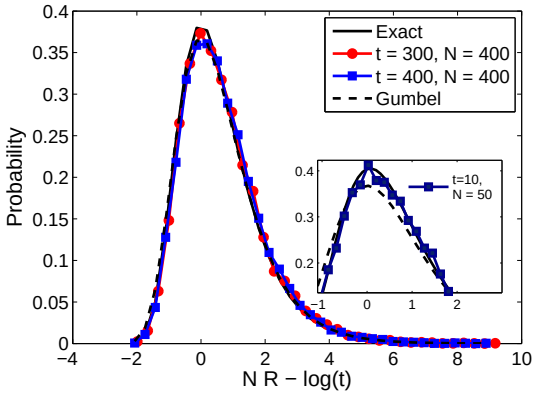

Figure 7: The distribution of the records when the index is t for eigenfunctions of the quantum standard map with $K = 10$. After re-scaling and a shift, the distributions are of the Gumbel type, except for small N (see inset) where deviations are seen and the exact formula for $P(R,t)$ is to be used.

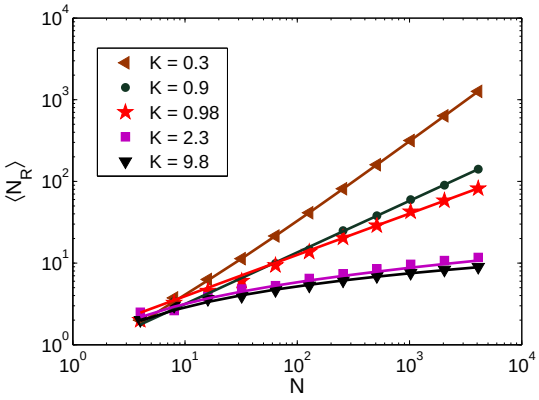

Figure 8: Average number of record in eigenfunction of the quantum standard map of length N vs N is plotted for various K values. Solid line (except $K = 9.8$) are fitted expression $a\log(N) + bN^{\delta}$, for $K = 9.8$ it is $\log(N) + \gamma$. a, b, δ for different K values are,(I) $K = 0.3$, $a = 0.45 \pm 0.15$, $b = 0.306 \pm 0.007$, $\delta = 1.001 \pm 0.003$,(II) $K = 0.9$, $a \approx 0$, $b = 0.73 \pm 0.06$, $\delta = 0.63 \pm 0.01$, (III) $K = 0.98$, $a \approx 0$, $b = 1.2 \pm 0.2$, $\delta = 0.50 \pm 0.01$ and (IV) $K = 2.3$, $a = 0.9 \pm 0.3$, $b = 0.7 \pm 0.6$, $\delta = 0.21 \pm 0.04$.

vector is continue to given by $\langle N_R \rangle = H_N \sim \log(N) + \gamma$ as in case of independent identically distributed random sequence despite the presence of a weak correlation. These follow from a classic result [Renyi 1962, Arnold 1998] that the probability of a record occurring at position j is $1/j$, independent of the past and future position of the records. In other words the probability of the position of the records is a Bernoulli process, Ber$(1/j)$. This can also be understood as the rank order of elements distributed in i.i.d. fashion does not change due to normalization, not surprisingly, the average number of records in complex vector case also turns out to be same.

To compare the results with a dynamical system, we have chosen the standard map, which has been very widely used in quantum chaos studies for over

30 years now. The eigenfunctions of quantized Floquet operator (Unitary matrix) of the standard map for large classical chaos on the torus with phases α, β around 0.25 behave as the complex random vector. We have shown that record statistics of intensity vectors of quantum standard map captures the classical transition to chaos. It is shown that in the mixed phase space regime, the number of intensity records is a power law in the dimensionality of the state in contrast to the logarithmic growth for the random states (see Fig. 8). The exponent of this power-law is exactly one-half at the critical value of the chaos parameter, $K \simeq 0.98$ of the standard map [Srivastava 2013]. Incidentally, in one of the very few exact results of record statistics of correlated time series, random walk, the record scales as square root of length of the sequence [Majumdar 2008]. These findings are based on the record statistics of complex, normalized random states for which we have shown that the probability of a record intensity is a Bernoulli process. Analytical results for lower records of the complex random vector are also presented in this thesis.

Summary

In the first part of the thesis, we have presented the calculation for joint probability distribution function and various spacing distributions of two $N \times N$ structured matrices - random cyclic, and, random reverse cyclic matrices. We also present their relation with exactly solvable models. Since cyclic matrices are pseudo-symmetric matrices, these calculations extend our understanding of random matrix theory of pseudo-symmetric matrices. We have also utilized this method to understand the random walk on a one-dimensional disordered lattice and analytically calculated the entropy and its time-dependence as the system approaches to a dynamical steady state. We have also shown that while random block cyclic matrices considered are themselves not cyclic but the joint probability distribution function has similar structure (only with more eigenval-

ues appearing) while in terms of spacing distribution they are identical. As it is well-known that quantum signatures of chaos are reflected in eigenvalues and eigenfunctions; random matrix theory has found quite a bit of success here too. However, at the same time, it is also well-known in literature that these fingerprints in terms of spacing distribution or spectral rigidity are not universally shared by all the dynamical systems. In second part of the thesis, motivated by this fact we have proposed a new measure, which differentiates among a range of dynamical systems based on whether classical dynamics is integrable or chaotic. This measure which we call stochasticity parameter is similar in definition given by Arnold to distinguish between the levels of stochasticity in arithmetic series and geometric series mod N. To see the order to chaos transition in eigenfunctions of the dynamical systems, we studied record statistics of intensity vectors. We have shown that order to chaos transition is not only captured when we study number of records and how does it scale with the dimensionality of the Hilbert space, but also we (possibly the first time) could capture in a quantum measure the transition point when last KAM torus breaks (*i.e.* $K \approx 0.98$).

List of Figures

Chapter 1

Introduction

Contents

Development of Random matrix theory (RMT) has been a cornerstone for explaining the fluctuation properties in diverse fields such as in Quantum chaos, Nuclear physics, Number theory, wireless communications, *etc.* Whenever the underlying dynamics is complex, or, the dimensionality involved is large, it is seen that fluctuation properties are governed by the symmetries respected by the Hamiltonian. This is the key idea behind development and successful application of random matrix theory in Nuclear physics, initiated by Wigner [Wigner 1957] and independently by Landau and Smorodinsky [Landau 1955]. As all physical systems studied then respected Hermiticity, most of the attention was paid to Hermitian matrices. The invariance enjoyed by the probability measure with respect to symmetry groups is the key to classify the RMT ensembles by Dyson [Dyson 1962a, Dyson 1962b, Dyson 1962c, Dyson 1962d]. The most popular ones are known as Gaussian (circular) orthogonal, unitary and symplectic ensembles of Hermitian (unitary) matrices. Mathematically rigorous analysis of eigenvalue density and spacing distributions were first carried out by Mehta and Gaudin. The book on Random matrices by Mehta remains a standard reference [Mehta 2004]. Around the same time, Ginibre studied the random matrix theory for non-Hermitian matrices [Ginibre 1965].

Though the joint probability distribution function for Ginibre unitary ensemble was obtained by Ginibre himself, the Ginibre orthogonal ensemble proved to be the most difficult one. The general results could only be found very recently thanks to the efforts largely by Sommers [Sommers 2008], Akemann [Akemann 2007], and others. Another class of matrices has become important after the pseudo-Hermitian extension of quantum mechanics [Bender 2002]. These non-Hermitian matrices either have completely real spectra or possess real and complex conjugate eigenvalues with corresponding eigenfunctions with unit and zero pseudo-norm respectively. A natural question arose about the statistical distribution of eigenvalues of this class of matrices. Although the answer is not known in full detail, some preliminary steps have been taken by developing the random matrix theory for 2×2 pseudo-Hermitian matrices by Ahmed and Jain [Ahmed 2003b].

Since one of the first signatures of classical chaos in quantum mechanical spectra was found in spacing distribution (local scale) and Δ_3-statistic (global scale), studies in quantum chaos involve random matrix theory to a great extent. It has been conjectured by Berry and Tabor that generic integrable systems (where number of functionally independent constant of motion which are in involution equals the number of degree of freedom of the system) have an exponential spacing distribution [Berry 1977b]. Similar conjecture by Bohigas, Giannoni, and Schmit (BGS) asserts, "Spectra of time reversal-invariant systems whose classical analogs are K systems show the same fluctuation properties as predicted by GOE" [Bohigas 1984].

Though, BGS conjecture has been successfully tested in many systems, exceptions have been found in a class of strongly chaotic systems in which the level spacings distribution and the two-point statistics approximately behave similar to classically integrable systems. This phenomenon gave rise to the no-

tion of arithmetical chaos [Bolte 1992]. This also motivated to look for other universal measures in energy level statistics which can distinguish between the classically integrable systems from chaotic ones. One such measure has been proposed as fluctuation in staircase function suitably normalized by $\Delta_\infty(x)$ ($\lim_{L\to\infty}\Delta_3(L,x)$). Then the conjecture is that such a normalized quantity will have a limit distribution (in a large x limit) converging to a Gaussian for classically chaotic systems while it will be non-Gaussian for integrable systems [Aurich 1994]. This has been further verified numerically for a range of dynamical systems [Alt 1998]. At the same time, it has been shown than to distinguish between Gaussianity and non-Gaussianity, a very large number of energy levels are required. This, in turn, makes this test equivalent to RMT where a large number of levels are required.

If the bulk spectrum have been studied extensively in quantum chaos literature, a recent development has been at the edges of density of spectrum or in fluctuation properties. Deviation of eigenvalue-density distribution from Wigner's semi-circle in tail region has been studied by Bronk and it has also been shown that about 6% of the eigenvalues come with larger magnitude than predicted by semi-circle law [Bronk 1964]. Starting from classic result of Tracy & Widom for extremal eigenvalues in case of Gaussian random matrix ensembles [Tracy 1994, Tracy 1996], to extremal intensities in case of complex random vectors [Lakshminarayan 2008], one has discovered various applications in bringing to fore various issues in quantum chaos and entanglement [Vivo 2011, Bhosale 2012].

In this thesis, we have extended the random matrix theory for two structured matrices, namely cyclic (pseudo-symmetric) and reverse cyclic (symmetric) ensembles. Corresponding many body problems have been presented and solved exactly. RMT for cyclic matrices extends our knowledge of RMT of pseudo-

Hermitian system while the same for reverse cyclic matrices has brought out the effect of reduction of independent matrix elements on the spectral properties of the symmetric matrices as well as the connection with exactly solvable "screened" harmonic potential. In both these cases, we have obtained explicit expressions for joint probability distribution function and various spacing distributions. It has been further shown that extreme value distribution for maximum eigenvalues of reverse random cyclic matrices is Gumbel while minimum is distributed exponentially in scaled variable.

Going beyond random matrix theory, we have proposed a stochasticity parameter to classify the quantum dynamical systems based on underlying classical dynamics. This is, in spirit, similar to studying the error terms in Gauss circle problem and their probability distribution functions. We show that it is very helpful in classifying the dynamical systems with only few thousand energy levels at our disposal. Further, to see the integrable-chaos transition in eigenfunctions of the standard map, we have studied the record statistics of intensity vectors and presented various analytical and numerical results. Record statistics though similar in spirit with extreme value statistics, have a different take on extremal properties. This not only asks the question about maximum component but also where they occur in the (random) process.

1.1 Random matrix theory : overview of classical ensembles

Complexity of a many-body system (specifically, interaction in a nucleus) gave birth to an astonishingly simple idea of Wigner, that fluctuation properties in the level-densities of different nuclei might behave like fluctuations in eigenvalues of a large random matrix which are invariant under certain symmetry

operations and have statistically independent matrix elements. The symmetry properties satisfied by the Hamiltonian are time-reversal invariance, rotation etc. If system does not possess an anti-unitary Time-reversal symmetry, then the Hamiltonian is Hermitian and such ensembles are called unitary ensembles. In case where system does possess anti-unitary Time-reversal symmetry $\mathcal{T}$, then it can always be written as $\mathcal{T} = UC$ where U is a unitary operator and C stands for complex-conjugation. Now as we know that composition of two anti-unitary operator is always unitary so $\mathcal{T}^2 = (UC)(UC)^\dagger = UU^\dagger$ and this in irreducible subspace will be multiple of identity, therefore $UU^\dagger = \lambda I$ with $\lambda = \pm 1$ due to U being unitary. The case with $\mathcal{T}^2 = 1$ corresponds to orthogonal ensemble and it is always possible to find a basis in which Hamiltonian is real. To show this explicitly let's start with a basis vector ϕ_1 and define $\psi_1 = \phi_1 + \mathcal{T}\phi_1$, clearly ψ_1 is an eigenvector of $\mathcal{T}$ with eigenvalue 1. Let's choose ϕ_2 orthonormal to ψ_1 and again define $\psi_2 = \phi_2 + \mathcal{T}\phi_2$ then it can be easily shown that ψ_2 is orthogonal to ψ_1. This procedure will yield a complete set of basis which are eigenvectors of $\mathcal{T}$ with eigenvalue 1. The matrix element for Hamiltonian H is

$$\begin{aligned} H_{kl} &= \langle \psi_k | H \psi_l \rangle = \langle \mathcal{T}\psi_k | \mathcal{T} H \psi_l \rangle^* \\ &= \langle \mathcal{T}\psi_k | H \mathcal{T} \psi_l \rangle^* \quad \text{as} \quad [H, \mathcal{T}] = 0 \\ &= \langle \psi_k | H \psi_l \rangle^* \quad \text{as} \quad \mathcal{T}\psi = \psi \\ &= H_{kl}^* \Rightarrow \ H \text{is real.} \end{aligned} \tag{1.1}$$

Orthogonal invariance will be guaranteed for systems where time-reversal and space rotation symmetries hold good or if space-rotation is broken then the spin of the particle should be integer. Symplectic ensembles are those where Hamiltonian is invariant under the symplectic group and is valid for systems which possess time-reversal symmetry but with space-rotation broken, they have to have half integer spin. This corresponds to the situation when $\mathcal{T}^2 = -1$,

as it can be easily seen that every eigenvalue will be doubly degenerate with eigenvectors ϕ and $\mathcal{T}\phi$. These two are independent eigenvectors as they can easily be shown to be orthogonal [Verbaarschot 2005].

$$\langle\phi_k|\mathcal{T}\phi_k\rangle = \langle\mathcal{T}\phi_k|\mathcal{T}^2\phi_k\rangle^* = -\langle\mathcal{T}\phi_k|\phi_k\rangle^* = -\langle\phi_k|\mathcal{T}\phi_k\rangle.$$

The trinity of orthogonal, unitary and symplectic ensembles is related with the possibility of only three associative division algebra of symmetry group representation (in terms of matrices) over real field. This is the famous "three fold way" of Dyson [Dyson 1962d, Frobenius 1906]. In general, the probability distribution function for H is given by

$$P(H) \propto \exp\{-[a\,\mathrm{Tr}(H^2) + b\,\mathrm{Tr}(H) + c]\}. \tag{1.2}$$

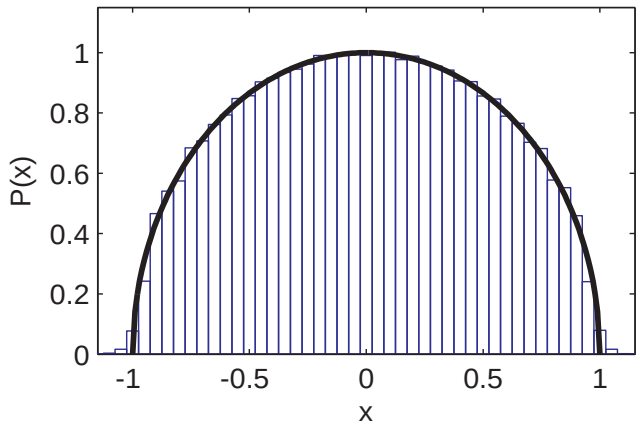

Figure 1.1: Numerical density of eigenvalues (in blue bar) of Gaussian unitary ensemble are compared with Wigner semi-circle (black line). In the bulk of the spectrum Wigner semi-circle matched nicely, but at the edges discrepancies can be seen which further is a subject of extreme value theory.

The joint probability distribution function of eigenvalues for the Gaussian orthogonal, unitary and symplectic matrices can be given by one formula using

an index β which takes values 1,2 and 4 respectively:

$$P\left(\{E_i\}\right) = C_\beta \prod_{i<j} \left(|E_i - E_j|\right)^\beta e^{-a\sum_{i=1} E_i^2}. \tag{1.3}$$

The density of eigenvalues for all the invariant classical ensembles is given by what is called the Wigner semi-circle law (shown in Fig. 1.1). Another interesting quantity that will recur quite frequently in RMT literature is the spacing distribution of the neighbouring eigenvalues. Nearest neighbour spacing distribution $p(s)$, is defined as

$$p(s) = \int_{-\infty}^{\infty} dE_1 \cdots \int_{-\infty}^{\infty} dE_N P(E_1, E_2, \cdots E_N)\delta(s - |E_1 - E_2|) \tag{1.4}$$

in terms of the JPDF. For invariant Gaussian ensembles again, the asymptotic spacing distribution can be given in a unified form,

$$p(s) = A_\beta s^\beta \exp(-B_\beta s^2), \quad \beta = 1, 2, 4. \tag{1.5}$$

$\beta = 1, 2$, and 4 corresponds to Gaussian orthogonal, unitary and symplectic ensembles respectively. A numerical comparison with spacing distributions obtained in Eq. 1.5 is shown in Fig. 1.2. The fluctuation properties also hold for non-Gaussian invariant ensembles where exponent of probability distribution function given in Eq. 1.2 contains an even degree polynomial in H in addition to quadratic term [Brézin 1978]. How the RMT results for invariant distribution are affected upon reducing the number of the independent matrix elements from $O(N^2)$ to $O(N)$ is one of the questions which we have tried to answer in this thesis. By studying the class of reverse random cyclic matrices, we have obtained explicit results of density which is zero at origin and a symmetric function of eigenvalues E. Possibility of three different spacing distributions

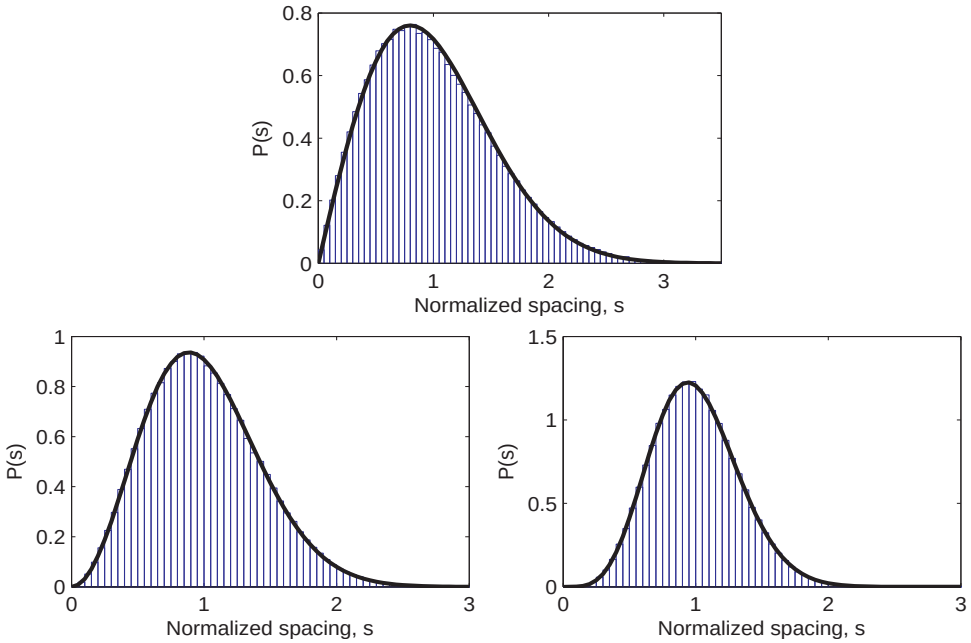

Figure 1.2: Numerical normalized spacing distribution for GOE (top) GUE (middle) and GSE (bottom) is compared with analytically obtained distribution. Solid black line denote the analytical expressions while blue bars denote numerical data.

has been identified and explicit forms have been obtained. We have obtained an exactly solvable many body problem which admits joint probability distribution function of eigenvalues of reverse random cyclic matrices as its ground state wavefunction. This potential is known as "screened-harmonic oscillator" potential and has been studied previously in different context [Perelomov 1971]. The form of potential (for a single particle) has been discussed in literature in quite a few physical situations. It has been interpreted as a screened, two-dimensional isotropic harmonic oscillator in a different context [Davidson 1932]. It has found use in explaining roto-vibrational states in the case of diatomic molecules by considering a five-dimensional version of Davidson oscillator [Rowe 2005]; in a different context of dynamical symmetries [Wu 2000], and uncertainty relations [Patil 2007].

1.2 Pseudo-Hermitian quantum mechanics: a brief introduction

Non-Hermitian Hamiltonians have been discussed in the literature for studying delocalization transition related to depinning of flux lines in type-II superconductors [Hatano 1996, Hatano 1997]. With the numerical observation of complete real eigen spectrum of a family of non-Hermitian Hamiltonians $H_\nu = \frac{1}{2}p^2 - (ix)^\nu$ with $\nu \geq 2$, Bender and his collaborators started a systematic study of parity-time $\mathcal{PT}$-symmetric quantum mechanics [Bender 2002]. It has been argued that non-Hermitian Hamiltonian having $\mathcal{PT}$-symmetry will possess either complete real spectrum (when Hamiltonian and $\mathcal{PT}$ operator share complete set of common eigenvectors) or complex eigenvalues will come in complex-conjugate pairs. When Hamiltonian and $\mathcal{PT}$ operator have complete set of common eigenvector, Hamiltonian is said to have exact $\mathcal{PT}$-symmetry. The other case corresponds to broken $\mathcal{PT}$-symmetry. Let's recall that $\mathcal{P}$ is linear operator with the action as $\hat{p} \to -\hat{p},\ \hat{x} \to -\hat{x}$ while $\mathcal{T}$ is an ani-linear operator with action as $\hat{p} \to -\hat{p},\ \hat{x} \to \hat{x},\ i \to -i$. Also notice $(\mathcal{PT})(\mathcal{PT}) = 1$, hence it is an involution operator and therefore eigenvalues will be pure phases, $\exp(\pm i\phi)$. The necessary condition for Hamiltonian operators of the form $H = \frac{\hat{p}^2}{2m} + V_r(x) + i\varepsilon V_i(x)$ to be $\mathcal{PT}$-symmetric is given by real part of the potential to be symmetric and imaginary part to be anti-symmetric in x. The $\mathcal{PT}$ phase transition has been realized in simple inductively coupled LCR-circuits, one with gain and other with loss. At transition point when two modes coalesce, the relative phase differences of their components acquire a definite value depending on the inductive coupling. Power oscillations reflected in the observed capacitive energy in the system and in fact grows exponentially beyond critical point with the growth rate controlled by the maximum imag-

inary eigenvalue. At critical point, interestingly the capacitive energy grows quadratically with time [Schindler 2011].

As optical beam propagation in a medium with complex refractive index (playing the role of potential) with real part as even function of position and imaginary part as odd function share a formal equivalence on mathematical level with Schrödinger equation; many properties of $\mathcal{PT}$-symmetric quantum mechanics are proposed and indeed observed in optical systems [Klaiman 2008, Makris 2008, Guo 2009, Ruter 2010]. As a function of a control parameter present in potential, it has been shown that below a critical point system possesses exact $\mathcal{PT}$-symmetry and at the critical point two eigenmodes coalesce and eigenvalues become equal. This point is called exceptional point and has been studied in various branches of physics [Heiss 1991, Rotter 2001, Cartarius 2007]. Beyond transition point eigenvalues become complex conjugate pairs and eigenmodes skewed. It is this skewed characteristic of eigenmodes coupled with the fact that power is no more constant of motion as a function of distance give rise to power oscillation observed in parity-time symmetric optical lattices. Total optical power of the propagating beam is defined as $P(z) = \int_{-\infty}^{\infty} |\psi(x,z)|^2 dx$. The dependence of power on travelled distance is derived below.

$$\begin{aligned}
\frac{dP}{dz} &= \int_{-\infty}^{\infty} (\frac{\partial \psi^*}{\partial z}\psi + \psi^* \frac{\partial \psi}{\partial z}) dx \\
&= \int_{-\infty}^{\infty} \{(-i\frac{\partial^2 \psi *}{\partial x^2} - iV^*(x)\psi^*)\psi + \psi^*(-i\frac{\partial^2 \psi}{\partial x^2} + iV(x)\psi)\} dx \\
&= \underbrace{\int_{-\infty}^{\infty} 2^{nd}\text{derivative}}_{\text{boundary term,0}} + i\int_{-\infty}^{\infty} (V(x) - V^*(x))\psi^*\psi dx \\
&= -2\int_{-\infty}^{\infty} \text{Im}(V(x))|\psi|^2 dx.
\end{aligned} \tag{1.6}$$

Following exactly the similar steps as in Eq. 1.6, it can be easily shown that con-

stant of motion is given by $Q(z) = \int_{-\infty}^{\infty} \psi(x,z)\overline{\psi}(-x,z)dx$ called quasi-power but then it may not necessarily be a real valued quantity. The transport properties, transmittance and reflectance in particular, of $\mathcal{PT}$-symmetric system with random index of refraction has been investigated in one-dimension. It has been shown that the transmission processes are reciprocal to left and right-incident waves but the reflection is enhanced from one side and is inversely suppressed from the other, making it a potential candidate for unidirectional coherent absorbers [Kalish 2012]. Calculation has been done utilizing the transfer matrix approach, which itself will become random as the refractive index has been chosen as a random variable.

$\mathcal{PT}$ - symmetric quantum mechanics has been shown as a special case of more general pseudo-Hermitian quantum mechanics. In fact, any non-Hermitian hamiltonian will have complete real eigen spectrum *iff* there exists a positive definite inner product with respect to which given Hamiltonian is Hermitian. This leaves a choice of choosing the inner product differently for different hamiltonian. Hamiltonian H will be called η-pseudo hermitian if it satisfies,

$$H^{\dagger} = \eta H \eta^{-1} \tag{1.7}$$

where η is an invertible Hermitian linear operator. In this formalism, the observable will be defined as in case of conventional quantum mechanics *i.e.* it will be Hermitian with respect to the inner product considered to find out the expectation value.

As we have seen that RMT has been successfully developed and applied to study the fluctuation properties for systems which are represented by Hermitian matrices in variety of areas. As the analysis has been carried out by taking into the account the various symmetry properties that system enjoys

and not the microscopic details of interactions, universality is lurking in the backdrop of RMT formalism. As pseudo-Hermitian systems are different from non-Hermitian systems, it is expected that RMT for them will be different. This is one of the motivation of studying RMT for cyclic matrices in this thesis. As we have not been able to construct the most general pseudo-Hermitian matrix of dimension $N(\neq 2)$, we have fallen back to study the specific model matrices which are pseudo-Hermitian. We have shown that cyclic matrix is one such example and have solved the RMT problem of this class completely. The explicit expressions for joint probability distribution function and all the spacing distribution have been obtained and these results have further been utilized to study the biased random walk problem on a disordered lattice.

1.3 Quantum Chaos

Bohr's correspondence principle which states that in classical limit ($\hbar \to 0$), quantum theory should reduce to classical physics has been a cornerstone of Quantum Mechanics [Liboff 1979, Ford 1991]. In Quantum Mechanics linearity of Schrödinger's equation rules out the exponential divergence in an arbitrary difference of nearby initial conditions. But even worse is the fact that there is no concept of trajectory in Quantum Mechanics which was very essential to define classical chaos. Now a puzzling question will be, where is the information hidden in quantum domain which reflects itself in classical limit by going to integrable and chaotic dynamics for relevant systems? This study of signatures of classical chaos in quantum domain is essentially the subject of "Quantum Chaos" (or quantum chaology as Berry argued [Berry 1989]). Though, the extreme sensitivity to the dynamics (Hamiltonian itself is different) persists in quantum domain [Chaudhury 2009], the more popular signatures have been in terms of spectral distributions and random matrix theory. As it has been

mentioned earlier that for generic integrable system the level tend to cluster and have an exponential spacing distribution $p(s) = \exp(-s)$ [Berry 1977b] in contrast to varying level of level repulsion in chaotic systems depending on the symmetry obeyed by the Hamiltonian [Bohigas 1984]. However, linear level repulsion is also obtained in polygonal billiards[1](e.g. rhombus) which are non-chaotic [Grémaud 1998].

Just to emphasize the remarkable difference in classical and quantum domain for chaotic systems, let's discuss the example of the kicked rotor. The dynamics of this well known example of chaotic (Hamiltonian) system can be captured by the stroboscopic map,

$$\begin{aligned} q_{n+1} &= (q_n + p_n) \bmod 1 \\ p_{n+1} &= p_n - \frac{K}{2\pi}\sin(2\pi q_{n+1}). \end{aligned} \tag{1.8}$$

This has got a phase-space geometry of cylinder and under reasonable assumptions of position q_n being random in fully chaotic domain it can be easily shown that $\langle \Delta p^2 \rangle$ grows linearly with number of kicks N for $K \gg 5$ [Chirikov 1979]. This diffusion is suppressed when one goes in quantum domain. It can be shown that this dynamical localization and Anderson localization are related [Fishman 1982]. But, at the spectral level, quasienergy spectrum of the Anderson model is pure point with fluctuation properties following Poisson distribution whereas the classically diffusive behaviour is possible with only absolutely continuous spectrum. This lack of correspondence is resolved in the semiclassical limit [Jain 1993].

Like eigenvalues of Schrödinger operator, eigenfunctions too carry signatures of chaos (classical) and indeed have been a topic of study. It is known that for

[1]Billiards are dynamical systems consisting of a freely moving particle in an enclosure, reflecting specularly from the boundary. The shape of the boundary is reflected in the name.

quasi-periodic dynamics, the semiclassical eigenfunction can be written as a superposition of plane waves,

$$\Psi_E(x) = \sum_n a_{n,E} e^{iS_n(x)/\hbar + i\phi_n} \tag{1.9}$$

where $S_n(x)$ is the classical action, ϕ_n is Maslov phase. The sum is over the number of ways a classical trajectory can reach position x, each with different momentum p_n. Quasiperiodicity implies the finite sum over n in Eq. 1.9 while chaotic dynamics mean the number of directions emanating or heading to point x is infinite and direction themselves are random in nature. For a chaotic wavefunction Berry conjectured that Eq. 1.9 is valid with random amplitude and phase factor with n now running upto ∞ [Berry 1977a]. Berry conjectured, "Each semi-classical eigenstate has a Wigner function concentrated on the region explored by a typical orbit over infinite times" [Berry 1977a]. In case of chaotic dynamics, a typical orbit fills up the whole available phase space uniformly and hence the local probability density in this case or the averaged Wigner function, under certain assumptions is given by,

$$\rho_m(x,p) = \delta(E - H(x,p))/d(E) \tag{1.10}$$

where $d(E)$ is the density of states. From random wave model (Eq. 1.9), it immediately follows that wavefunction amplitude is distributed in Gaussian manner. This has been numerically shown for number of systems [McDonald 1988, Aurich 1993]. Apart from density, spatial autocorrelation function for random waves can be shown to follow,

$$C(q,\delta q) := \int \Psi^*(q)\Psi(q+\delta q)dq = \frac{1}{\mathrm{vol}\Omega} J_0(\sqrt{E}|\delta q|) \tag{1.11}$$

where Ω is area, J_0 is the Bessel function of order 0. Utilizing $\rho_m(x,p)$, the intensity patterns can be found and compared with wavepacket dynamics in chaotic billiards (in particular Stadium). It has been found that isolated unstable periodic orbits leave their mark on certain eigenfunctions rather prominently in intensity patterns especially whenever the frequency to sum of real positive characteristic exponents of monodromy matrix ω/λ is large. This phenomenon is called scarring [Heller 1984]. It has been latter observed that even when ω/λ is not very large, in $\hbar \to 0$ limit scarring persists.

Distribution of these extreme values of intensities and their position are very important topic of studies in themselves. In case of deep chaotic regime, for systems with broken time-reversal symmetry the maximum intensities are shown to follow Gumbel distribution asymptotically. In fact, for small N the explicit expression has been obtained and they differ significantly from Gumbel, which further may be utilized to extract the system size. The minimum intensities are shown to follow the exponential distribution [Lakshminarayan 2008].

Characterization of such high intensity patterns in the wavefunction is one of our motivations to study the record distribution of wavefunction intensities. As the largest record is also the global maximum of the intensity vector, the statistics of maximum has also been obtained via records distribution and this agrees well with result obtained otherwise. Similar results have also been obtained with lower records which now become the minimum of intensity vector and again relevant statistics has been obtained. In fact we have shown that the phase transition in standard map from integrable to chaotic dynamics can be captured by studying how the number of records depend on length of the intensity vector. Also, in terms of distribution of the position of maximum intensity, a transition from non-quantum unique ergodicity to quantum unique ergodicity can be captured as ergodicity implies that the position of the maximum

intensity is uniformly distributed.

The thesis is broadly comprised of two parts- (i) Chapters 2-4, where we have developed random matrix theory of cyclic and reverse cyclic matrices and applied to case of random walk problem; (ii) Chapters 5-6, where we study two different measures stochasticity parameter and record statistics for studying the various aspect of quantum chaos in eigenvalues and eigenvectors respectively (though by no means it is implied that they cannot be extended for opposite cases).

In Chapter 2, we start with summarizing the existing RMT results in case of non-Hermitian matrices and then discuss the preliminary steps taken for advancing the RMT to the case of pseudo-Hermitian matrices of dimension two. We develop then the random matrix theory for real random cyclic matrices and obtain the joint probability distribution function. We also obtain the various spacing distributions explicitly and compared with numerical distributions. As this class of matrices are examples of pseudo-Hermitian matrices, by solving the RMT problem for general $N \times N$ dimension we have argued to find out the glimpses of general features of RMT for pseudo-Hermitian class of matrices.

In Chapter 3, we have developed first the random matrix theory for random reverse cyclic matrices and obtained the JPDF and explicit expressions for spacing distributions. As reverse cyclic matrices are symmetric matrices, one would expect the results of Gaussian orthogonal ensemble to appear. It is shown that reduced number of independent matrix elements affects the density and various spacing distribution too. In fact JPDF itself comes as a product measure. We have then shown that JPDF is the ground state wavefunction of an exactly solvable N-body problem. The potential is known as the screened harmonic oscillator potential. In this Chapter, we also have shown the maximum of eigenvalues to be distributed as Gumbel in contrast to Tracy-Widom

distribution of GOE while minimum positive eigenvalue is distributed as exponential.

In Chapter 4, we have utilized the results obtained in Chapter 2 to study the biased random walk problem on one dimensional disordered circular lattice. We have obtained the ensemble-averaged entropy evolution for this system from non-equilibrium statistical mechanics.

Carrying out further the studies in quantum chaos, in Chapter 5 we have used the record statistics to study integrable to chaos transition in standard map. For this, we have developed the record statistics for δ-correlated random variables. We have obtained the explicit expressions for number of records as a function of length of the sequence, probability of life-time of record and the distribution of records themselves. We have shown that all the upper records are distributed as Gumbel when properly scaled and shifted while lower records according to exponential distribution. Looking at number of records $\langle N_R \rangle$ as a function of length for intensity vectors of unitary operator of standard map in various regime, we have shown that $\langle N_R \rangle$ varies as a power law in integrable regime while in chaotic regime it varies as logarithmic function of length N. The exponent in power law becomes 0.5 at $K = 0.98$, the value where Golden torus breaks down in case of standard map. As we know that diffusion starts in classical phase space as Golden torus breaks, and it is known that number of records set goes as square-root of number of steps in random walk, we believe to have capture this transition in a measure calculated from quantum mechanical spectra.

In Chapter 6 we have proposed a new measure called stochasticity parameter λ for fluctuations in staircase function of eigenvalue spectrum. We have shown that such a measure scales as a power law ($\propto n^{-\alpha}$) with length of the spectrum. We numerically have found out the probability distribution function of

stochasticity parameter $\Phi'(\Lambda) = \frac{d\Phi}{d\lambda}\big|_{\lambda=\Lambda}$ for typical integrable systems as well as chaotic systems. It has been shown that two class of dynamical systems possess two different kind of PDF of stochasticity parameter, $\sim \exp(-\lambda^{\beta})$ for integrable system while $(a+\lambda)^{-\gamma}$ for chaotic system where λ is the stochasticity parameter. As based on just 5000 eigenlevels PDF of stochasticity parameter has been calculated and have shown marked difference between two kind of dynamical systems, these can be used to classify them. We finally plot a graph between α and $\Phi'(\Lambda)$ which clearly shows that all the integrable systems (considered) tend to cluster at one place while chaotic ones at other. Λ is stochasticity parameter evaluated at last member of spectrum considered (in our case, 5000).

Finally, we summarise in Chapter 7 and present some future directions. Some technical details have been presented in the Appendix.

Chapter 2

Random cyclic matrices

Contents

2.1 Introduction

In 1964, Ginibre initiated the studies on non-Hermitian random matrix theory when he introduced complex, quaternion and real ensembles much alike their Hermitian counterpart [Ginibre 1965]. The matrix ensemble is defined by specifying the algebraic set of matrices, Z (complex, quaternion, and real $N \times N$ matrices) and the measure $d\mu(H) = d\mu_L(H) \exp(-\mathrm{Tr}(H^\dagger H)/4a^2)$ (H is generic element of Z). The measure further satisfies the invariance under an adjoint representation[1] of Z and the elements of H are statistically invariant. $d\mu_L(H)$ is a linear measure on the algebraic set of matrices, Z, and defined as a product of independent elements of H. The joint probability distribution function (JPDF) and the correlation function are obtained by choosing the algebraic set

[1] $d\mu(H) = d\mu(U^\dagger H U)$

of matrices on a complex field:

$$P_N(E_1, E_2, \ldots, E_N) = [1!2! \ldots N!(2\pi)^N]^{(-1)} \prod_{i<j} |E_i - E_j|^2 \exp[-\sum_{i=1}^{N} |E_i|^2],$$

$$R_n(E_1, E_2, \ldots, E_n) = (2\pi)^{-n} \exp[-\sum_{i=1}^{n} |E_i|^2] \det[\exp(E_i E_j^*)]$$

where the n-level correlation function is defined as,

$$R_n(E_1, E_2, \cdots, E_n) = \frac{N!}{(N-n)!} \int \cdots \int P_N(E_1, E_2, \ldots, E_N) dE_{n+1} \cdots dE_N. \tag{2.1}$$

The JPDF of the quaternion ensemble is

$$P_N(E_1, E_2, \ldots, E_N) = [1!2! \ldots (2N-1)!(4\pi)^N]^{(-1)} \prod_{i=1}^{N} |E_i - E_i^*|^2 \times \prod_{i<j\leq N} |E_i - E_j|^2 |E_i - E_j^*|^2 \exp[-\sum_{i=1}^{N} |z_i|^2].$$

The correlation functions for the quaternion case are given by [Mehta 1967, Mehta 1991]

$$R_n(E_1, E_2 \ldots E_n) = \prod_{i=1}^{n} (E_i - E_i^*) e^{-|E_i|^2} \left\{ \det \begin{bmatrix} \phi(E_i, E_j) & \phi(E_i, E_j^*) \\ \phi(E_i^*, E_j) & \phi(E_i^*, E_j^*) \end{bmatrix} \right\}^{1/2},$$

$$\phi(u, v) = \frac{1}{2\pi}(v-u)e^{uv} \int_0^1 \exp\left(\frac{1}{2}(u-v)^2 x\right) \frac{dx}{\sqrt{1-x}}. \tag{2.2}$$

For the real non-Hermitian ensemble, Ginibre found the JPDF for a very special situation when all the eigenvalues were real to be

$$P_N(E_1, E_2, \ldots, E_N) = \frac{C\pi^{N(N-1)/4}}{2^N N!} \prod_{i<j} |E_i - E_j| \exp[-\sum_{i=1}^{N} E_i^2].$$

The real non-Hermitian ensemble proved to be the hardest among three (complex, quaternion and real) and a formal solution for JPDF and correlation function were obtained very recently [Kanzieper 2005, Akemann 2007]. A very nice summary is presented in the Section 1.2 of [Akemann 2007], we are reproducing here the same (almost verbatim) for the sake of completeness.

Let $\mathcal{H}_k$ be an $n \times n$ random real matrix with k real eigenvalues such that its entries are statistically independent random variables picked from a normal distribution $\mathsf{N}(0,1)$. Then, the JPDF of its $2\ell = n - k$ complex eigenvalues is

$$P_{\boldsymbol{\mathcal{H}}_k}(E_1, \cdots, E_\ell) = \tfrac{p_{n,n}}{\ell!} \left(\tfrac{2}{i}\right)^\ell \prod_{j=1}^{\ell} \operatorname{erfc}\left(\tfrac{E_j - \bar{E}_j}{i\sqrt{2}}\right) \operatorname{pf} \begin{bmatrix} \mathcal{D}_n(E_i, E_j) & \mathcal{D}_n(E_i, \bar{E}_j) \\ \mathcal{D}_n(\bar{E}_i, E_j) & \mathcal{D}_n(\bar{E}_i, \bar{E}_j) \end{bmatrix}_{2\ell \times 2\ell} \tag{2.3}$$

Here, pf denotes the Pfaffian[2] and erfc denotes the complementary error function. $p_{n,n} (= 2^{-n(n-1)/4})$ is the probability of having all the eigenvalues real for $n \times n$ matrices $\mathcal{H}$. This JPDF is supported for $(\operatorname{Re} E_1, \cdots, \operatorname{Re} E_\ell) \in \mathbb{R}^\ell$, and $(\operatorname{Im} E_1, \cdots, \operatorname{Im} E_\ell) \in (\mathbb{R}^+)^\ell$. The antisymmetric kernel $\mathcal{D}_n(E, E')$ is given explicitly by (2.4) – (2.10). For $n = 2m$ even, the kernel function is given by

$$\mathcal{D}_{2m}(x,y) = \frac{1}{2} e^{-(x^2+y^2)/2} \sum_{j=0}^{m-1} \frac{q_{2j+1}(x)\, q_{2j}(y) - q_{2j}(x)\, q_{2j+1}(y)}{h_j} \tag{2.4}$$

while for $n = 2m+1$ odd, it equals

$$\mathcal{D}_{2m+1}(x,y) = \frac{1}{2} e^{-(x^2+y^2)/2} \sum_{j=0}^{m-1} \frac{\tilde{q}_{2j+1}(x)\, \tilde{q}_{2j}(y) - \tilde{q}_{2j}(x)\, \tilde{q}_{2j+1}(y)}{h_j}. \tag{2.5}$$

[2]Determinant of any even dimensional skew-symmetric matrix can be expressed as square of a polynomial (in matrix elements), this polynomial is called Pfaffian of the matrix(*Courtesy* Wikipedia). Each entry of Pfaffian if denoted by $\operatorname{pf}(a_1, a_2)$, then Pfaffian is an anti-symmetric function of $a_1,\ a_2$. General even dimensional Pfaffian can be defined recursively as

$$\operatorname{pf}(a_1, a_2, \cdots, a_{2n}) = \sum_{i=2}^{2n} \operatorname{pf}(a_1, a_i)(-1)^i \operatorname{pf}(a_2, \cdots, \overline{a_i}, \cdots, a_{2n})$$

where $\overline{a_i}$ represents elimination of a_i.

Both representations (2.4) and (2.5) involve the polynomials $q_j(x)$ skew orthogonal on $\mathbb{R}$ with respect to the GOE skew product [Mehta 2004]

$$\langle f,\, g\rangle = \frac{1}{2}\int_{\mathbb{R}} dx\, e^{-x^2/2} \int_{\mathbb{R}} dy\, e^{-y^2/2}\mathrm{sgn}(y-x)\, f(x)\, g(y) \tag{2.6}$$

such that

$$\langle q_{2k}, q_{2\ell+1}\rangle = -\langle q_{2k+1}, q_{2\ell}\rangle = h_k\delta_{k,\ell}, \quad \langle q_{2k}, q_{2\ell}\rangle = \langle q_{2k+1}, q_{2\ell+1}\rangle = 0. \tag{2.7}$$

The skew orthogonal polynomials $q_j(x)$ can be expressed in terms of Hermite polynomials as [3]

$$\begin{aligned} q_{2j}(x) &= \frac{1}{2^{2j}}\, H_{2j}(x), \\ q_{2j+1}(x) &= \frac{1}{2^{2j+1}}\left[H_{2j+1}(x) - 4j\, H_{2j-1}(x)\right] \end{aligned} \tag{2.8}$$

while "tilde" polynomials $\tilde{q}_j(x)$ [4] entering (2.5) are related to $q_j(x)$ via

$$\begin{aligned} \tilde{q}_{2j}(x) &= q_{2j}(x) - \frac{(2j)!}{2^{2j}j!}\,\frac{2^{2m}m!}{(2m)!}\, q_{2m}(x), \\ \tilde{q}_{2j+1}(x) &= q_{2j+1}(x), \end{aligned} \tag{2.9}$$

with the normalisation,

$$h_j = \langle q_{2j},\, q_{2j+1}\rangle = \frac{\sqrt{\pi}\,(2j)!}{2^{2j}} \tag{2.10}$$

Let $\boldsymbol{\mathcal{H}}_0$ be an $n\times n$ random real matrix with no real eigenvalues such that its entries are statistically independent random variables picked from a normal distribution $\mathsf{N}(0,1)$. Then, the p-point correlation function ($1\le p\le \ell$) of its

[3] Equation (2.8) assumes that $H_{-1}(x)\equiv 0$.
[4] Note that the $\tilde{q}_{2j}(x)$ is no longer a polynomial of the degree $2j$.

complex eigenvalues, equals

$$R_{0,p}^{(\boldsymbol{\mathcal{H}}_0)}(E_1,\cdots,E_p;n) = p_{n,n}\,\frac{\prod_{j=0}^{\ell-1} r_j}{\prod_{j=1}^{n}\Gamma(j/2)}\prod_{j=1}^{p}\operatorname{erfc}\left(\frac{E_j-\bar{E}_j}{i\sqrt{2}}\right)\exp\left(-\frac{E_j^2+\bar{E}_j^2}{2}\right) \times \operatorname{pf}\begin{bmatrix}\kappa_\ell(E_i,E_j) & \kappa_\ell(E_i,\bar{E}_j)\\ \kappa_\ell(\bar{E}_i,E_j) & \kappa_\ell(\bar{E}_i,\bar{E}_j)\end{bmatrix}_{2p\times 2p} \tag{2.11}$$

Here, $n = 2\ell$ and the 'pre-kernel' κ_ℓ equals

$$\kappa_\ell(E,E') = i\sum_{j=0}^{\ell-1}\frac{1}{r_j}\Big[p_{2j}(E)p_{2j+1}(E') - p_{2j}(E')p_{2j+1}(E)\Big]. \tag{2.12}$$

The polynomials $p_j(E)$ are skew orthogonal in the complex half-plane ($\operatorname{Im} E > 0$),

$$\langle p_{2j+1}, p_{2k}\rangle_{\mathrm{c}} = -\langle p_{2k}, p_{2j+1}\rangle_{\mathrm{c}} = i\,r_j\,\delta_{jk}, \tag{2.13}$$

$$\langle p_{2j+1}, p_{2k+1}\rangle_{\mathrm{c}} = \langle p_{2j}, p_{2k}\rangle_{\mathrm{c}} = 0, \tag{2.14}$$

with respect to the skew product

$$\langle f,g\rangle_{\mathrm{c}} = \int_{\operatorname{Im}E>0} d^2E\operatorname{erfc}\left(\frac{E-\bar{E}}{i\sqrt{2}}\right)\exp\left(-\frac{E^2+\bar{E}^2}{2}\right)\big[f(E)g(\bar{E}) - f(\bar{E})g(E)\big] \tag{2.15}$$

In case of Gaussian asymmetric matrices having real and complex eigenvalues, Sommers *et al.* [Sommers 1988] derived the expression for the average density of eigenvalues, $\rho(E)$ to be uniform inside a circle. It was shown that in $N\to\infty$ limit,

$$\rho(E) = \begin{cases}\frac{1}{\pi ab}, & \text{if } \left(\frac{x}{a}\right)^2+\left(\frac{y}{b}\right)^2 \le 1\\ 0, & \text{otherwise}\end{cases} \tag{2.16}$$

where $E = x + iy$. It came very nicely by invoking the similarity of Green's

function of eigenvalues in this problem to that of 2D-Coulomb problem with a very special potential function, given by,

$$\mathbf{\Phi}(E) = \frac{1}{N} \ln \left[\int \left(\frac{d^2 z_i}{\pi} \right) \exp \left\{ -\varepsilon \sum_i |z_i|^2 - \sum_{i,j,k} z_i^* (E^* \delta_{ik} - H_{ik}^T)(E\delta_{kj} - H_{kj}) z_j \right\} \right]_H . \tag{2.17}$$

The bracket $[\dots]_H$ denotes ensemble average. After realizing this connection, it boils down to calculating potential function in the large N limit (N being the dimension of matrix) utilizing saddle point method. It is then straightforward to calculate the Green's function and thereby the density.

Further the joint probability distribution function for real and complex eigenvalues was obtained in [Lehmann 1991]. An outline of this result which being a very important milestone is summarized in Section 2.2. Essentially the same results were rediscovered by Edelman [Edelman 1997].

2.2 JPDF of Random Real matrices

In this Section, we will sketch the proof of joint probability distribution function of eigenvalues given that R of them are real for Ginibre orthogonal ensemble [Lehmann 1991]. We will then illustrate this result for 2×2 matrix H, it is largely based on the reference [Sommers 2008]. Here, it will be prudent to remind that general JPDF obtained in [Kanzieper 2005] is sum of these JPDF for $R = 0$ to N. The correlation functions for this class have been obtained in [Kanzieper 2005]. Let's recall a simple identity that a diagonal matrix with complex conjugate entries can be transformed into a 2×2 matrix with real elements as

$$\frac{1}{\sqrt{2}} \begin{bmatrix} 1 & 1 \\ i & -i \end{bmatrix} \begin{bmatrix} a+ib & 0 \\ 0 & a-ib \end{bmatrix} \frac{1}{\sqrt{2}} \begin{bmatrix} 1 & 1 \\ i & -i \end{bmatrix} = \begin{bmatrix} a & b \\ -b & a \end{bmatrix} \tag{2.18}$$

This enables one to write a diagonal eigenvalue matrix having R real eigenvalues and Q complex conjugate eigenvalues into a matrix having R diagonal entries and Q blocks of type referred in Eq. 2.18 on diagonals, with rest being zero. From elementary algebra we know that any real matrix with distinct eigenvalues can be reduced by a non-singular real matrix X as

$$H = X\tilde{\Lambda}X^{-1}, \quad \det(X) \neq 0 \tag{2.19}$$

where

$$\tilde{\Lambda} = U\Lambda U^{-1}, \quad \Lambda_{ij} = \lambda_i \delta_{ij} \tag{2.20}$$

with U given by an almost diagonal matrix such that first R diagonal entries are 1 and next Q are 2×2 matrices of the form

$$\frac{1}{\sqrt{2}} \begin{bmatrix} 1 & 1 \\ i & -i \end{bmatrix} \tag{2.21}$$

Again from (incomplete) Schur decomposition, X can be written as $X = OT\tilde{D}$ where O is a real orthogonal matrix, T is an upper triangular matrix with diagonal elements as 1, and $\tilde{D}$ is a diagonal matrix of the same type as $\tilde{\Lambda}$. As $\tilde{D}$ and $\tilde{\Lambda}$ commute, H can be written as $H = O\tilde{H}O^{-1}$ with $\tilde{H} = T\tilde{\Lambda}T^{-1}$. One can verify that both the sides have correct number of independent entries. H has N^2 and on right hand side both O and T have $N(N-1)/2$ plus N coming from the $\tilde{\Lambda}$.

It is then easy to show that $\mathrm{Tr}HH^T = \mathrm{Tr}\tilde{H}\tilde{H}^T$ utilizing the fact that $H = O\tilde{H}O^{-1}$ and O is orthogonal matrix. Therefore it is most convenient to consider $\Lambda,\ O,\ $ and $\tilde{H_{ij}}(i < j)$ as independent variables. Further integration on O (which is easy) and $\tilde{H_{ij}}(i < j)$ will produce the joint probability distribution

function (JPDF) of Λ:

$$P(\lambda_1, \lambda_2, \ldots, \lambda_N) = K_N \prod_{i>j} |\lambda_i - \lambda_j| \left(\prod_{i=1}^{N} \exp(-\lambda_i^2) \mathrm{erfc}(|\lambda_i - \lambda_i^*|/\sqrt{2}) \right)^{1/2}. \tag{2.22}$$

Let's work through for $N = 2$ case which captures essentially all the interesting ingredients. Through this calculation we intend to show that measure of eigenvalues Λ_+, Λ_- of matrix H is given by,

$$d\mu(\Lambda_+, \Lambda_-) = \frac{1}{2\sqrt{2\pi}} d\Lambda_+ d\Lambda_- (\Lambda_+ - \Lambda_-) \exp(-(\Lambda_+^2 + \Lambda_-^2)/2) \mathrm{erfc}(\sqrt{2}|\mathrm{Im}\Lambda_+|).$$

We know that any real 2-dimensional matrix H can be written in the following form,$H = O\tilde{H}O^T$,

$$H = \begin{bmatrix} \cos\phi & \sin\phi \\ -\sin\phi & \cos\phi \end{bmatrix} \begin{bmatrix} \lambda_1 & \delta \\ -\delta & \lambda_2 \end{bmatrix} \begin{bmatrix} \cos\phi & -\sin\phi \\ \sin\phi & \cos\phi \end{bmatrix} \tag{2.23}$$

with $\lambda_1 > \lambda_2,\ 0 \leq \phi \leq \pi,\ -\infty < \delta < \infty$. $\lambda_1,\ \lambda_2$ are the eigenvalues of symmetric part of H, ϕ is the angle of rotation which diagonalizes the symmetric part of H and δ determines the skew-symmetric part of H. As an anti-diagonal matrix with δ and $-\delta$ commutes with rotation matrix, it can not be diagonalized by rotations. As $O^TO = 1$, so $dO^TO + O^TdO = 0$ or O^TdO is skew symmetric matrix. Let's evaluate dH:

$$\begin{aligned} dH &= dO\tilde{H}O^T + Od\tilde{H}O^T + O\tilde{H}dO^T \\ &= O(O^TdO\tilde{H} + \tilde{H}dO^TO + d\tilde{H})O^T \\ &= O(O^TdO\tilde{H} - \tilde{H}O^TdO + d\tilde{H})O^T. \end{aligned} \tag{2.24}$$

As Jacobian is invariant under O-symmetry, we focus on the quantities in paren-

thesis which can be written as

$$O^T dO\tilde{H} - \tilde{H}O^T dO + d\tilde{H} = \begin{bmatrix} d\lambda_1 & d\delta + d\phi(\lambda_2 - \lambda_1) \\ -d\delta + d\phi(\lambda_2 - \lambda_1) & d\lambda_2 \end{bmatrix}. \quad (2.25)$$

Hence, Jacobian is $2(\lambda_2 - \lambda_1)$. Let's go finally from λ to Λ which are eigenvalues of H, viz.,

$$\Lambda_\pm = \frac{\lambda_1 + \lambda_2}{2} \pm \sqrt{\left(\frac{\lambda_1 - \lambda_2}{2}\right)^2 - \delta^2}. \quad (2.26)$$

From Eq. 2.26, it is clear that both the roots are real for $\left(\frac{\lambda_1-\lambda_2}{2}\right)^2 \geq \delta^2$ and complex conjugate otherwise. The Jacobian of transformation given in Eq. 2.26 is given by $\frac{\lambda_1-\lambda_2}{\Lambda_+-\Lambda_-}$. This gives the spectral measure

$$\begin{aligned} d\mu(H) &= \frac{1}{(2\pi)^2} d\phi d\delta d\Lambda_+ d\Lambda_- 2(\Lambda_+ - \Lambda_-) \exp(-\mathrm{Tr}(\tilde{H}\tilde{H}^T)) \\ &= \frac{1}{(2\pi)^2} d\phi d\delta d\Lambda_+ d\Lambda_- 2(\Lambda_+ - \Lambda_-) \exp(-(\Lambda_+^2 + \Lambda_-^2 + 4\delta^2)/2) \quad (2.27) \end{aligned}$$

From 2.26, one can easily invert and write

$$\lambda_{1,2} = \frac{\Lambda_+ + \Lambda_-}{2} \pm \sqrt{\left(\frac{\Lambda_+ - \Lambda_-}{2}\right)^2 + \delta^2}. \quad (2.28)$$

Now if $\Lambda_\pm$ are real then $\lambda_{1,2}$ being real will allow the range of δ to be $(-\infty, \infty)$ so measure for (real)eigenvalues is given by

$$\begin{aligned} d\mu(\Lambda_+, \Lambda_-) &= \frac{1}{(2\pi)^2} \int_0^\pi d\phi \int_{-\infty}^{\infty} d\delta d\Lambda_+ d\Lambda_- 2(\Lambda_+ - \Lambda_-) \exp(-(\Lambda_+^2 + \Lambda_-^2 + 4\delta^2)/2) \\ &= \frac{1}{2\sqrt{2\pi}} d\Lambda_+ d\Lambda_- (\Lambda_+ - \Lambda_-) \exp(-(\Lambda_+^2 + \Lambda_-^2)/2). \quad (2.29) \end{aligned}$$

On the other hand, for $\delta^2 > \left(\frac{\lambda_1-\lambda_2}{2}\right)^2$ the $\Lambda_\pm$ are complex-conjugate, so for δ-integration lower limit, will be $|\mathrm{Im}\Lambda_+|$ with upper limit ∞. This gives the

measure as

$$d\mu(\Lambda_+,\Lambda_-)=\frac{1}{2\sqrt{2\pi}}d\Lambda_+d\Lambda_-(\Lambda_+-\Lambda_-)\exp(-(\Lambda_+^2+\Lambda_-^2)/2)\mathrm{erfc}(\sqrt{2}|\mathrm{Im}\Lambda_+|). \tag{2.30}$$

In contrast to this result, we will see how a smaller number of independent elements in the matrix modify this result. The case in present will be of cyclic matrices which even though are asymmetric matrices have very small number of independent elements (N). Cyclic matrices are also an example of pseudo-symmetric (Hermitian) matrix as it will be shown and discussed in Sections 2.3, 2.4.

2.3 RMT for 2×2 pseudo-Hermitian matrices

A complete new class of matrices are being studied which though not symmetric (rather generally Hermitian) possess real eigenvalues in a certain parameter interval present in the Hamiltonian matrix. These classes are known as pseudo-Hermitian matrices and already have captured attention of physicists both theoretical and experimental as well as mathematicians alike. The random matrix theory for general $N\times N$ pseudo-Hermitian matrices has been elusive so far, nevertheless some concrete and closed-form expressions for 2×2 matrices have already been found [Ahmed 2003b]. In 3×3 and $N\times N$, the most general form of pseudo-hermitian matrix is not known, thereby making the random matrix theory untenable. It is useful to mention here that cyclic matrices form a special cases of pseudo-hermitian matrices on the real field.

In any physical experiment we measure a (real) eigenvalue of some linear operator belonging to a Hilbert space. Let us consider a linear wave theory(*e.g.* quantum mechanics) where a system is represented at any instant by a state in a Hilbert space, with a time-independent norm. Denoting by $|\psi\rangle$ a vector and

its conjugate partner by $\langle\psi\eta|$, the inner product may be given by the volume integral, $\int \psi^* \eta \psi dV$ = constant. Accordingly, the linearity and continuity of evolution implies

$$\begin{aligned} \frac{d}{dt}\int \psi^*\eta\psi dV &= 0, \\ \int \frac{\partial\psi^*}{\partial t}\eta\psi dV &+ \int \psi^*\eta\frac{\partial\psi}{\partial t}dV = 0, \\ \int i\psi^*\mathcal{H}^\dagger\eta\psi dV &- \int i\psi^*\eta\mathcal{H}\psi dV = 0, \\ \int i\psi^*\eta(\eta^{-1}\mathcal{H}^\dagger\eta - \mathcal{H})\psi dV &= 0, \\ \mathcal{H}^\dagger &= \eta\mathcal{H}\eta^{-1}. \end{aligned} \tag{2.31}$$

We have made use of linearity (via, e.g., Schrödinger equation)

$$\mathcal{H}\psi = i\hbar\frac{\partial\psi}{\partial t}. \tag{2.32}$$

Thus Eq. 1.7 is motivated from here (Eq. 2.31) and as a special case taking η as identity operator will give the Hermitian quantum mechanics and the norm as the usual Euclidean norm in Hilbert space.

Let us consider a symmetry transformations which preserves the η-norm ($\langle x|\eta y\rangle$) between the vectors $\mathbf{x}$ and $\mathbf{y}$. By considering the Cayley form, $D = e^{iH}$ as a symmetry transformation acting on $\mathbf{x}$, $\mathbf{y}$ where H is pseudo-Hermitian in accordance with $\eta H\eta^{-1} = H^\dagger$, it is easy to show that $D^\dagger = \eta D^{-1}\eta^{-1}$, *i.e.* pseudo-unitary with respect to η. If x, y are two vectors in Hilbert space which transform to x', y' and the transformation operator is given by D, then the inner product $\langle x'|\eta y'\rangle$ is invariant under transformation D. Also the matrix element of an arbitrary operator A will transform as $\langle x'|\eta A'|y'\rangle = \langle x|\eta A|y\rangle$ provided A itself transforms as $DAD^{-1} = A'$ [Ahmed 2003b]. The closure law for two pseudo-unitary matrices is trivial if both are pseudo-unitary with respect to

the same η. Also, D^{-1} is pseudo-unitary with respect to η if D is pseudo-unitary: $\eta^{-1}(e^{-iH})^{\dagger}\eta = e^{i\eta^{-1}H^{\dagger}\eta} = e^{iH}$. With identity matrix as a unit element of the symmetry transformation, and with associativity guaranteed, the $N \times N$ pseudo-unitary matrices form a pseudo-unitary group of order N, $PU(N)$.

Starting with the simplest case of a pseudo-Hermitian matrix [Ahmed 2003a],

$$H = \{H_{ij}\} = \begin{bmatrix} a & -ib \\ ic & a \end{bmatrix}, \tag{2.33}$$

a, b, c being real, it is easy to show that metric is

$$\eta = \begin{bmatrix} 0 & i \\ -i & 0 \end{bmatrix}. \tag{2.34}$$

Interpreting the matrix $\begin{bmatrix} 1 & 0 \\ 0 & -1 \end{bmatrix}$ which is σ_z as parity ($\mathcal{P}$), and usual complex conjugation, $\mathcal{K}_0$ as time-reversal operator $\mathcal{T}$, the matrix is $\mathcal{PT}$- symmetric[5]. The diagonalizing matrix for H is given by D, *i.e.*,

$$D = \begin{bmatrix} 1 & i/r \\ ir & 1 \end{bmatrix}. \tag{2.35}$$

The eigenvalues of H are $E_{\pm} = a \pm \left[\frac{c}{2r} + \frac{br}{2}\right]$ ($r = \sqrt{c/b}$ ($r \in [0, \infty]$)). Here, we would also like to mention that $H(D)$ may not be pseudo-Hermitian (unitary) with respect to the same metric, as is the case here. The metric for D is

$$\delta = \begin{bmatrix} 0 & 1 \\ 1 & 0 \end{bmatrix}. \tag{2.36}$$

[5] $\mathcal{PT}$ symmetry implies $[H, \mathcal{PT}] = 0$ which in turn reduces to $\mathcal{P}H^{*}\mathcal{P}^{-1} = H$ if $\mathcal{T}H\mathcal{T}^{-1} = H^{*}$ *i.e.* $\mathcal{T}$ is usual complex-conjugation.

In the parameter space, the joint probability density function for the matrix H is taken of the Gaussian form,

$$P(H) = \mathcal{N} e^{-\frac{1}{2\sigma^2} \text{ Tr } H^\dagger H} \tag{2.37}$$

and this reduces to

$$P(a,b,c) = \frac{1}{2(\pi\sigma^2)^{\frac{3}{2}}} e^{-\frac{1}{2\sigma^2}\left[2a^2+b^2+c^2\right]}. \tag{2.38}$$

By inserting the relation of eigenvalues in terms of parameters and, using the Jacobian for this transformation, we get the joint probability distribution function (JPDF) of eigenvalues:

$$P(E_+,E_-) = \frac{|E_+ - E_-|}{2(\pi\sigma^2)^{\frac{3}{2}}} K_0\left(\frac{(E_+-E_-)^2}{4\sigma^2}\right) e^{-\frac{(E_++E_-)^2}{4\sigma^2}} \tag{2.39}$$

where $K_0(x)$ is 0^{th} order modified Bessel function of second kind and it can further be represented as $K_0(x) = \int_0^\infty \cos(x \sinh t) dt$. Perhaps historically one of the most studied quantity in random matrix literature is the nearest neighbour level spacing distribution, $P(S)$. It is well known that for the Wigner-Dyson ensembles the spacing distribution very well-approximated by, $P(S) \sim S^\beta e^{-\gamma S^2}$ where β is 1, 2, and 4 corresponds to the orthogonal, unitary, and symplectic ensembles [Mehta 1991, Haake 1991, Zelevinsky 1996]. However, there are systems such as billiards in polygonal enclosures, three-dimensional Anderson model at the metal-insulator transition point, and many more which display intermediate statistics [Parab 1996, Grémaud 1998, Bogomolny 1999].

The spacing distribution for the present case , $P(S)$, is given in terms of

the JPDF by

$$\begin{aligned} P(S) &= \int_{-\infty}^{\infty}\int_{-\infty}^{\infty} P(E_+, E_-)\delta(S - |E_+ - E_-|)dE_+dE_- \\ &= \frac{|S|}{\pi\sigma^2}K_0\left(\frac{S^2}{4\sigma^2}\right). \end{aligned} \tag{2.40}$$

Remarkably, as $S \to 0$, $P(S) \sim S\log(1/S)$ (it is non-algebraic level repulsion, in contrast with Wigner-Dyson ensembles). In Table 2.1, we summarize the results for various 2×2 pseudo-Hermitian matrices which form their own class.

It is clear that unlike Hermitian cases, simply because of the presence of a larger number of parameters, more forms of spacing distributions are expected. The natural extension of these results to the general $PU(N)$ case remains open. However, we have exact results for a special kind of pseudo-Hermitian matrices, *viz.* cyclic matrices or circulants, which we now turn to.

2.4 Random cyclic matrices

Let us consider an $N \times N$ cyclic matrix with real elements, $\{a_i\}$:

$$\mathbf{M} = \begin{bmatrix} a_1 & a_2 & \ldots & a_N \\ a_N & a_1 & \ldots & a_{N-1} \\ \vdots & & & \\ a_2 & a_3 & \ldots & a_1 \end{bmatrix}. \tag{2.41}$$

Table 2.1: A summary of 2×2 pseudo-hermitian random matrices

H	η	D	δ	P(S) $(S \to 0)$
$\begin{bmatrix} a & -ib \\ ic & a \end{bmatrix}$	$\begin{bmatrix} 0 & i \\ -i & 0 \end{bmatrix}$	$\frac{1}{\sqrt{2}}\begin{bmatrix} 1 & \frac{i}{r} \\ ir & 1 \end{bmatrix}$ $(0 \le r < \infty)$	$\begin{bmatrix} 0 & 1 \\ 1 & 0 \end{bmatrix}$	$-S \log S$
$\begin{bmatrix} a+c & ib \\ ib & a-c \end{bmatrix}$	$\begin{bmatrix} 1 & 0 \\ 0 & -1 \end{bmatrix}$	$\begin{bmatrix} \frac{\cos\theta}{\sqrt{\cos 2\theta}} & \frac{i\sin\theta}{\sqrt{\cos 2\theta}} \\ \frac{-i\sin\theta}{\sqrt{\cos 2\theta}} & \frac{\cos\theta}{\sqrt{\cos 2\theta}} \end{bmatrix}$ $\theta = -\frac{1}{2}\sin^{-1}(b/c)$ $(-\pi/4 < \theta < \pi/4)$	Not known	$-S \log S$
$\begin{bmatrix} a & -i\varepsilon c \\ \frac{ic}{\varepsilon} & b \end{bmatrix}$	$\begin{bmatrix} \frac{1}{\varepsilon} & 0 \\ 0 & \varepsilon \end{bmatrix}$	$\begin{bmatrix} \cos\theta & i\varepsilon\sin\theta \\ -i\sin\theta/\varepsilon & \cos\theta \end{bmatrix}$ $\theta = -\frac{1}{2}\tan^{-1}\frac{2c}{a-b}$ $(-\pi/4 < \theta < \pi/4)$	$\begin{bmatrix} \frac{1}{\varepsilon} & 0 \\ 0 & \varepsilon \end{bmatrix}$	$Sf(\gamma)$, $\varepsilon = e^{\gamma}$
$\begin{bmatrix} a+ib & c \\ d & a-ib \end{bmatrix}$	$\begin{bmatrix} 0 & 1 \\ 1 & 0 \end{bmatrix}$	$\begin{bmatrix} \frac{re^{i\theta}}{\sin\theta} & -\frac{re^{i\theta}}{\sin\theta} \\ 1 & 1 \end{bmatrix}$ $r = (b/d)$ $\cot\theta = \sqrt{\frac{cd}{b^2} - 1}$	Not known	S with large coefficient
$\begin{bmatrix} a+b & d+ic \\ -d+ic & a-b \end{bmatrix}$	$\begin{bmatrix} 1 & 0 \\ 0 & -1 \end{bmatrix}$	$\begin{bmatrix} i\cos\theta & e^{i\phi}\sin\theta \\ e^{-i\phi}\sin\theta & -i\cos\theta \end{bmatrix}$ $\phi = -\frac{1}{2}\tan^{-1}\frac{c}{d}$ $(-\frac{\pi}{2} < \phi < \frac{\pi}{2})$ $\sin 2\theta = \sqrt{\frac{c^2+d^2}{b^2}}$ $(0 < \theta < \pi/2)$	$\begin{bmatrix} 1 & 0 \\ 0 & -1 \end{bmatrix}$	S

It is important to note that this matrix is, in fact, pseudo-Hermitian (pseudo-symmetric) with respect to η

$$\eta = \begin{bmatrix} 1 & 0 & 0 & \dots & 0 & 0 \\ 0 & 0 & 0 & \dots & 0 & 1 \\ 0 & 0 & 0 & \dots & 1 & 0 \\ \vdots & & & & & \\ 0 & 1 & 0 & \dots & 0 & 0 \end{bmatrix}, \tag{2.42}$$

that is,

$$\mathbf{M}^{\dagger} = \mathbf{M}^{T} = \eta \mathbf{M} \eta^{-1}. \tag{2.43}$$

Since $\eta^2 =$ identity, $\mathbf{I}$, η is introduced here as "generalized parity". Thus, we have an ensemble of random cyclic matrices (RCM) which are pseudo-symmetric in the sense of (Eq. 2.43). In general there are two distinct scenario with respect to time-reversal, $\mathcal{T}$ and parity, $\mathcal{P}$: (a) standard case where $\mathcal{T}$ and $\mathcal{P}$ are preserved, this case is trivially $\mathcal{PT}$-symmetric, and, (b) the case of $\mathcal{PT}$-symmetry where $\mathcal{T}$ and $\mathcal{P}$ both are broken. In case (a), one may study the fluctuations properties of energy levels after classifying the eigenfunctions according to definite parity (odd or even); however the case (b) belongs to a different class altogether. Whereas case (a) corresponds to the invariant ensembles of random matrix theory [Mehta 1991], case (b) has not been fully studied, only some partial results exist [Ahmed 2003b, Ahmed 2003a, b. Gong 2012] and RCM belong to this case. To our knowledge, the discrete symmetries for operators represented by cyclic matrices are clearly spelt out here for the first time.

The eigenvalues of $\mathbf{M}$ are given by [Kowaleski 1948]

$$E_l = \sum_{p=1}^{N} a_p \exp \frac{2\pi i}{N}(p-1)(l-1); \tag{2.44}$$

$(l = 1, 2, ..., N)$, the maximum real eigenvalue being $\sum_i a_i$. The diagonalizing matrix is given by

$$U_{jl} = \frac{1}{\sqrt{N}} \exp \frac{2\pi i}{N}(j-1)(l-1). \tag{2.45}$$

We consider a Gaussian ensemble of cyclic matrices with a distribution,

$$P(\mathbf{M}) \sim \exp -A \text{ Tr } (\mathbf{M}^\dagger \mathbf{M}) \tag{2.46}$$

where A sets the scale (of energy, for instance).

For the sake of simplicity, we present the analysis for an ensemble of 3×3 matrices. We would like to obtain the joint probability distribution function (JPDF) of eigenvalues because all the correlations are related to it. To have a feeling how the eigenvalues themselves are distributed in the complex domain, a graph of eigenvalues of 3×3, 100×100 and 101×101 are shown in Fig. 2.1. Also, we would like to show results on the spacing distribution as they

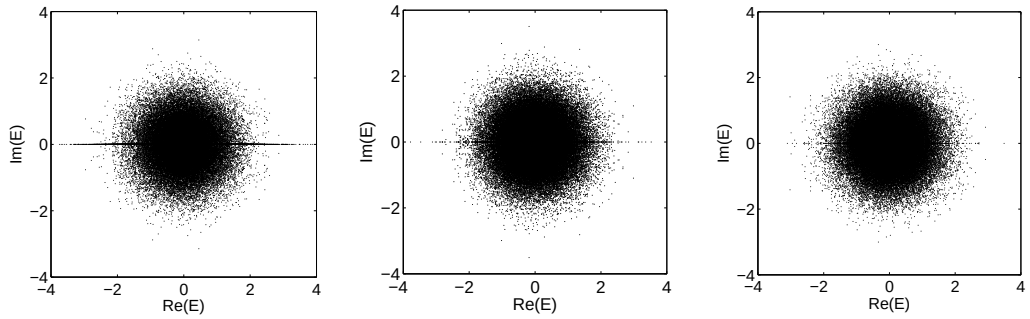

(a) 3×3, sample=25000 (b) 100×100, sample = 750 (c) 101×101, sample = 750

Figure 2.1: Real and imaginary part of eigenvalues of cyclic matrices are plotted against each other. The cyclic matrix elements are chosen from Gaussian with mean 0 and variance 1 and then the total matrix is normalized by $\sqrt{N}$, N being the dimension of the matrix.

enjoy a central place in discussions in quantum chaos, universality arguments, and rule the dominant long-time tail in correlation functions [Jain & Gaspard

1996 unpublished]. We immediately see that $\mathrm{Tr}\mathbf{M}^\dagger\mathbf{M} = 3(a_1^2 + a_2^2 + a_3^2)$. In effect, we have $P(\{a_i\}) = \left(\frac{3A}{\pi}\right)^{\frac{3}{2}} e^{-3A\sum_i a_i^2}$. There are three eigenvalues - one real, $E_1 = \sum_i a_i$ and a complex conjugate pair, (E_2, E_2^*). We may define spacing as $S_{23} := |E_2 - E_3| = \sqrt{3}(a_3 - a_2)$ as well as $S_{12} := |E_1 - E_2| = |\frac{3}{2}(a_2 + a_3) + \frac{i\sqrt{3}}{2}(a_2 - a_3)|$. Obviously, $S_{12} = S_{13}$. The JPDF of eigenvalues $P(\{E_i\})$ can be obtained by calculating the Jacobian and trace utilizing the relation between matrix elements and eigenvalues and is written as

$$P(E_1, E_2, E_2^*) = \left(\frac{A}{\pi}\right)^{\frac{3}{2}} e^{-A(E_1^2 + 2|E_2|^2)}. \tag{2.47}$$

With this JPDF, "spacing" distributions can be found. Spacing distribution for the complex conjugate pair, $P_{cc}(S_{23})$ is given by

$$P_{cc}(S_{23}) \;=\; \int \prod_{i=1}^{3} da_i P(\{a_i\}) \delta(S_{23} - \sqrt{3}|a_3 - a_2|) \sqrt{\frac{2A}{\pi}} e^{-\frac{A}{2}S_{23}^2}. \tag{2.48}$$

Using this, we may define an average spacing, $\overline{S_{23}}$ through the first moment and obtain finally a normalized spacing distribution in terms of the variable $z = S_{23}/\overline{S_{23}}$:

$$p_{cc}(z) = \frac{2}{\pi} e^{-\frac{z^2}{\pi}}. \tag{2.49}$$

Similarly, the spacing distribution, $P_{rc}(S_{12})$ is obtained:

$$P_{rc}(S_{12}) = \frac{4A}{\sqrt{3}} S_{12} e^{-\frac{4}{3}S_{12}^2} I_0\left(\frac{2}{3}AS_{12}^2\right) \tag{2.50}$$

where $I_0(x)(= J_0(ix))$ is 0^{th} order modified Bessel function of first kind. It can also be written as $I_0(x) = \frac{1}{\pi}\int_0^\pi e^{x\cos\theta} d\theta$. Mean spacing turns out to be $\overline{S_{12}} = \frac{3}{8}\sqrt{\frac{\pi}{A}}c$ where $c = \;{}_2F_1\left[\frac{3}{4}, \frac{5}{4}; 1; \frac{1}{4}\right] = 1.31112...$ (a hypergeometric function).

Defining $z = S_{12}/\overline{S_{12}}$,

$$p_{rc}(z) = \frac{3\sqrt{3}\pi}{16} c^2 z \exp\left(-\frac{3\pi}{16} c^2 z^2\right) I_0\left(\frac{3\pi}{32} c^2 z^2\right). \tag{2.51}$$

We can now make following observations : (i) the (semi-)Gaussianity of $p_{cc}(z)$ implies that there is no level repulsion among the complex conjugate pairs, at the same time there is no attraction, there is no tendency of clustering as in Poissonian spacing distribution; (ii) real and complex eigenvalues display linear level repulsion. These results are also borne out by the numerical simulations in Fig. 2.2 and Fig. 2.3.

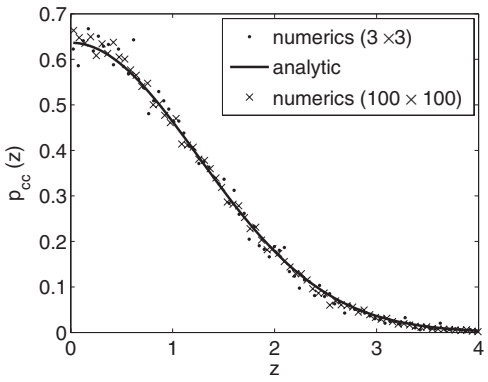

Figure 2.2: Probability distribution of the absolute spacing between the complex conjugate pair of eigenvalues of a Gaussian ensemble of 3×3 cyclic matrices. The numerical result obtained by considering 10000 realizations agrees with the analytic result (2.49). The (semi-)Gaussian spacing distribution may be interpreted to give an accumulation of eigenvalues resulting in a maximum at zero spacing, but no tendency to cluster as the first derivative is zero. This is different from a Poisson distribution.

For the general case of $N \times N$ matrices, we need to invert (2.44). This inversion leads us to the following relation:

$$a_i = \frac{1}{N} \sum_l \mathsf{S}_{il} E_l \tag{2.52}$$

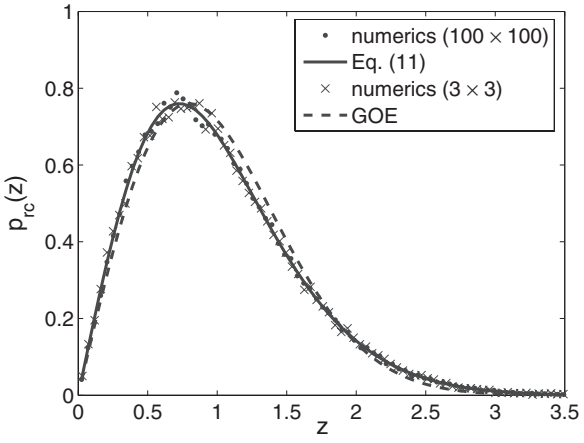

Figure 2.3: Probability distribution of the absolute spacing between a real and a complex eigenvalue of a Gaussian ensemble of 3×3 cyclic matrices. The numerical result obtained by considering 10000 realizations for 3×3 matrices and 1000 realizations of 100×100 matrices agrees with the analytic result (2.51). We observe a linear level repulsion near zero spacing, however the result is distinctly different from the Wigner surmise for GOE.

where $\mathbf{S}_{il} = \omega^{(i-1)(N-(l-1))}$ and $\omega = e^{2\pi i/N}$ is a root of unity. $\mathbf{S}$ is a symmetric matrix and $\mathbf{S}^2 = N\eta$. Employing these relations, we can find $\sum_i a_i^2$, and hence the following result for the JPDF for even N:

$$P(\{E_i\}) = \left(\frac{A}{\pi}\right)^{\frac{N}{2}} \exp\left[-A\left(E_1^2 + E_{\frac{N}{2}+1}^2 + \sum_{i\neq 1,\frac{N}{2}+1}^{N} E_i E_{N+2-i}\right)\right] \quad (2.53)$$

where E_1 and $E_{\frac{N}{2}+1}$ real and the rest of the eigenvalues may be complex. For odd N, the above result will hold except that there will be only one real eigenvalue, E_1 and the summation in the second term will extend over all i except 1. Employing this general result on JPDF, we can now calculate the spacing distributions for the general case. There are three cases : (i) spacing among the complex conjugate pair of eigenvalues is found to be distributed again as a Gaussian; (ii) spacing between a real and a complex eigenvalue is distributed according to (2.51); (iii) two complex eigenvalues, $E_j = x_j + iy_j$ and

$E_k = x_k + iy_k$ are spaced according to

$$p(s) = \frac{\int \prod_i d\Re E_i d\Im E_i P(\{E_i\}) \delta(|E_j - E_k| - s)}{\int \prod_i d\Re E_i d\Im E_i P(\{E_i\})}, \tag{2.54}$$

which reduces to the following integral on change of variables, $\xi(\eta)_\pm = x(y)_k \pm x(y)_j$

$$\begin{aligned} p(s) &= \frac{A}{\pi} \int d\xi_- d\eta_- e^{-A(\xi_-^2 + \eta_-^2)} \delta(\sqrt{\xi_-^2 + \eta_-^2} - s) \\ &= \frac{\pi s}{2} \exp\left(-\frac{\pi s^2}{4}\right) \end{aligned} \tag{2.55}$$

which is exactly the Wigner distribution (Fig. 2.4). Let us recall that Wigner's result holds exactly for 2×2 real symmetric matrices only, it serves as an excellent approximation for $N \times N$ matrices though. We also know that the spacing distribution for a Poissonian random process in a plane is exactly the same mathematical form as Wigner's, discovered by Rayleigh. Thus our result proves that the complex eigenvalues of random cyclic matrices describe such a process. This is a very beautiful, non-intuitive result which brings out yet another characteristic of RCM.

The eigenfunctions of $\mathbf{M}$ corresponding to the real eigenvalues (E_1 and $E_{\frac{N}{2}+1}$) are also simultaneously eigenfunctions of "generalized parity" η. However, the eigenfunctions of $\mathbf{M}$ corresponding to the complex conjugate pair of eigenvalues are not simultaneously eigenfunctions of η. Thus, when these complex eigenvalues occur, "generalized parity" is said to be spontaneously broken. Also, the eigenfunctions corresponding to the complex conjugate pair of eigenvalues have zero $\mathcal{PT}$ - norm. This is expected from the earlier works [Bender 2002, Ahmed 2006] on $\mathcal{PT}$-symmetric quantum mechanics. This observation then fully embeds our findings into the new random matrix theory developed recently for pseudo-Hermitian Hamiltonians. However, we also note that the

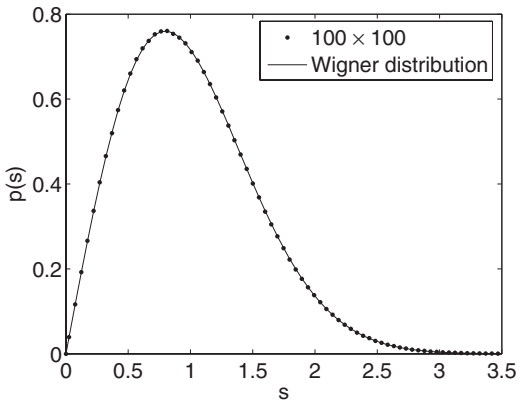

Figure 2.4: We observe a linear level repulsion between two eigenvalues which are neither real nor complex conjugate pairs for an ensemble of 100×100 matrices with 5000 realizations. The agreement with GOE is deceptive; in fact, this suggests that the eigenvalues describe a Poisson process on a plane.

eigenvectors ψ_1 (ψ_2) corresponding to complex conjugate eigenvalues, λ (λ^*) satisfy orthogonality defined with respect to η. Since these results are found for $N \times N$ matrices, we believe that this work extends the random matrix theory in a significant way. The findings on the spacing distributions have led us to a linear level repulsion among distinct complex eigenvalues, whereas the spacing between complex-conjugate pair is Gaussian-distributed.

2.5 Random cyclic block matrices

Extension of random matrix theory for cyclic block matrices (with individual blocks as cyclic matrix) has been a natural step forward. As a matter of notation size of the individual sub-blocks are denoted by m while that of block-considered-as-element-matrix is by n. The size of the complete matrix, hence is given by mn and will be denoted by N.

A cyclic block matrix is denoted by

$$H = \begin{bmatrix} A_1 & A_2 & \dots & A_n \\ A_n & A_1 & \dots & A_{n-1} \\ \vdots & & & \vdots \\ A_2 & A_3 & \dots & A_1 \end{bmatrix}, \text{ with } A_i = \begin{bmatrix} a_1^i & a_2^i & ... & a_m^i \\ a_m^i & a_1^i & ... & a_{m-1}^i \\ \vdots & & & \\ a_2^i & a_3^i & ... & a_1^i \end{bmatrix} \tag{2.56}$$

It is easy to see that cyclic block matrices are normal matrices *i.e.* $HH^\dagger = H^\dagger H$. Hence, these matrices will admit the spectral decomposition using unitary matrices.

These matrices like cyclic matrices are examples of pseudo-Hermitian (symmetric) matrices. The corresponding η operator is given by,

$$\eta = \begin{bmatrix} \sigma & 0 & \dots & 0 \\ 0 & 0 & \dots & \sigma \\ \vdots & & & \vdots \\ 0 & \sigma & \dots & 0 \end{bmatrix}, \text{ with } \sigma = \begin{bmatrix} 1 & 0 & \dots & 0 \\ 0 & 0 & \dots & 1 \\ \vdots & & & \\ 0 & 1 & \dots & 0 \end{bmatrix}. \tag{2.57}$$

It is easy to verify then, $H^\dagger = \eta H \eta^{-1}$.

It is shown in [Friedman 1961] that if ω is the n^{th} root of unity, then eigenvalues of H will be given by the eigenvalues of n, m-dimensional matrices, T_k defined as,

$$T_k = \sum_{j=1}^{n} \omega^{(k-1)(j-1)} A_j, \ (1 \leq k \leq n). \tag{2.58}$$

Now it is straightforward to find the eigenvalues of T_k, let us apply the Fourier matrix, F from left and $F^\dagger$ from right,

$$FT_kF^\dagger = \sum_{j=0}^{n-1} \omega^{kj} F A_j F^\dagger = \sum_{j=0}^{n-1} \omega^{kj} \Lambda_k. \tag{2.59}$$

Hence, the spectral decomposition of a block cyclic matrix A is given by,

$$H = \left(F^{(n)} \otimes F^{(m)}\right) \Lambda \left(F^{(n)} \otimes F^{(m)}\right)^{\dagger} = U \Lambda U^{\dagger} \tag{2.60}$$

where $\otimes$ denotes tensor product[6].As the dimensionality of H is N, there are total N eigenvalues coming from n blocks of m-dimensional matrices. We can level the eigenvalues of H carrying the information about the block and its place in that particular block. This helps in identifying the complex-conjugate pair eigenvalues of H. For N odd, one of the eigenvalue is real and is given by the sum of the first row elements of the matrix H, while rest of the eigenvalues occur as complex conjugate pairs. Let's recall that labeling of eigenvalues in a cyclic matrix is done so that the first eigenvalue is sum of the first row elements while k^{th} eigenvalue is complex conjugate of $(n+2-k)^{th}$ eigenvalue. Here it is always understood that $n+2-k$ is taken as $\bmod n$.

Similarly here, $[(k-1)m+j]^{th}$ eigenvalue will be complex conjugate of $[((n+2-k)-1)m+(m+2-j)]^{th}$ eigenvalue with k taking the values $1, 2, \ldots n$ and j from 1 to m. Again it is understood that $n+2-k$ is taken as $\bmod n$ while $(m+2-j)$ is $\bmod m$.

Let's take an example of a block-cyclic matrix of dimension 3 with a sub-block dimension 2. This captures all the flavours of random matrix theory of these class of matrices. The matrix H is given by

$$H = \begin{bmatrix} A_1 & A_2 & A_3 \\ A_3 & A_1 & A_2 \\ A_2 & A_3 & A_1 \end{bmatrix} \text{ with } A_i = \begin{bmatrix} a_i & b_i \\ b_i & a_i \end{bmatrix} \tag{2.61}$$

Each A_i can be diagonalized by a Fourier matrix of order 2. The eigenvalues of

[6] A tensor product of 2 matrices $A = (a_{ij})$ of size $m \times n$ and $B = (b_{ij})$ of size $p \times q$ will produce a matrix $C = a_{ij}B$ of size $mp \times nq$.

A_is are given by $a_i + b_i$ and $a_i - b_i$. From Eq. 2.58, the matrices can be written as,

$$
\begin{aligned}
T_1 &= A_1 + A_2 + A_3 \\
&= \begin{bmatrix} a_1 + a_2 + a_3 & b_1 + b_2 + b_3 \\ b_1 + b_2 + b_3 & a_1 + a_2 + a_3 \end{bmatrix} \\
T_2 &= A_1 + e^{i\frac{2\pi}{3}} A_2 + e^{-i\frac{2\pi}{3}} A_3 \\
&= \begin{bmatrix} a_1 + a_2 e^{i\frac{2\pi}{3}} + a_3 e^{-i\frac{2\pi}{3}} & b_1 + b_2 e^{i\frac{2\pi}{3}} + b_3 e^{-i\frac{2\pi}{3}} \\ b_1 + b_2 e^{i\frac{2\pi}{3}} + b_3 e^{-i\frac{2\pi}{3}} & a_1 + a_2 e^{i\frac{2\pi}{3}} + a_3 e^{-i\frac{2\pi}{3}} \end{bmatrix} \\
T_3 &= A_1 + e^{-i\frac{2\pi}{3}} A_2 + e^{i\frac{2\pi}{3}} A_3 \\
&= \begin{bmatrix} a_1 + a_2 e^{-i\frac{2\pi}{3}} + a_3 e^{i\frac{2\pi}{3}} & b_1 + b_2 e^{-i\frac{2\pi}{3}} + b_3 e^{i\frac{2\pi}{3}} \\ b_1 + b_2 e^{-i\frac{2\pi}{3}} + b_3 e^{i\frac{2\pi}{3}} & a_1 + a_2 e^{-i\frac{2\pi}{3}} + a_3 e^{i\frac{2\pi}{3}} \end{bmatrix}
\end{aligned}
$$

The eigenvalues of H can be easily listed now as

$$
\begin{aligned}
&E_1 = a_1 + a_2 + a_3 + b_1 + b_2 + b_3,\ E_2 = a_1 + a_2 + a_3 - b_1 - b_2 - b_3 \\
&E_3 = (a_1 + b_1) + (a_2 + b_2)e^{i\frac{2\pi}{3}} + (a_3 + b_3)e^{-i\frac{2\pi}{3}} \\
&E_4 = (a_1 - b_1) + (a_2 - b_2)e^{i\frac{2\pi}{3}} + (a_3 - b_3)e^{-i\frac{2\pi}{3}} \\
&E_5 = (a_1 + b_1) + (a_2 + b_2)e^{-i\frac{2\pi}{3}} + (a_3 + b_3)e^{i\frac{2\pi}{3}} \\
&E_6 = (a_1 - b_1) + (a_2 - b_2)e^{-i\frac{2\pi}{3}} + (a_3 - b_3)e^{i\frac{2\pi}{3}}.
\end{aligned}
\tag{2.62}
$$

From 2.62, it is clear that for $k = 1, j = 1$, $[(k-1)m + j(= 1)]^{th}$ eigenvalue is complex conjugate of $[((n+2-k)-1)m + (m+2-j)(= 1)]^{th}$ eigenvalue. Similarly $k = 1, j = 2$, *i.e.* second eigenvalue is it's own complex conjugate (real). For $k = 2, j = 1$, $[(k-1)m + j(= 3)]^{th}$ is complex conjugate of $[((n+2-k)-1)m + (m+2-j)(= 5)]^{th}$ eigenvalue and similarly the rest. This scheme of labeling works for all orders irrespective of N being even or odd.

It can also be verified easily that $\vec{E} = \sqrt{3}F^{(3)} \otimes \sqrt{2}F^{(2)}\vec{a}$ where $\vec{a}$ is the first row of the composite matrix H and hence inversion is rather easy, $\vec{a} = \frac{1}{\sqrt{6}}F^{(3)\dagger} \otimes F^{(2)\dagger}\vec{E}$

Now let's consider the ensemble of $N = 6$ with $n = 3, m = 2$ cyclic block matrices drawn from a Gaussian distribution,

$$P(H) \sim \exp\left(-A\mathrm{Tr}H^{\dagger}H\right). \tag{2.63}$$

then,

$$P(\{a_i, b_i\}) = \left(\frac{6A}{\pi}\right)^3 e^{-6A\sum_{k=1}^{3}(a_i^2+b_i^2)} \tag{2.64}$$

Using the relation between eigenvalues and a_i, b_i, we can immediately find out that Jacobian of transformation from parameter space to eigenvalue space is given by $(\sqrt{6})^6$, and

$$\sum_{k=1}^{3}(a_i^2 + b_i^2) = \vec{a}^T.\vec{a} = \frac{1}{6}\vec{E}^T.\vec{E} = \frac{1}{6}(E_1^2 + E_2^2 + 2E_3E_5 + 2E_4E_6). \tag{2.65}$$

Hence, the joint probability distribution function of eigenvalues can be written using Eq. 2.64 as,

$$P(E_1, E_2, E_3, E_3^*, E_4, E_4^*) = \left(\frac{A}{\pi}\right)^3 e^{-A(E_1^2+E_2^2+2|E_3|^2+2|E_4|^2)}. \tag{2.66}$$

After deriving the joint probability distribution function, let's try to evaluate the different possible spacing distributions. There can be three types altogether (i) spacing between two real eigenvalues or between two complex conjugate eigenvalues, (ii) spacing between a real eigenvalue and a complex eigenvalue, and (iii) spacing between two complex eigenvalues which are not conjugate to each other. Here, let's remind ourselves that due to complex nature of eigenvalues, ordering between them can not be defined and hence for spacing

the Euclidean distance between two eigenvalues has been used.

It is easy to calculate all the three spacing distribution as has been done in [Jain 2008b]. Let's first consider the spacing distribution between two real or two complex-conjugate pairs. As we know the real eigenvalues are either sum or alternating sum of first row of the matrix, H. These elements are normal distributed random numbers and hence spacing will be basically a linear combination of normal distributed random numbers endowing the distribution as normal. If we see the complex conjugate pairs the difference is simply i times a linear combination of Gaussian distributed random numbers and as we are using the notion of Euclidean distance, the distribution of such spacings again become normal. The other two spacing distribution can be exactly calculated as in [Jain 2008b], and here the results are only stated.

Let's say E_j is the real eigenvalue while E_k is the complex one, then probability distribution of spacings between E_j and E_k, can be defined by,

$$p_{rc}(s) = \int P(\{E_i\})\delta\left(s - |E_j - E_k|\right) d\{E_i\}. \tag{2.67}$$

Integration over different eigenvalues will give 1(as they are properly normalized) and hence we need to integrate only with respect to E_j and E_k. As E_k is complex, let's denote $\mathrm{Re}(E_k) = x_k$ and $\mathrm{Im}(E_k)$=y_k, then the relevant integral is,

$$p_{rc}(s) = \left(\frac{A}{\pi}\right)^{\frac{3}{2}} \int 2dx_j dx_k dy_k e^{-A(x_j^2+2x_k^2+2y_k^2)} \delta\left(s - \sqrt{(x_k - x_j)^2 + y_k^2}\right) \tag{2.68}$$

which results after proper normalization to

$$p_{rc}(z) = \frac{3\sqrt{3}\pi}{16} c^2 z \exp\left(-\frac{3\pi}{16} c^2 z^2\right) I_0\left(\frac{3\pi}{32} c^2 z^2\right). \tag{2.69}$$

where $c = {}_2F_1\left[\frac{3}{4}, \frac{5}{4}; 1; \frac{1}{4}\right] = 1.31112....$ Here, $p_{rc}(z)$ is normalized spacing distribution with mean 1.

The complex eigenvalues which are not conjugate to each other can be shown to behave as poisson process on a plane and hence there spacing distribution is given by,

$$p(s) = \frac{\pi s}{2} \exp\left(-\frac{\pi s^2}{4}\right) \tag{2.70}$$

A numerical comparison with different spacing distributions are shown in Fig. 2.5. The agreement found is good.

These results can immediately be generalized for general n and m. While the JPDF will be given as,

$$P(E_1, E_2, \ldots E_N) = \left(\frac{A}{\pi}\right)^{\frac{N}{2}} e^{-A\sum_{i=1}^{N}|E_i|^2} \tag{2.71}$$

the spacing distribution remain unaffected and are given by Gaussian, 2.69, 2.70 for spacing between two real or complex-conjugate eigenvalues, between real and complex eigenvalues, between two complex (not conjugate) eigenvalues respectively. The indices of complex conjugate eigenvalues can again be calculated as illustrated in previous example. The comparison with numerical spacing distribution with analytical formulas are again excellent as shown in Fig. 2.5.

It is interesting to note that while block cyclic matrices considered here are themselves not cyclic but the joint probability distribution function has similar structure (only with more eigenvalues appearing), more so in terms of spacing distribution they are identical. To my knowledge, this is first instant when asymmetric block structures have been considered and joint probability distribution function, spacing distributions are calculated analytically exactly and in closed form.

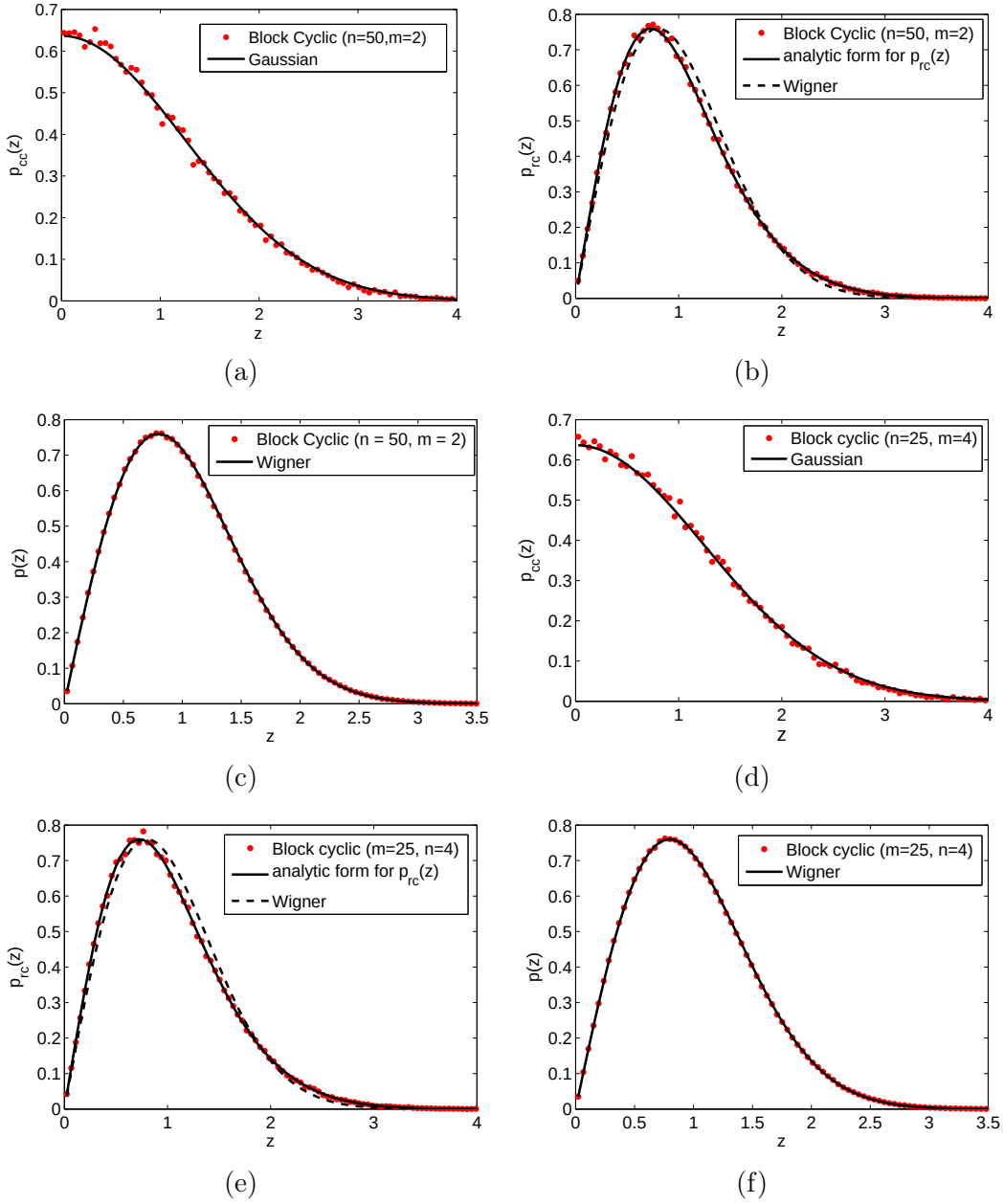

Figure 2.5: Various spacing distributions

Further, we present another special case of random matrices with block entries. Firstly, let us consider

$$\mathbf{B} = \begin{bmatrix} A_1 & A_2 & ... & A_N \\ A_N & A_1 & ... & A_{N-1} \\ \vdots & & & \\ A_2 & A_3 & ... & A_1 \end{bmatrix} \tag{2.72}$$

where each entry A_i is

$$A_i = \begin{bmatrix} a_i & -b_i \\ c_i & a_i \end{bmatrix}. \tag{2.73}$$

A realization of a random matrix is constructed by drawing real elements a_i, b_i, and c_i independently from a Gaussian distribution with zero mean and unit variance. In this way, we will obtain a rather simple random matrix ensemble with real elements. However, seen as scalar entries, the resulting matrix is not a cyclic one. The matrix $\mathbf{B}$ is pseudo-symmetric with respect to the "generalized parity",

$$\Sigma = \begin{bmatrix} \sigma & 0 & ... & 0 \\ 0 & 0 & ... & \sigma \\ \vdots & & & \\ 0 & \sigma & ... & 0 \end{bmatrix} \tag{2.74}$$

where σ happens to be Pauli matrix,

$$\sigma = \begin{bmatrix} 0 & 1 \\ 1 & 0 \end{bmatrix} \tag{2.75}$$

for this example. Consequently, $\mathbf{B}^\dagger = \Sigma \mathbf{B} \Sigma^{-1}$.

However, as we shall see below, the spectral fluctuations are just like the one for the scalar cyclic matrices. For instance, numerical investigations for 50 $\times$ 50 matrix, comprised of fifty 2×2 blocks per row reveal that the spacing distributions among complex conjugate pairs, real-complex pair, complex-complex pair follow Figures 2.6, 2.7, and 2.8 respectively.

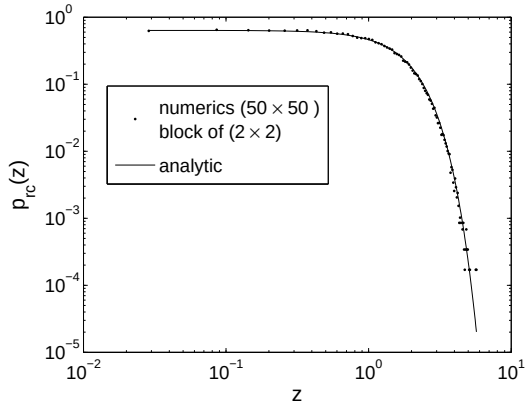

Figure 2.6: Log-log plot of the distribution of spacing among complex-conjugate pairs. The result is exactly in agreement with (12) for scalar entries (Sec. II).

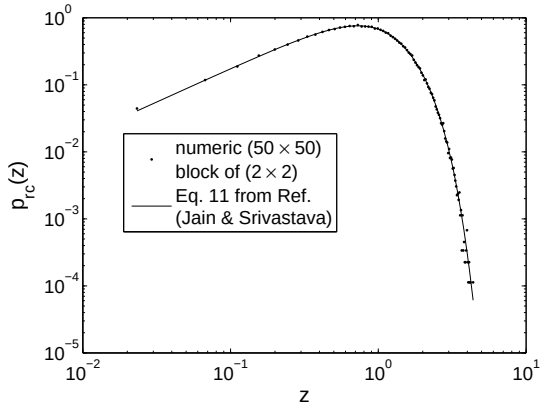

Figure 2.7: Log-log plot of the distribution of spacing among real and complex eigenvalues. The result is exactly in agreement with (13) for scalar entries (Sec. II).

These results are not at all obvious, considering the fact that the resulting matrix with scalar entries is not a cyclic matrix. This example encourages us to explore a possible universal class within the pseudo-orthogonal ensemble of random matrices.

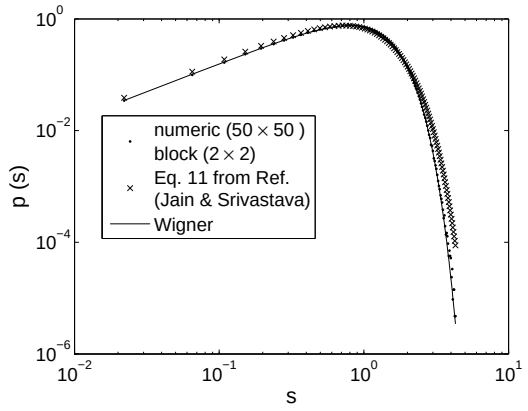

Figure 2.8: Log-log plot of the distribution of spacing among complex eigenvalues. The result is exactly in agreement with (15) for scalar entries (eq. (11) from [Jain 2008b]).

2.6 Summary

We saw how the random matrix theory of Ginibre orthogonal ensemble has been a rich and a very demanding problem, be it the spectral measure or correlation (which we have not focussed here for the general case). Pseudo-Hermitian (symmetric) matrices though non-hermitian (symmetric) have spectral measure and spacing distribution which are very different from those obtained for general asymmetric cases. For order 3 and above, a general form of a pseudo-hermitian (symmetric) matrix has eluded us. Cyclic matrices and cyclic block matrices are very specific examples of such matrices. We have obtained the JPDF and spacing distributions for these matrices in full generality. We also saw that being asymmetric matrices and having very small number of independent elements also make them attractive for the studies. The deviation in JPDF and spacing distribution from general results are studied in detail.

CHAPTER 3

Random reverse cyclic matrices

Contents

3.1 Introduction

In this Chapter, we study random, reverse cyclic matrices, that are real-symmetric,

$$H = \begin{bmatrix} a_1 & a_2 & \dots & a_n \\ a_2 & a_3 & \dots & a_1 \\ \vdots & & \dots & \vdots \\ a_n & a_1 & \dots & \end{bmatrix} \tag{3.1}$$

with matrix elements chosen from an appropriate distribution function. Bose *et al.* [Bose 2002] derived the limiting spectral distribution for reverse-cyclic matrices, but the JPDF and the spacing distribution function remained open problems. In fact it will be interesting to see how the special symmetric matrices having a very small independent matrix elements (only N in this case), differ from the results known for their counterparts having all the matrix elements independent up to restriction due to symmetry[*i.e.* $\frac{N(N+1)}{2}$]. In Chapter

2, we obtained the JPDF for the cyclic matrices, which forms another example in which the number of the matrix elements are constrained (again only N). On the one hand, there is a vast literature about different results for random cyclic matrices in literature (see [Bose 2009], [Meckes 2009] *etc.*). However, the same is not true for random reverse-cyclic matrices. Interestingly, reverse cyclic matrices appear (albeit with the name reverse circulant and retro-circulant) in models for particle masses, flavour mixing, and CP violation. Here families of particles can be shown to emerge by a spontaneous breakdown of discrete $\mathbf{Z}_6$ (group under congruence modulo 6) chiral symmetry, by the Higgs sector [Adler 1998]. The presence of reverse-cyclic matrices is due to S_3 cyclic permutation symmetry of the Lagrangian. Quoting Adler, "...in the limit of S_3 cyclic permutation symmetry, we shall find that the fermion mass matrices in both the three and six doublet models are retrocirculants..." [Adler 1998]. In another instance, while exploring whether discrete flavor symmetry S_3 can explain the pattern of neutrino masses and mixings, reverse-cyclic matrices (again referred to as retro circulant) have been used as a perturbation matrix [Dev 2011]. It was also shown in [Dev 2011] that after third order perturbation, neutrino mixing depends only on perturbation parameter, consistent with experimental data. One may speculate that the background and statistical errors may make these matrices random.

Here, we present the JPDF, spacing distributions and extreme value distribution of eigenvalues for the random reverse-cyclic matrices. In Chapter 4 we present a connection of JPDF and an exactly solvable model that we refer to as screened harmonic potential model.

We collect some known results related to the eigen-decomposition of reverse-cyclic matrices. A known eigen-decomposition becomes a very advantageous tool, to derive the joint probability distribution function for eigenvalues. Karner

et al. [Karner 2003] have shown that the eigen-decomposition for an odd-dimensional ($n = 2k + 1$) reverse cyclic matrix is given by

$$H = F^{\dagger} \begin{bmatrix} 1 & 0 \\ 0 & R \end{bmatrix} \Lambda \begin{bmatrix} 1 & 0 \\ 0 & R^{\dagger} \end{bmatrix} F \tag{3.2}$$

$$\Lambda = (E_1, |E_2|, \ldots, |E_{(n-1)/2}|, -|E_{(n-1)/2}|, \ldots, -|E_2|)$$

$$F_{r,s}(n) = \frac{1}{\sqrt{n}} e^{2\pi i (r-1)(s-1)/n}; \quad r, s = 1, 2, \ldots, n \tag{3.3}$$

$$R := \begin{bmatrix} \Phi^{\dagger} & i\Phi^{\dagger}\hat{I}_k \\ \hat{I}_k\Phi & -i\hat{I}_k\Phi\hat{I}_k \end{bmatrix} \in \mathbb{C}^{2k\times 2k}, \quad k = 1, 2, \ldots \tag{3.4}$$

$$\text{with} \quad \Phi = \frac{1}{\sqrt{2}} \text{diag}\left(e^{i\phi_1/2}, \ldots, e^{i\phi_k/2}\right),$$

$\hat{I}_k$ is an anti-diagonal identity matrix, and $0 \leq \phi_j < 2\pi$ while $\mathbb{C}^{2k\times 2k}$ represents $2k$ dimensional matrices with complex elements. The eigen-decomposition for an even-dimensional reverse cyclic matrix takes following form,

$$H = F^{\dagger} \begin{bmatrix} 1 & 0 \\ 0 & R \end{bmatrix} \Lambda_1 \begin{bmatrix} 1 & 0 \\ 0 & R^{\dagger} \end{bmatrix} F \tag{3.5}$$

$$\Lambda_1 = \text{diag}(E_1, |E_2|, \ldots, |E_{(n-2)/2}|, E_{n/2}, -|E_{(n-2)/2}|, \ldots, -|E_2|)$$

$$\text{with} \quad R := \begin{bmatrix} \Phi^{\dagger} & 0 & i\Phi^{\dagger}\hat{I}_k \\ 0 & 1 & 0 \\ \hat{I}_k\Phi & 0 & -i\hat{I}_k\Phi\hat{I}_k \end{bmatrix} \in \mathbb{C}^{2k+1\times 2k+1} \quad k = 1, 2, \ldots \tag{3.6}$$

where $\mathbb{C}^{2k+1\times 2k+1}$ represents $2k + 1$ dimensional matrices with complex elements. To prove the special form of eigenvalues, let's recall that a reverse cyclic matrix,C_r can be essentially written as product of a permutation matrix, say

P with cyclic matrix, C:

$$\begin{bmatrix} a_1 & a_2 & ... & a_N \\ a_N & a_1 & ... & a_{N-1} \\ \vdots & & & \\ a_2 & a_3 & ... & a_1 \end{bmatrix} = \begin{bmatrix} 1 & 0 & \dots & 0 \\ 0 & 0 & \dots & 1 \\ \vdots & & & \\ 0 & 1 & \dots & 0 \end{bmatrix} \begin{bmatrix} a_1 & a_2 & ... & a_N \\ a_2 & a_3 & ... & a_1 \\ \vdots & & ... & \vdots \\ a_N & a_1 & ... & \end{bmatrix}. \tag{3.7}$$

We observe that $P = F^\dagger \overline{F}$, but P being real, complex conjugation of both side will lead to $P = F^T F$ and P is also symmetric so $P = FF^T$ therefore once more taking complex conjugation of both side will lead to $P = \overline{F}F^\dagger$ where $\overline{F}$ stands for complex conjugate of F and similarly F^T for transpose while $F^\dagger$ for Hermitian conjugate. This, along with the fact that Fourier matrix is symmetric and unitary suffices to show that

$$\begin{aligned} F^\dagger C_r F = F^\dagger P C F = F^\dagger \overline{F} F^\dagger C F = P\Lambda_C, \quad \text{with} \\ \Lambda_C = \text{diag}(E_1, E_2, E_3, \dots, \overline{E_3}, \overline{E_2}). \end{aligned} \tag{3.8}$$

The characteristic determinant for C_r is $|\Lambda \mathbf{I} - C_r|$. Using properties of determinants, it is easy to show that this is equivalent to $|\Lambda \mathbf{I} - F^\dagger C_r F|$ and hence,

$$|\Lambda \mathbf{I} - C_r| = \begin{vmatrix} \lambda - E_1 & 0 & 0 & \dots & 0 & 0 & 0 \\ 0 & \lambda & 0 & \dots & 0 & 0 & -\overline{E_2} \\ 0 & 0 & \lambda & \dots & 0 & -\overline{E_1} & 0 \\ \vdots & & & & & & \\ 0 & 0 & -E_3 & \dots & 0 & \lambda & 0 \\ 0 & -E_2 & 0 & \dots & 0 & 0 & \lambda \end{vmatrix} \tag{3.9}$$

$$= (\lambda - E_1) \prod_{i=2}^{(N+1)/2} (\lambda^2 - |E_i|^2) \quad \text{for odd } N; \tag{3.10}$$

$$|\Lambda \mathbf{I} - C_r| = (\lambda - E_1)(\lambda - E_{n/2+1}) \prod_{i=2}^{N/2} (\lambda^2 - |E_i|^2) \quad \text{for even } N. \tag{3.11}$$

This proves the special form of eigenvalues of reverse cyclic matrices [Aitken 1962]. All the eigenvalues of reverse cyclic matrices are real and modulus sign | | is used to take absolute value. Let's note in passing that eigenvectors in case of reverse cyclic matrices display a little more freedom by having some phases Φ in contrast to random cyclic matrices which had same set of eigenvectors namely the discrete Fourier basis for the whole class.

3.2 JPDF, spacing distribution

Consider an ensemble of reverse cyclic (RC) matrices, drawn from a Gaussian distribution,

$$P(H) \sim \exp\left(-A\mathrm{Tr}(H^\dagger H)\right). \tag{3.12}$$

Let us start with the simplest case, namely an ensemble of 3×3 reverse cyclic matrices,

$$H = \begin{bmatrix} a & b & c \\ b & c & a \\ c & a & b \end{bmatrix}. \tag{3.13}$$

The JPDF in matrix space will be given by, using (3.12),

$$P(a, b, c) = \left(\frac{3A}{\pi}\right)^{(3/2)} \exp[-3A\left(a^2 + b^2 + c^2\right)]. \tag{3.14}$$

From Eq. (3.2), we can diagonalize H and it is also clear that there are only $(n+1)/2$ independent eigenvalues for odd-dimensional matrices. For the 3×3

case, the explicit form of R is

$$R = \begin{bmatrix} 1 & 0 & 0 \\ 0 & \frac{1}{\sqrt{2}}\exp(-i\theta/2) & \frac{i}{\sqrt{2}}\exp(-i\theta/2) \\ 0 & \frac{1}{\sqrt{2}}\exp(i\theta/2) & -\frac{i}{\sqrt{2}}\exp(i\theta/2) \end{bmatrix}. \tag{3.15}$$

It takes some simple algebra then to show that

$$\begin{aligned} a &= \frac{1}{3}(E_1 + 2|E_2|\cos\theta), \\ b &= \frac{1}{3}\left(E_1 - |E_2|\left(\cos\theta + \sqrt{3}\sin\theta\right)\right), \\ c &= \frac{1}{3}\left(E_1 - |E_2|\left(\cos\theta - \sqrt{3}\sin\theta\right)\right). \end{aligned} \tag{3.16}$$

Using (3.16) in (3.14), we can find the JPDF for eigenvalues and an independent parameter θ coming from the eigenvector. Note that in H, the independent parameters are three in number, namely a, b and c; while in the eigen-decomposition, we have E_1, E_2, θ. The Jacobian for the transformation (3.16) is given by $\frac{2|E_2|}{3\sqrt{3}}$. The JPDF for eigenvalues is

$$\begin{aligned} &P(E_1, |E_2|, \theta) = \frac{2|E_2|}{3\sqrt{3}}\left(\frac{3A}{\pi}\right)^{(3/2)} \exp[-A\left(E_1^2 + 2E_2^2\right)] \\ &\text{where } E_1 \in (-\infty, \infty), |E_2| \in [0, \infty), \theta \in [0, 2\pi). \end{aligned} \tag{3.17}$$

The Eq. 3.17 can also be written as to reflect the relation of E_2 and E_3 being negative of each other and allowing the domain of integration now to go over $-\infty$ to ∞ (this can also be argued that the domain of $|E_2|$ is $[0, \infty)$, and that the function on the right hand side is an even function of E_2, so we can change the domain) as follows,

$$P(E_1, E_2, E_3) = 2\pi\frac{|E_2|}{3\sqrt{3}}\left(\frac{3A}{\pi}\right)^{(3/2)} e^{-A\left(E_1^2+E_2^2+E_3^2\right)}\delta(E_2 + E_3). \tag{3.18}$$

The θ variation has been taken as uniform as any dependence on θ will be seen in the Jacobian which comes out to be independent of it. Thus θ integration has been done in the JPDF causing the presence of factor 2π.

The density of E_1 (called as the trivial eigenvalue and given by $\mathrm{Tr}H$) comes out to be Gaussian as expected because of E_1 is a sum of Gaussians. On the other hand, the density of non-trivial eigenvalue E_2 is given by (3.19).

$$\rho(E) = 2A|E| \exp(-2AE^2) \tag{3.19}$$

Also, due to product structure of the JPDF, the density of non-trivial eigen-

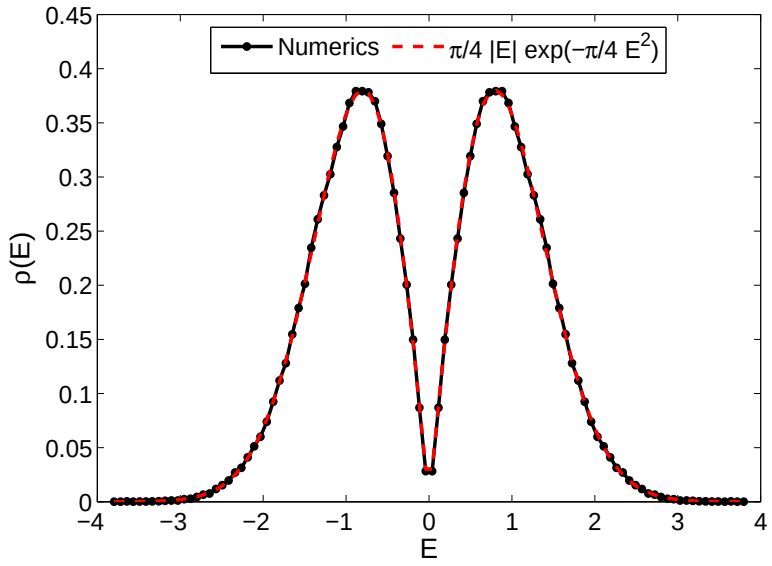

Figure 3.1: Normalized density of non-trivial eigenvalues for an ensemble of 20000 reverse cyclic matrices of size 15×15 is compared with the analytical form. The density is normalized such that averaged density for positive eigenvalues is $1/2$.

value will remain the same for higher-dimensional matrices. The presence of $|E|$ ensures that there are no non-trivial eigenvalues present at origin while they increase linearly along both the positive and negative real axis. It is as if there is a hole in the density of non-trivial eigenvalues (see Fig. 3.1). This has been

independently derived by Bose *et al.* [Bose 2002] without obtaining the JPDF. Also notice that, it is the limiting distribution in the case of [Bose 2002] while here it is an exact result for any dimension (matrix). The spacing distribution between E_1, E_2 can now be calculated as

$$\begin{aligned} P(s_{12}) &= \int_{-\infty}^{\infty} dE_1 \int_{-\infty}^{\infty} dE_2 P(E_1, E_2)\delta(s_{12} - |E_1 - E_2|) \\ &= \frac{12\sqrt{A}e^{-As_{12}^2}}{9\sqrt{\pi}} + \frac{4Ae^{-2A\frac{s_{12}^2}{3}}\sqrt{3\pi}s_{12}\mathrm{erf}\left(\sqrt{\frac{A}{3}}s_{12}\right)}{9\sqrt{\pi}} \end{aligned} \tag{3.20}$$

where $\mathrm{erf}(x)(= \frac{2}{\sqrt{\pi}}\int_0^x e^{-t^2}dt)$ is error function. The value of A can be chosen so that $\int_0^\infty s_{12}P(s_{12})ds_{12} = 1$. A numerical histogram is compared with (3.20) in Fig. 3.2. One could think of spacing between the second and third eigenvalue of H, but due to their special form as $|E_2|$ and $-|E_2|$, it is simply given by $s_{23} = 2|E_2|$, so the spacing distribution as expected is very similar to the density of $|E_2|$ and is given by (3.21):

$$P(s_{23}) = As_{23}e^{-\frac{A}{2}s_{23}^2}. \tag{3.21}$$

Again, the value of A is chosen such that $\int_0^\infty s_{23}P(s_{23})ds_{23} = 1$, which turns out to be $\pi/2$. A comparison with the numerical data is shown in Fig. 3.3.

In the case of 5×5, a similar procedure will give the JPDF as in (3.22) with $E_i \in (-\infty, \infty)$ and $\theta_i \in [0, 2\pi)$:

$$P(E_1, E_2, E_3, E_4, E_5, \theta_1, \theta_2) = \frac{|E_2||E_3|}{25\sqrt{5}}\left(\frac{5A}{\pi}\right)^{5/2} e^{-A\sum_{i=1}^5 E_i^2}\delta(E_2+E_5)\delta(E_3+E_4). \tag{3.22}$$

The density of E_is and the spacing distribution[1] for the cases appearing in 3×3 reverse cyclic matrices remain the same. There is an additional spacing

[1]The spacing distribution defined here is not nearest neighbour spacing distribution, rather distribution of all possible spacings between two concerned eigenvalues.

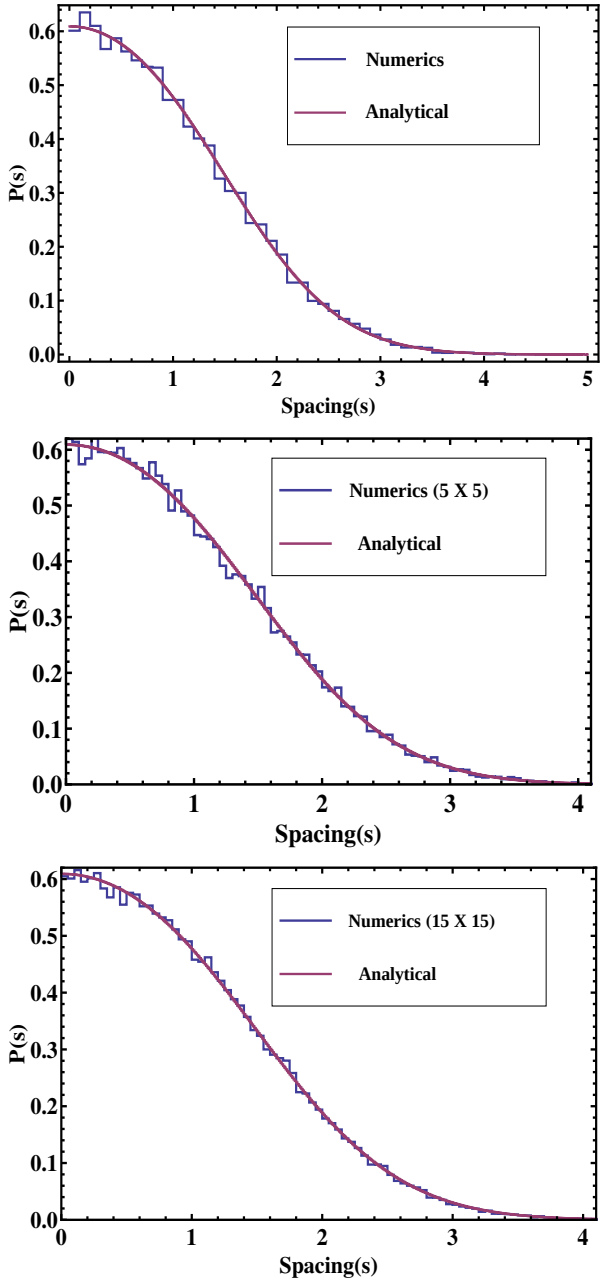

Figure 3.2: Spacing distribution s_{12} for an ensemble of 20000 reverse cyclic matrices of size 3×3, 5×5 and 15×15 is compared with the analytical form (Eq. 3.20).

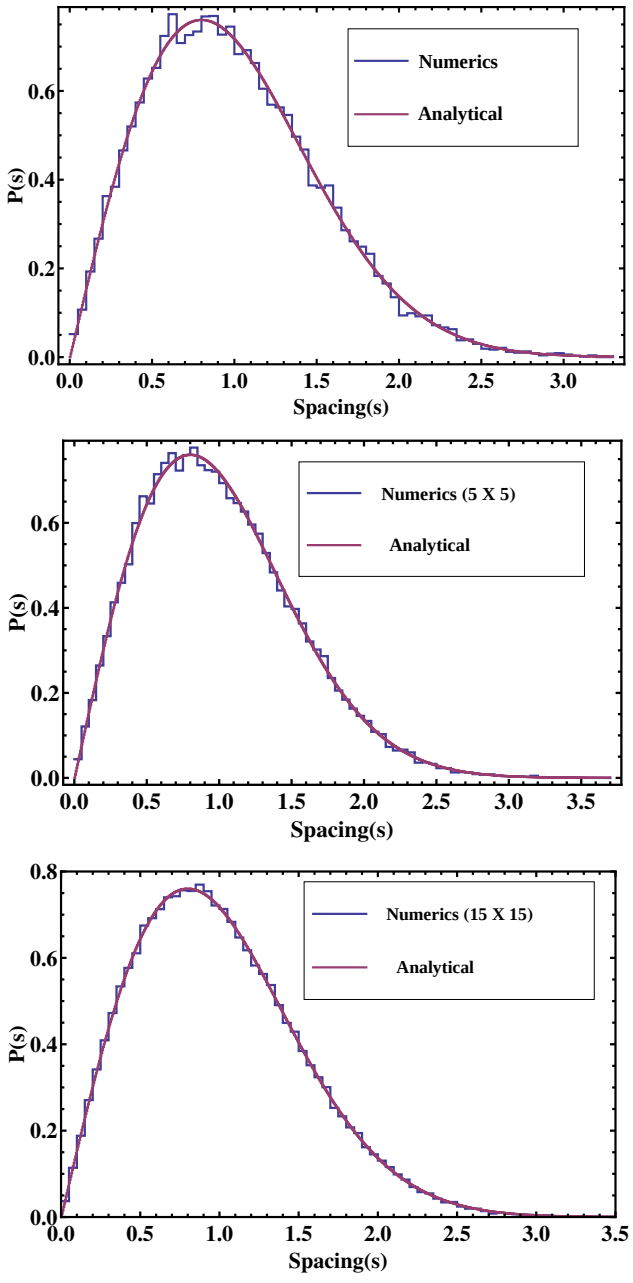

Figure 3.3: Spacing distribution s_{23} for an ensemble of 20000 reverse cyclic matrices of size 3×3, 5×5 and 15×15 is compared with the analytical form (Eq. 3.21).

possible, namely between two positive eigenvalues $|E_2|$ and $|E_3|$. Let us denote this by s_{pp}. Its distribution is

$$\begin{aligned} P(s_{pp}) &= \int_{-\infty}^{\infty} dE_1 \int_0^{\infty} dE_2 \int_0^{\infty} dE_3 4P(E_1, E_2, E_3)\delta(s_{pp} - |E_2 - E_3|) \\ &= As_{pp}e^{-2As_{pp}^2} - \frac{1}{2}\sqrt{\pi A}e^{-As_{pp}^2}(-1 + 2As_{pp}^2)\text{erfc}(\sqrt{A}s_{pp}) \end{aligned} \tag{3.23}$$

where $\text{erfc}(x)(= 1 - \text{erf}(x))$ is complementary error function. The area under this distribution is $1/2$. Taking care of the domains of $|E_2|$ and $|E_3|$, and accounting for the spacing between these and between $-|E_2|$ and $-|E_3|$, we obtain the correctly normalized distribution. This can be seen to be in agreement with the numerical data (see Fig. 3.4). This same distribution (Eq. 3.23) has been compared with the distribution of spacings among all positive eigenvalues except the Gaussian distributed one of an ensemble of higher-dimensional reverse-cyclic matrices (*e.g.* 15×15). The agreement is good. For the $(n = 2k + 1)$-dimensional reverse-cyclic matrix JPDF is a straightforward generalization of (3.22) and is given by (3.24):

$$P(E_1, E_2, \ldots, E_{k+1}, \theta_1, \ldots, \theta_{2k}) = \left(\frac{A}{\pi}\right)^{(2k+1)/2} |E_2| \ldots |E_{k+1}| e^{-A(E_1^2 + 2\sum_{i=2}^{k+1} E_i^2)}. \tag{3.24}$$

This generalization of JPDF can be understood as follows. Clearly, the nature of the first (trivial) eigenvalue is very different from the others (nontrivial), and its distribution will be Gaussian. We focus on the rest of the eigenvalues. With $O = F^{\dagger}R$ an orthogonal matrix [Karner 2003], the diagonalizing equation, $H = O\Lambda O^T$ has the correct number of independent parameters. For a $(2k + 1)$-dimensional matrix H, the left hand side has only $(2k + 1)$ independent variables while the right hand side has $(k + 1)$ independent eigenvalues with k angle variables in O. As dH will contain $(2k + 1)$ independent differentials,

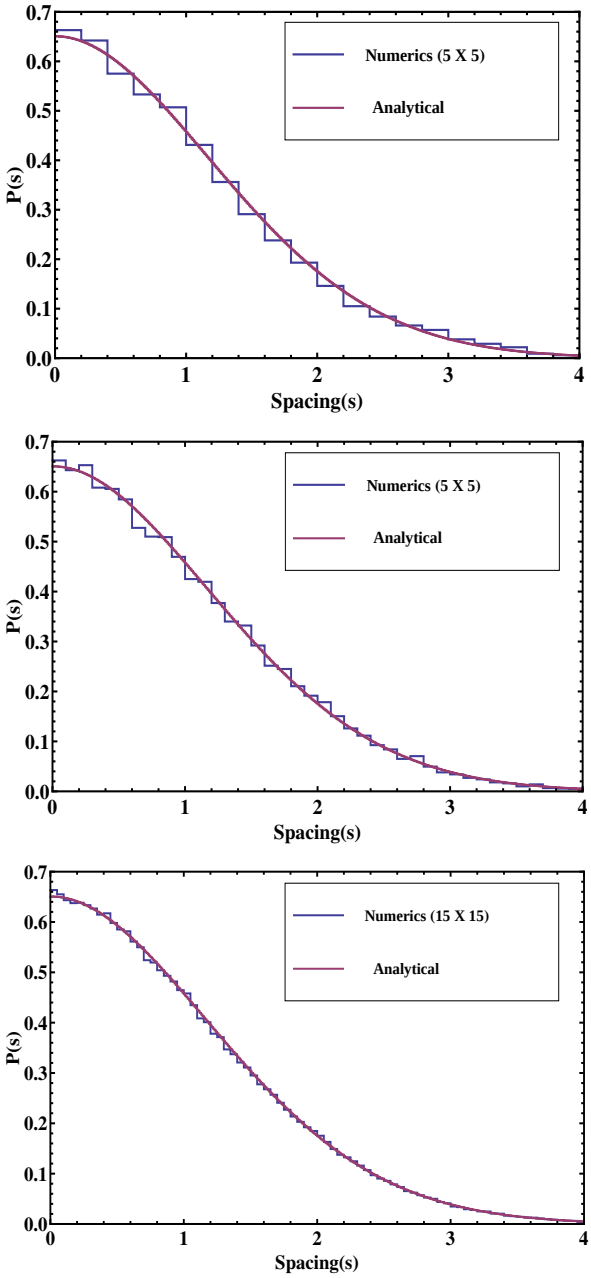

Figure 3.4: Spacing distribution s_{pp} for an ensemble of 5000 and 20000 reverse cyclic matrices of size 5×5 (in top and middle) and 20000 reverse cyclic matrices of size 15×15 (in bottom) is compared with the analytical form (Eq. 3.23). This figure also shows that analytical results matches very well even with ensemble of 5000 matrices.

a multiplication of H with a scalar a will satisfy $d(aH) = a^{2k+1}dH$. Now, $(k+1)$ of them will be absorbed in the scaling of measure $d\Lambda$ (as independent eigenvalues are $(k+1)$). Hence, from the scaling property of $d(aH)$, dH will be a homogeneous polynomial of degree k [Forrester 2010]. Our prototype examples for $n = 3$ and 5 has shown that they vanish linearly as eigenvalues approach the origin, hence the polynomial in the eigenvalues is necessarily proportional to $|E_2| \ldots |E_{k+1}|$. The even case is not very different from the odd one, except that $E_{k/2+1}$ appears along with E_1, the rest being the same as that in (3.24).

The linear level repulsion obtained here has its origin in the product of the absolute value of the eigenvalues in the JPDF. This is reflected in the interaction among eigenvalues if we write the JPDF as a partition function for an n-particle system. This interaction, in the context of random matrices is the Coulomb interaction in two dimensions. In contrast, the case of random-cyclic matrices [Jain 2008b] has a JPDF which is just the exponential containing a sum of the square of the modulus of the complex eigenvalues. The eigenvalues are in a plane, and the level repulsion comes out as a Rayleigh distribution for the Poisson process on a plane, which has the same functional form as Wigner's spacing distribution for the orthogonal ensemble. Thus, we have a very interesting situation for the random reverse-cyclic and random cyclic matrices in that we obtain the same formula for the spacing distribution but the origin is different.

3.3 Distribution of extreme eigenvalues

The eigenvalues of a cyclic matrix is given by [Kowaleski 1948]

$$E_l = \sum_{p=1}^{N} a_p \exp \frac{2\pi i}{N}(p-1)(l-1); \tag{3.25}$$

where $l = 1, \ldots, N$ these eigenvalues can equivalently be thought of being the discrete Fourier transform of first row of the matrix. As a_ps are random numbers, E_l in Eq. 3.25 can be interpreted as position of l^{th} Random walker after N steps in a 2-dimensional space where different directions possible for walker to jump along is given by roots of unity and length of the jump in that particular direction is given by a_p. The modulus of E_l will then give the distance travelled by l^{th} Random walker from origin after N-steps (see Fig. 3.5). It is clear that in a given realization each walker can be characterized by the combination of the directions chosen and not the length of step which is same for each Random walker. Hence it would be interesting to ask which walker travels maximum distance after N-step or how the records of distance travelled by Random walkers behave? Hence distance travelled by different Random walkers can be taken as time series.

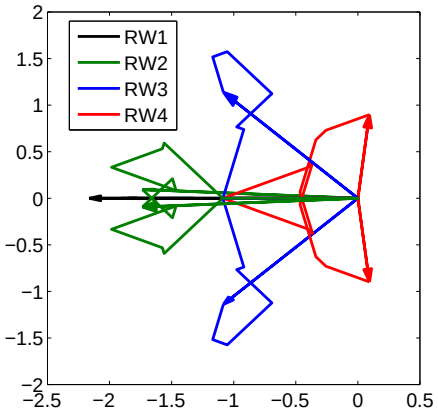

Figure 3.5: For $N = 7$ cyclic matrix, eigenvalues are given by Eq. 3.25 and here they are graphically shown as random walk being done by different Random walkers. The final position of Random walker is shown by an arrow. The length of the arrow represents the net distance travelled from origin and also the positive eigenvalues of reverse cyclic matrices. It is clear that 3 eigenvalues are complex conjugate of each other and hence they are labelled with same Random walker as they travel same net distance from origin (also shown in same colour).

As we have shown that (positive) eigenvalues of reverse cyclic matrices are precisely the same (modulus of E_l). Hence, $|E_l|$ can be taken as time-series *i.e.* $(|E_1|, |E_2|, \ldots, |E_{(N+1)/2}|)$ (for odd dimensional matrices)[2] with index i signifying the eigenvalue corresponding to i^{th} discrete Fourier basis and record statistics for such time series can be studied. The maximum of this time-series will also give the maximum eigenvalue of reverse-cyclic matrix. As reverse cyclic matrix is a symmetric matrix, one would expect that edge distribution of eigenvalues may be given by Tracy-Widom. However, we have seen that bulk spectrum measures (JPDF, spacing distributions) for this class of matrices are different despite these being symmetric. The reason may be attributed to the specific pattern of matrix element which restricts the independent number of parameters to only N in contrast to $N(N+1)/2$. Indeed, it has been shown in [Bose 2011] that the largest eigenvalue for these class of matrices are distributed in accordance with Gumbel distribution. Here, we are presenting record statistics of non-trivial eigenvalues of RRCM. With this, it has been shown that not only the largest eigenvalue but any record once properly shifted and re-scaled follows Gumbel distribution. We have also shown that the smallest positive non-trivial eigenvalue is distributed as an exponential which is equivalent in our Random walker description to say that least distance travelled by a Random walker is exponentially distributed. Let's remind ourselves that if we associate the Euclidean distance with the eigenvalues of cyclic matrices and ask the question about statistics of farthest eigenvalue from origin in complex plane, the result turns out to be same as that of distribution of largest eigenvalue of reverse cyclic matrices. As the record statistics has been dealt in detail in Chapter 5, let's just briefly recall here that sequence of upper records for a sequence which can be ordered are defined by $R_t = \max(x_t, R_{t-1})$ for all

[2] the index is restricted to $(N+1)/2$ as rest of the eigenvalues will be complex conjugate of eigenvalues E_2 to $E_{(N+1)/2}$

index (time) $t \geq 2$ with $R_1 = x_1$. Let $P(x_1, \ldots, x_N)$ be the JPDF of N random variables. The probability that the record at time t, R_t, is less than R is given by

$$Q(R,t) = \int_0^R dx_1 ... dx_t P_t(x_1, ...x_t) \tag{3.26}$$

where $P_t(x_1, \ldots, x_t) = \int P(x_1, \ldots, x_N) dx_{t+1} ... dx_N$ is the marginal JPDF of the first t random variables. It follows that the probability density for the record variable to be R, at time t, $P(R,t)$ is given by $P(R,t) = dQ(R,t)/dR$.

The JPDF of non-trivial eigenvalues of reverse random cyclic matrices have product structure, given by Eq. 3.24. As we have earlier shown that each non-trivial eigenvalue of RRCM comes as $\pm$ pair, hence it is sufficient to look far the positive non-trivial eigenvalues. The $Q(R,t)$ for these eigenvalues are

$$\begin{aligned} Q(R,t) &= \prod_{i=1}^{t} \int_0^R dE_i 2E_i e^{-E_i^2} \\ &= \left(1 - e^{-R^2}\right)^t \end{aligned} \tag{3.27}$$

For large t, asymptotically, Eq. 3.27 can be written as $\sim \exp(-\exp(-x))$ (Gumbel), with $x = R^2 - \log t = (R + \sqrt{\log t})(R - \sqrt{\log t}) \approx 2\sqrt{\log t}(R - \sqrt{\log t})$. It is clear that last record is also the maximum eigenvalue of the sequence, and hence the maximum eigenvalue (among non-trivial eigenvalues) are distributed as Gumbel distribution with shift as $\sqrt{\log t}$ and scaling $2\sqrt{\log t}$ (see Fig. 3.6a). To calculate the record statistics the procedure followed is outlined in following steps here, (i) take the first row of random reverse cyclic matrix (ii) obtain the complex eigenvalues (of corresponding random cyclic matrices) using Eq. 3.25 (iii) as has been shown the nontrivial positive eigenvalues are modulus of first $(N-1)/2$ eigenvalues of corresponding cyclic matrix with order of eigenvalues maintained (iv) these are the time-series to do the record statistics. As the minimum of non-trivial eigenvalue is simply negative of the maximum in case

of RRCM, hence the question of minimum eigenvalues is answered. In case of cyclic matrices, what is the distribution of closest eigenvalue (again distance is in Euclidean sense) or the minimum distance travelled by the walker translates into the minimum positive eigenvalue statistics of RRCM. This again can be answered easily in terms of record distribution only now we need to consider the lower records. In this case $Q(R,t)$ for lower records of non-trivial positive eigenvalues of RRCM is given by,

$$\begin{aligned} Q(R,t) &= \prod_{i=1}^{t} \int_{R}^{\infty} dE_i 2E_i e^{-E_i^2} \\ &= e^{-tR^2}. \end{aligned} \tag{3.28}$$

Again $t = N$ will give the result for minimum (positive) eigenvalue, which is $Q = \exp(-x^2)$ where $x = \sqrt{t}R$ with shift as 0 and scale factor as $\sqrt{t}$ (see Fig. 3.6b).

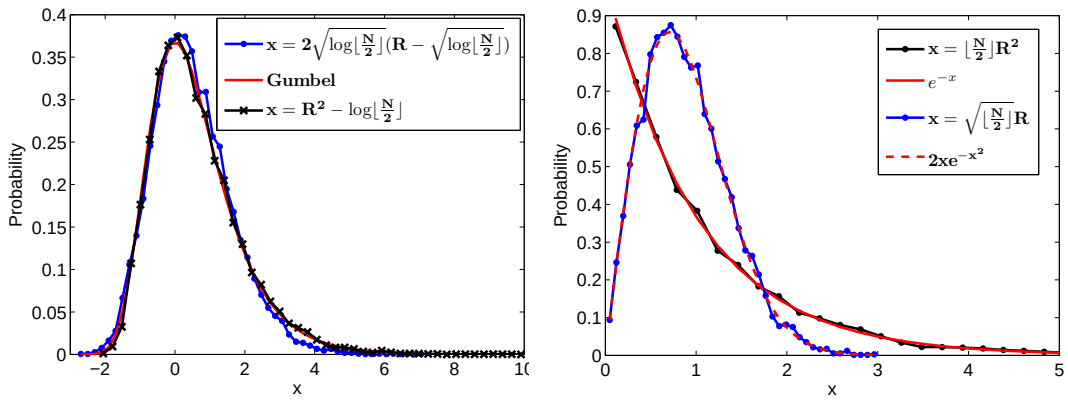

(a) (b)

Figure 3.6: The probability distribution of last upper (lower) record *i.e.* maximum (minimum) is shown, matching with Gumbel (Wigner type) distribution in properly shifted and scaled variables are found good. In each graph we have also compared with a nonlinear transform which in case of maximum seems to be better approximation. N is 101.

3.4 Screened harmonic oscillator and Reverse cyclic matrices

Connections between random matrix theory and exactly solvable models are very important and interesting [Sutherland 1971, Sutherland 2005, Jain 2006, Jain 1999, Auberson 2001]. It is well-known that the invariant random matrix ensembles are related to some exactly solvable many-body problems in one dimension, as was found by Calogero and Sutherland [Calogero 1969, Sutherland 1972, Moser 1975]. In particular, the joint probability distribution function (JPDF) of the eigenvalues of random matrices shares the functional form with the probability density corresponding to the ground state of the quantum N-body problem. This observation is important as it allows one to obtain the correlation functions of one problem by knowing those for the other, comparing terms using a dictionary. In the same vein, even for the explanation of intermediate statistics [Grémaud 1998], a random matrix model was found [Bogomolny 2001] which, in turn, was related to an N-particle system with an inverse-square, repulsive two-body interaction, and, an inverse-square, attractive three-body interaction [Jain 1999, Auberson 2001]. Even for pseudo-Hermitian Hamiltonians (where there exists a metric η such that $H^\dagger = \eta H \eta^{-1}$), a random matrix theory can be built [Ahmed 2003b, Ahmed 2003a]. The connection of this with exactly solvable models is explored in [Jain 2006]. In turn, the models found in [Calogero 1969, Sutherland 1972, Moser 1975] and [Jain 1999, Auberson 2001] can be mapped to integrable [Rey 1997] and chaotic systems [Jain 2002] for which, quite remarkably, analytically exact eigenfunctions are obtained.

Now we show the exactly solvable n-body problem, the ground-state wave function of which is such that the probability density has the same mathematical form as (3.24). It can be verified that (3.24) corresponds to $|\Psi(x_1, x_2, ..., x_n)|^2$

where $\Psi(x_1, x_2, ..., x_n)$ is the ground state wave function with eigenvalue $(4n-3)A$ of the n-body problem with the Hamiltonian:

$$\mathcal{H}(x_1, x_2, ..., x_n) = -\nabla^2 + \left[A^2 x_1^2 + \sum_{i=2}^{n}\left(4A^2 x_i^2 - \frac{1}{4x_i^2}\right)\right]. \tag{3.29}$$

To illustrate that this is so, let us verify for $n = 2$. This will also be sufficient for general n due to the identical form of separable $\mathcal{H}$. As we need to take double derivatives of the wave function, it will be prudent to replace $|E_i|$s by $\sqrt{E_i^2}$. Hence, $\Psi(x_1, x_2) = c\sqrt{\sqrt{x_2^2}}\exp\left(-A/2\left(x_1^2 + 2x_2^2\right)\right)$, the JPDF for a corresponding three-dimensional reverse-cyclic matrix,

$$\frac{\partial^2}{\partial x_1^2}\Psi(x_1, x_2) = A\left(-1 + Ax_1^2\right)\Psi(x_1, x_2)$$
$$\frac{\partial^2}{\partial x_2^2}\Psi(x_1, x_2) = \frac{\left(-1 + 16Ax_2^2\left(-1 + Ax_2^2\right)\right)}{4}\Psi(x_1, x_2)$$
$$\left(-\frac{\partial^2}{\partial x_1^2} - \frac{\partial^2}{\partial x_2^2} + A^2x_1^2 + 4A^2x_2^2 - 1/(4x_2^2)\right)\Psi(x_1, x_2) = 5A\Psi(x_1, x_2).$$

This proves our assertion.

This system has been the subject of a lot of work, initiated by Perelomov [Perelomov 1971]. The only potential that can be added to a harmonic interaction is $2a/x^2$ if we want to successfully construct the creation and annihilation operators for the above model [Hoppe 1992]. For Hamiltonian,

$$H = \frac{1}{2}\left(-\partial_x^2 + x^2 + \frac{2\alpha}{x^2}\right),\ \alpha > 0,\ 0 < x < \infty \quad H\psi = E\psi \text{ with } \psi(0) = 0 \tag{3.30}$$

admits the solution

$$\psi_p(x) = \sqrt{2}\sqrt{\frac{p!}{\Gamma(p+\varepsilon+1/2)}}x^{\varepsilon}L_p^{\varepsilon-1/2}(x^2)e^{-x^2/2}$$
$$E_p = 2p+\varepsilon+1/2, \quad \varepsilon = \frac{1}{2}+\sqrt{\frac{1}{4}+2\alpha}.$$

$L_p^{\varepsilon-1/2}$ is the Laguerre polynomial. Here $\psi_p(x)$ is p^{th} excited state of single particle Hamiltonian given in Eq. 3.30.

This work relates this well-known model to a random matrix theory for reverse-cyclic matrices, which constitutes a remarkable addition to the known connections along similar lines.

3.5 Summary

In summary, we have shown that reverse-cyclic matrices though a subset of symmetric matrices have an unusual density and spacing distribution. In contrast to semi-circle density, this ensemble admits a density with a hole at the origin. Again, the spacing distribution has a variety ranging from Gaussian-looking distributions to Wigner type distributions. We have obtained the record statistics of eigenvalues and shown that the upper records, when properly shifted and scaled, follow Gumbel distribution while lower records follow Wigner-type distribution. As the last upper record is also largest eigenvalue of the sequence, we have re-derived the largest eigenvalue distribution to be Gumbel. Similarly the last lower record is the smallest eigenvalue of the given sequence of positive non-trivial eigenvalues, we have shown that they, when properly shifted and scaled, follow a Wigner-type distribution. The records of eigenvalues are interpreted is terms of records of net distance travelled by different Random walkers after N-steps from origin in two-dimension. The jumps in this two-dimensional

space is restricted along the directions given by roots of unity. We also observed that the JPDF is just the square of the modulus of the ground-state eigenfunction of an exactly solvable many-body Hamiltonian in one dimension, of a screened harmonic oscillator potential. Hence the correlations between the different particles in the potential will be the same as that derived from the joint probability distribution function for the random matrix theory.

Chapter 4

Random cyclic matrices and random walks

Contents

4.1 Introduction

The theory of random walks is at the heart of statistical mechanics. It has been employed in a wide range of phenomena across various disciplines of science. Beginning from its connection with Brownian movement [Einstein 1956], it has been applied to understand polymer physics [de Gennes 1979], locomotion of micro-organisms [Berg 1993, Berg 2003] etc. The subject of random walks has also been the basis of understanding in a simple manner many fundamental ideas like universality in the language of renormalization group [Raposo 1991]. One of the paradigms for non-equilibrium physics is the asymmetric exclusion process (ASEP) [Spohn 1991, Mallick 2009]. Related to it, we consider biased random walks on a one-dimensional lattice with periodic boundary conditions. We first show the connection of this problem with the spectral properties of cyclic matrices [Jain 2008b], this is a simple extension of an earlier work [Franceschetti 1993]. Then, we treat the problem of random walk on a

disordered medium where the randomness is modelled via the randomness of the asymmetric cyclic matrix. The connection of master equation for exclusion processes is known to present a difficult mathematical problem as the Hamiltonian turns out to be non-Hermitian. Thus, with the exact results on spectral properties of an ensemble of asymmetric cyclic matrices, it is natural for us to demonstrate their application in the relevant case of random walks. For this case, we also find the entropy of the system in its nonequilibrium steady state. Recently, there has been a lot of interest in understanding these states and their connection with microscopic chaos [Dorfman 1999]. The well-known connection of random walks and diffusion suggests application of random matrices to nonequilibrium statistical mechanics in a more general manner.

4.2 Biased random walks on a regular lattice

Let us consider a random walk on a one-dimensional lattice of N equally spaced sites with periodic boundary conditions. Let us assume that the particle jumps with probability w. Let the jump probability to the left or right neighbour be pw and $qw(=(1-p)w)$ respectively. The case of w=1 is well known [Feller 1968]. The other special case of $p = q$, $w \neq 1$ has been studied as an eigenvalue problem [Franceschetti 1993]. Moreover, let us consider an ensemble of lattices, $N_{ens} = \sum_{i=1}^{N} N_i$ where N_i denotes the number of lattices (realizations) with a particle occupying the i^{th} site. This allows us to define the probability of occupation of the site, i by

$$p_i = N_i/N_{ens}. \tag{4.1}$$

At time t, a state of an ensemble can be written as a vector

$$\vec{p}(t) = \Big[p_1(t), ..., p_N(t)\Big]^T, \tag{4.2}$$

where T stands for transpose. The time evolution of the ensemble is given by

$$\vec{p}(t+1) = \mathbf{M}\vec{p}(t) \tag{4.3}$$

where

$$\mathbf{M} = \begin{bmatrix} (1-w) & pw & 0 & ... & qw \\ qw & (1-w) & pw & ... & 0 \\ 0 & qw & (1-w) & ... & pw \\ ... & & & & \\ pw & 0 & qw & ... & (1-w) \end{bmatrix}, \tag{4.4}$$

Matrix $\mathbf{M}$ is a transition matrix which can be easily recognized as an asymmetric cyclic matrix. Since this matrix is not Hermitian, its eigenvalues occur in complex conjugate pairs, in addition to some of them being real.

For a general cyclic matrix

$$\mathbf{A} = \begin{bmatrix} a_1 & a_2 & ... & a_N \\ a_N & a_1 & ... & a_{N-1} \\ ... & & & \\ a_2 & a_3 & ... & a_1 \end{bmatrix}, \tag{4.5}$$

it is well-known [Kowaleski 1948] that the eigenvalues are given by

$$\lambda_l = \sum_{p=1}^{N} a_p \exp\left[\frac{2\pi i}{N}(p-1)(l-1)\right], \tag{4.6}$$

$(l = 1, 2, ..., N)$. The maximum eigenvalue is $\sum_{i=1}^{N} a_i$ for $a_i \geq 0$. The diagonal-

izing matrix is discrete Fourier matrix and given by

$$U_{jl} = \frac{1}{\sqrt{N}} \exp\left[\frac{2\pi i}{N}(j-1)(l-1)\right]. \tag{4.7}$$

The n^{th} component of the l^{th} eigenvector corresponding to λ_l is

$$(\hat{e}_l)_n = \frac{1}{\sqrt{N}} \exp\left[\frac{2\pi i}{N}(n-1)(l-1)\right]. \tag{4.8}$$

We can easily see that given an initial distribution

$$\vec{p}(0) = \sum_{l=1}^{N} c_l \hat{e}_l \tag{4.9}$$

with

$$c_l = \frac{1}{\sqrt{N}} \sum_{n=1}^{N} p_n(0) \exp\left[\frac{-2\pi i}{N}(n-1)(l-1)\right], \tag{4.10}$$

the probability $\vec{p}(t)$ is given by a product of matrices $\mathbf{M}$, acting on $\vec{p}(0)$. Thus

$$\vec{p_i}(t) = \sum_{l=1}^{N} c_l \lambda_l^t \hat{e}_l. \tag{4.11}$$

This equation is used to calculate the time evolution of $p_i(t)$ for lattices of several different numbers of sites and for given values of w.

For calculating the entropy of this system in its non-equilibrium steady state, we can use Boltzmann's relation

$$S = k_B \ln \Omega \tag{4.12}$$

with the thermodynamic probability, Ω. Let us obtain a version of this formula which can be used with a probability distribution of the type given in Eq. 4.11.

The thermodynamic probability is given by

$$\Omega = \frac{N_{ens}!}{(N_1!)(N_2!)...(N_N!)}. \tag{4.13}$$

Using Stirling's approximation for large m, $\ln m! \approx m \ln m - m$, we can write

$$\ln \Omega = N_{ens} \ln N_{ens} - N_1 \ln N_1 - N_2 \ln N_2 - ... - N_N \ln N_N. \tag{4.14}$$

On dividing by N_{ens} and using Eq. 4.1, the ensemble averaged entropy, $s = S/N_{ens}$ an ensemble may be written as

$$\frac{s}{k_B} = -\sum_{i=1}^{N_{site}} p_i \ln p_i. \tag{4.15}$$

Since, in a lattice which reaches equilibrium, all the p_i will equal $1/N_{site}$ the limiting value of s/k_B will be $\ln N_{site}$.

Using the result of Eq. 4.11 in Eq. 4.15 we calculate the corresponding entropy as a function of time (Fig.4.1).

4.3 Biased random walks on a disordered lattice

Generalizing the basic model considered above by allowing the particle to jump not only at nearest neighbour but at any site will make transition matrix full in contrast to almost tri-diagonal form considered in earlier section. We further introduce randomness by making the elements of the transition matrix random. This is achieved by considering the transition matrix to belong to a Gaussian ensemble of cyclic matrices with a distribution,

$$p(\mathbf{M}) \sim \exp\big[-\alpha \mathrm{Tr}(\mathbf{M}^{\dagger}.\mathbf{M})\big]. \tag{4.16}$$

The maximum eigenvalue being $\sum_i a_i$ (for $a_i \geq 0$). We employ the results of theory of random cyclic matrices [Jain 2008b] to find the ensemble average. However, there is an important modification to be made owing to the fact that the matrix elements are probabilities and the sum of these is unity. This can be easily done and will be used in the calculation of the average over random matrix ensemble. To calculate numerically the entropy, the transition matrix is populated first by Gaussian random number with a very high positive mean and variance one, once the positivity of all elements are ensured (first row of the transition matrix which is a cyclic matrix) they are normalized by sum of them to have them between 0 and 1. This makes the M as correct stochastic matrix. Let us define the average by ($\lambda = re^{i\theta}$)

$$\langle \vec{p}(t) \rangle_{RCM} = \frac{\int_0^1 dr \int_{-\pi}^{\pi} d\theta \vec{p}(t) \rho(r,\theta) r}{\int_0^1 dr \int_{-\pi}^{\pi} d\theta \rho(r,\theta) r} \tag{4.17}$$

where $\rho(r,\theta)$ is the density of eigenvalues. As we have seen in Chapter 3 that modulus of eigenvalues of random cyclic matrices are the eigenvalues of reverse random cyclic matrices upto a sign. We have also shown that these joint probability distribution function of these eigenvalues have a product structure and given by Eq. 3.24. Hence, the r ($= |\lambda|$) is distributed by a Wigner-like distribution of random matrix theory.

The time evolution is given by

$$p_j(t) = \sum_{l=1}^{N} c_l \lambda_l^t (\hat{e}_l)_j \tag{4.18}$$

substituting the eigen vector in the above equation we get,

$$p_j(t) = \frac{1}{\sqrt{N}} \sum_{l=1}^{N} c_l \lambda_l^t \exp\left[\frac{2\pi i}{N}(l-1)(j-1)\right] \tag{4.19}$$

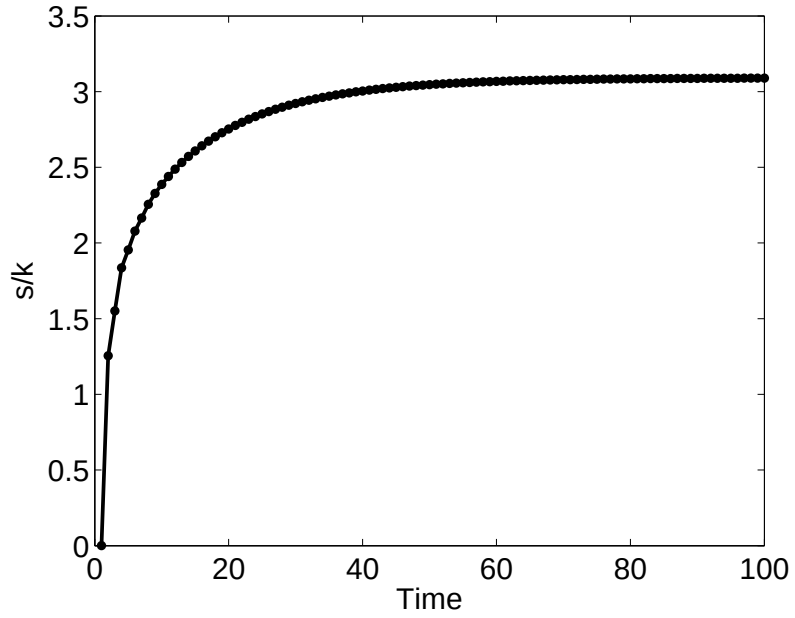

Figure 4.1: For the case of random walkers on a periodic lattice with 22 sites, $a_1 = 0.2, a_2 = 0.24, a_{22} = 0.56$ (other a_i's are zero) with the jump probability, $w = 0.8$, the entropy is seen here.

$p_j(t)$ can be re-written as

$$\begin{aligned} p_j(t) &= \frac{1}{N}\sum_{n=1}^{N} p_n(0)\left(\lambda_1^t + \sum_{l=2}^{N}\lambda_l^t \exp\left[\frac{2\pi i}{N}(l-1)(j-n)\right]\right) \\ p_j(t) - \frac{1}{N} &= \frac{1}{N}\sum_{n=1}^{N} p_n(0)\sum_{l=2}^{N}\lambda_l^t \exp\left[\frac{2\pi i}{N}(l-1)(j-n)\right] \\ p_j(t) - \frac{1}{N} &= \frac{1}{N}\sum_{n=1}^{N} p_n(0)\sum_{l=2}^{N}\lambda_l^t \Omega_{jn}^{l-1} \end{aligned} \tag{4.20}$$

where we have $\exp\left[\frac{2\pi i}{N}(j-n)\right] := \Omega_{jn}$ and also made use of $\sum_{n=1}^{N} p_n(0) = 1$. Now, we can average over the joint probability distribution function of eigenvalues, $J(\lambda_2, ..., \lambda_N)$. Denoting the average as $\langle p_j(t) - \frac{1}{N}(\{\lambda_i\})\rangle_{RMT}$, we can write

$$
\begin{aligned}
\langle \tilde{p}_j(t)(\{\lambda_i\})\rangle_{RMT} &= \frac{1}{N}\sum_{n=1}^{N} p_n(0)\sum_{l=2}^{N}\Omega_{jn}^{l-1}\int d\lambda_2 ... d\lambda_l ... d\lambda_N J(\lambda_2,...,\lambda_N)\lambda_l^t \\
&= \frac{1}{N}\sum_{n=1}^{N} p_n(0)\sum_{l=2}^{N}\Omega_{jn}^{l-1}\left[\frac{1}{N-1}\int_{-\infty}^{+\infty} d\lambda \lambda^t \rho(\lambda)\right] \\
&= \frac{1}{N(N-1)}\sum_{n=1}^{N} p_n(0)\sum_{l=2}^{N}\Omega_{jn}^{l-1}.\left[\int_0^{+\infty}\int_{-\pi}^{+\pi} k dr d\theta\right. \\
&\quad \left. r^t \exp\left[it\theta\right]\frac{\pi}{2}r^2\exp\left(-\frac{\pi r^2}{4}\right)\left(\frac{1}{\pi}-\delta(\theta)\right)\right] \\
&= \frac{k}{N(N-1)}\sum_{n=1}^{N} p_n(0)\sum_{l=2}^{N}\Omega_{jn}^{l-1}.2^{1+t}\pi^{-\frac{1}{2}-\frac{t}{2}}\left[\Gamma\left(\frac{3+t}{2}\right)\right. \\
&\quad \left.-\Gamma\left(\frac{3+t}{2},\frac{\pi}{4}\right)\right]\left(-1+\frac{2\sin[\pi t]}{\pi t}\right) \\
&= \frac{k}{N(N-1)}\sum_{n=1}^{N} p_n(0)(-1)2^{1+t}\pi^{-\frac{1}{2}-\frac{t}{2}}\left[\Gamma\left(\frac{3+t}{2}\right)\right. \\
&\quad \left.-\Gamma\left(\frac{3+t}{2},\frac{\pi}{4}\right)\right](-1) \\
&= \frac{1}{N}\frac{2^{1+t}\pi^{-\frac{1}{2}-\frac{t}{2}}}{\left(-e^{-\pi/4}+\mathrm{erf}\left[\frac{\sqrt{\pi}}{2}\right]\right)}\left[\Gamma\left(\frac{3+t}{2}\right)-\Gamma\left(\frac{3+t}{2},\frac{\pi}{4}\right)\right] \\
&= \frac{1}{N}\frac{1}{\left(-e^{-\pi/4}+\mathrm{erf}\left[\frac{\sqrt{\pi}}{2}\right]\right)}\left(\frac{2}{\sqrt{\pi}}\right)^{1+t}\gamma\left(\frac{3+t}{2},\frac{\pi}{4}\right) \quad (4.21) \\
&\qquad\qquad \forall\ t>0
\end{aligned}
$$

For the behaviour of $N\langle \tilde{p}_j(t)(\{\lambda_i\})\rangle_{RMT}$ for large time t, we make use of the identity for large a ($\neq 0,-1,-2,...$) and fixed z, [DLMF 2010]

$$\gamma\left(a,z\right) = z^a e^{-z}\sum_{k=0}^{\infty}\frac{z^k\Gamma(a)}{\Gamma(a+k+1)} \quad (4.22)$$

After a little algebra,

$$N\langle \tilde{p}_j(t)(\{\lambda_i\})\rangle_{RMT} \approx \frac{\pi}{4}\frac{e^{-\frac{\pi}{4}}}{\left(-e^{-\pi/4}+\mathrm{erf}\left[\frac{\sqrt{\pi}}{2}\right]\right)}\left[\frac{2}{3+t}\right. \quad (4.23)$$

$$+ \frac{\pi}{(t+3)(t+5)} + O\left(\frac{1}{t^3}\right)\Bigg]$$

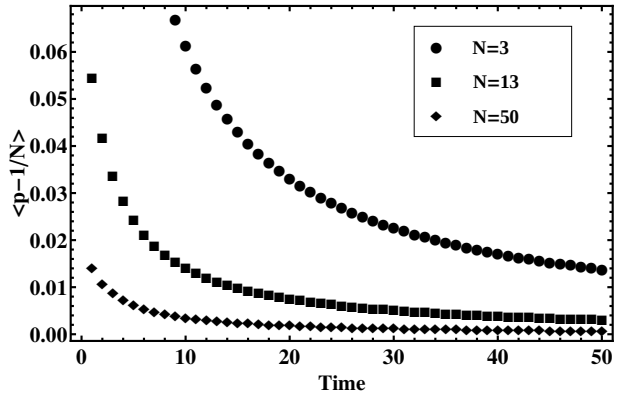

Figure 4.2: With time p becomes more and more uniform, for three different N values the curves show how fast the uniformity sets in with time.

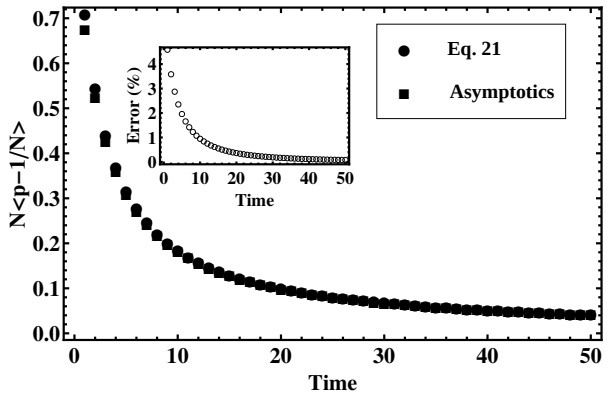

Figure 4.3: After absorbing N in $\langle \tilde{p}_j(t)(\{\lambda_i\})\rangle_{RMT}$, the exact time dependence and first two term of asymptotic series expansion is plotted, in inset the difference between the two in % is plotted. It is clear that the convergence of the series is very fast. Asymptotically, the time dependence is given by $\sim \frac{\text{constant}}{t+3}$.

In the above we have used,

$$\begin{aligned}
\Gamma(a) &= \int_0^\infty t^{a-1}e^{-t}dt \quad \Gamma(a,z) = \int_z^\infty t^{a-1}e^{-t}dt \\
\gamma(a,z) &= \int_0^z t^{a-1}e^{-t}dt \quad \text{with } \Gamma(a) = \Gamma(a,z) + \gamma(a,z).
\end{aligned}$$

As we have mentioned earlier, that modulus of eigenvalue are distributed as Wigner-like distribution, the proportionality constant k has been evaluated by normalizing the distribution of all eigenvalues except 1, to number of eigenvalue (N-1).

$$\begin{aligned}\int_{-\infty}^{+\infty} d\lambda\rho(\lambda) &= k\int_0^1\int_{-\pi}^{+\pi} rdrd\theta\rho(r)\rho(\theta)\\ (N-1) &= k\int_0^1\int_{-\pi}^{+\pi} drd\theta\frac{\pi}{2}r^2\exp\left(-\frac{\pi r^2}{4}\right)\left(\frac{1}{\pi}-\delta(\theta)\right)\\ k &= \frac{(N-1)}{\left(-e^{-\pi/4}+\mathrm{erf}\left[\frac{\sqrt{\pi}}{2}\right]\right)}\end{aligned} \tag{4.24}$$

Let's note that $\theta = 0$ is the case for first eigenvalue which we have excluded from the joint probability distribution function. Hence the density of this angle ($\delta(\theta)$) is excluded from the uniform density of θ, valid for the rest of the eigenvalues.

The time dependence of $\langle\tilde{p}_j(t)(\{\lambda_i\})\rangle_{RMT}$ is shown in Fig.4.2. We see that all the probabilities tend to $1/N$, thus the evolution of the walk is shown to produce a non-equilibrium steady state with maximum entropy given by $\log N$. This is not surprising.

4.4 Summary

Using the distribution functions obtained for random cyclic matrices in Chapter 2, we have applied in a problem of random walks of statistical mechanics. We trivially generalized the biased random walk as an eigenvalue problem and have shown that the transfer matrix is cyclic matrix. Once we demand that jump probabilities are random in nature, this has been cast as biased random walk in disordered lattice. The evolution of entropy has been calculated and expectedly found as $\log N$. Importantly, the rate of approach to equilibrium for ensemble averaged jump probabilities has been shown to follow $1/t$ law. The point to

note is that any other form of randomness or bias can be modeled using the general scheme here by a suitable modification of the distribution of matrix elements. The main advantage is the simplicity of the treatment given here. We may recall the usual process where one sets up a master equation with a non-Hermitian Hamiltonian [Mallick 2009] and solves for the steady state solution to study the approach to equilibrium.

Chapter 5

Records and eigenvectors

Contents

5.1 Introduction

Sports and finance interest most, if not all, of the human beings and consequently, the records set (or broken) in various events. How we long for a particular record to be set by our favourite sportsman or when the sensex reaches the height it has never touched before. Similarly for engineers in designing a dam, one of the most important data is when and by how much the river level has exceeded it's all the previous levels; similar questions are asked about rainfall when the planning for agricultural policies is taken up. Naturally, these are the requirements which have got first few applications of study of the events which

exceed themselves in some aspect and are often called as "Record". Questions about how the records increase with time, or the number of records set, are of natural interest in all these contexts and have been studied [Gembris 2002, Vogel 2001, Redner 2006]. A mathematical theory of records for i.i.d. random variables has been developed [Renyi 1962, Glick 1978, Arnold 1998]. The physics applications started a little later, but have found use in various problems from random walks, spin-glasses, Type II super-conductors. In this thesis, we have applied the record statistics in quantum chaos. Now to define records more precisely, given $\{x_t, t = 1, \cdots N\}$ as a finite time series, the first element, R_1, of the corresponding records series is x_1 itself and at subsequent times t it will be $R_t = \max(x_t, R_{t-1})$. As x_t is a random variable, so is R_t and properties of this random variable is of interest.

Some of the recent works concerning random walks and records are now reviewed here. In case of random walks, x_t represents the position of a random walker at a time step, t. For discrete time step, and, the jump-lengths drawn from an i.i.d. symmetric distribution, probability $P(M, N)$ of M records in $t = N$ steps is given by

$$P(M, N) = \binom{2N - M + 1}{N} 2^{-2N+M-1}, \quad M \leq N + 1 \tag{5.1}$$

with mean $\langle M \rangle \sim \frac{2}{\sqrt{\pi}}\sqrt{N}$. Age statistics of record *i.e.*, how long a record survives before it is broken, is given by $\langle l \rangle \sim \frac{N}{\langle M \rangle} \sim \sqrt{\frac{\pi N}{4}}$ [Majumdar 2008]. In case of continuous time random walk, *i.e.* when position of a random walker is now observed at equal discrete time steps with time interval τ_0, the probability of finding M records within a given time duration t, $P(M, t)$ attains a scaling

form given as,

$$\begin{aligned} P(M,t) &\sim (t/\tau_0)^{-\alpha/2} g_\alpha \left(M(t/\tau_0)^{-\alpha/2}\right) \\ g_\alpha(x) &= \frac{2}{\alpha} x^{-(1+2/\alpha)} L_{\alpha/2}(x^{-2/\alpha}), \quad 0 < \alpha \leq 1, \end{aligned} \tag{5.2}$$

where $L_{\alpha/2}(x)$ is one-sided Lévy stable probability distribution function. The moments of records, asymptotically goes as

$$\langle M^\nu \rangle \sim \frac{(2/\alpha)\Gamma(\nu)}{\Gamma(\nu\alpha/2)} (t/\tau_0)^{\nu\alpha/2}. \tag{5.3}$$

The mean-age of the record is

$$\langle l \rangle = \langle t/M \rangle \sim \frac{\tau_0(\alpha/2)}{\Gamma(1-\alpha/2)} [\ln(t/\tau_0) - \Psi(1-\alpha/2)](t/\tau_0)^{(1-\alpha)}, \tag{5.4}$$

where $\Psi(x)$ is di-gamma function [Sabhapandit 2011]. In another generalization, the record distribution for a random walk with discrete time steps but asymmetric jump distribution, has been calculated for the model governed by $x_n = x_{n-1} + \xi_n + c$ with ξ_n being the jump length with symmetric distribution while c is the constant drift. For Gaussian jump distribution with variance σ, in the limit of small drift (smallness is compared with respect to $c = 0$ case) *i.e.* $\left(\frac{c}{\sigma} << \frac{1}{\sqrt{n}}\right)$, the mean number of records and record rate (*i.e.* probability of n^{th} event being a record), is given by,

$$\begin{aligned} \langle M_n(c) \rangle &\approx \frac{2\sqrt{n}}{\sqrt{\pi}} + \frac{c}{\sigma}\frac{\sqrt{2}}{\pi}(n \arctan(\sqrt{n}) - \sqrt{n}), \\ P_n(c) &\approx \frac{1}{\sqrt{\pi n}} \frac{c}{\sigma} \frac{\sqrt{2}}{\pi} \arctan(\sqrt{n}). \end{aligned} \tag{5.5}$$

In the large drift limit, $P_n(c)$ approaches a constant value [Wergen 2011].

The geometric feature of random systems such as size of the largest cluster in percolation on a finite lattice of size N, has been shown to follow Gumbel

distribution in the large-N limit [Bazant 2000]. In Type-II superconductor, temperature independence of magnetic creep rate *i.e.* rate of change of magnetic field in the sample at a constant temperature for a range of temperatures has been understood in terms of record dynamics, namely, the dynamical properties of the times at which a stochastic fluctuating signal (in this case thermal noise due to non-zero temperature) establishes records. This puzzling temperature independence of the creep rate, which at non-zero temperatures has its origin due to thermal fluctuations, has been sorted out by showing that the process of vortex penetration into the sample can be described in terms of a Poisson process with logarithmic time argument, called the log-Poisson process; a result from record dynamics [Oliveira 2005]. The application of record statistics in case of quantum chaos has been treated in [Srivastava 2013] and the details of this work will be subject matter of current chapter.

This chapter focusses on record statistics of random vectors and this is compared to the record statistics of eigenvectors of a quantized dynamical system, the standard map. For this purpose, we will derive the exact record statistics for complex random vectors, correlated via the normalization. It is known that the eigenstate intensities in fully chaotic systems with no particular symmetries are conjectured to behave exactly as these random vectors subject only to a normalization constraint. These are also the statistical properties of eigenvectors of the classical ensembles of random matrix theory. For chaotic systems, the applicability of random matrix theory [Mehta 2004, Brody 1981] has been well appreciated for long [Bohigas 1984]. As we will discuss in detail in Sections 5.4 and 5.5 that in standard map the breaking of last KAM torus allows the diffusion in phase space and diffusion being connected with random walks, we expect and indeed observe the average number of records in eigenvectors to go as square-root of N. In fact this is first known instance where K values

at which the last KAM torus breaks has been seen in a quantity derived from quantum mechanical spectrum.

5.2 Record statistics

5.2.1 Definition

Let's take a time-series $\{X_1, X_2, \cdots X_n\}$. An entry X_j will be defined as an upper (a lower) record if

$$X_j = \max\ (\min)\{X_1, X_2, \cdots X_j\}.$$

To illustrate the definition of records, let's take a time series consisting of just six elements, $X = \{0.8, 0.6, 0.3, 0.9, 0.4, 0.5\}$. Corresponding upper record sequence will be $R = \{0.8, 0.8, 0.8, 0.9, 0.9, 0.9\}$ while lower record sequence will be $\{0.8, 0.6, 0.3, 0.3, 0.3, 0.3\}$. Let's note that first element will always be record no matter whether we are looking for upper or lower record and in general records are fewer. From the definition of record, it is clear that last upper (lower) record is also the global maximum (minimum) of the sequence $\{X_j\}$. Hence, the statistics of last record will correspond to similar results of maximum or minimum from extreme value theory. A word of caution is warranted here, as second last upper (lower) record will not be the second maximum (minimum) of the sequence. This can be easily understood by visualizing a sequence where global maximum (minimum) occurs before second maximum (minimum). As in that case, record statistics will not sense the presence of second maximum (minimum). To develop more familiarity with record sequence, let's take $\sin x,\ 0 \leq x \leq 2\pi$ as an example. In the range $[0, \pi/2]$ the upper record sequence is $\sin x$ itself and beyond that the entries will be constant 1.

5.2.2 Independent and identically distributed (i.i.d.) random variables

Consider entries of $\{X_j\}$ being independent and identically distributed random numbers. As we have exchangeable entries, symmetry of the sequence determines the probability of X_j being a record to be $1/j$ at the j^{th} trial [Renyi 1962, Arnold 1998]. Consider temperatures in a particular city, despite all the fluctuations, it is clear that it beats its own record. In a formal language, the process of setting a record is persistent. Let's denote the number of record in a sequence of length n by N_n, then above statement can be rephrased as $N_n \to \infty$ with length of sequence $n \to \infty$. To prove this let's consider that in a sequence of length $n_1 + n_2$, all the records have occurred in the first batch of length n_1; then, since there is no record set from n_1 to $n_1 + n_2$, the probability can be calculated as

$$\left(1 - \frac{1}{n_1 + 1}\right)\left(1 - \frac{1}{n_1 + 2}\right) \cdots \left(1 - \frac{1}{n_1 + n_2}\right)$$

and hence

$$P\{N_{n_1} = N_{n_1+n_2}\} = \frac{n_1}{n_1 + n_2}.$$

Now by increasing n_2 this value can be made arbitrarily small. Let's take r such batches of lengths $n_2,\ n_3,\ \cdots n_{r+1}$; for an arbitrary $\varepsilon > 0$,

$$\sum_{k=1}^{r} P\{\text{no record value in } k^{\text{th}} \text{ batch}\} = r(\varepsilon/r) = \varepsilon.$$

But the probability of obtaining at least r records in a sequence with length $n > n_1 + n_2 + \cdots + n_r$, is then

$$P\{N_n \geq r\} \geq P\{\text{at least one record occurs in r batches}\}$$

$$
\begin{aligned}
&= 1 - P\{\text{at least one bacth has no record}\} \\
&\geq 1 - \sum_{k=1}^{r} P\{\text{no record value in } k^{\text{th}} \text{ batch}\} \\
&> 1 - \varepsilon
\end{aligned}
$$

As ε is small, so $P\{N_n \geq r\} \to 1$ for arbitrary large number r. This proves the assertion [Glick 1978].

The next natural question is about the frequency of record breaking, Let's define an indicator function

$$
I_j = \begin{cases} 1 & \text{if there is a record at } j \text{ ,} \\ 0 & \text{otherwise.} \end{cases} \tag{5.6}
$$

Calculating the expected value of I_j is equivalent to calculating the probability of I_j taking the value 1, but this is precisely the probability of X_j being the record- which is $1/j$. Similarly, for variance, we note that expected value of I_j^2 is the same as expected value of I_j. This immediately give the variance as $1/j - 1/j^2$. Another important property of I_j being pairwise uncorrelated (statistically independent) can be proven as follows,

$$
\begin{aligned}
\langle I_j I_k \rangle &= P\{I_j = 1 \text{ and } I_k = 1\} \\
&= P\{X_j = \max\{X_1, \cdots X_j\} \text{ and } X_k = \max\{X_1, \cdots X_k\}\} \\
&= P\{X_j = \max\{X_1, \cdots X_j\} < \max\{X_{j+1}, \cdots X_k\} = X_k\} \\
&= P\{X_j = \max\{X_1, \cdots X_j\}\} \times \\
&\quad P\{X_j = \max\{X_1, \cdots X_j\} < X_k = \max\{X_1, \cdots X_k\}\} \\
&\quad \times P\{\max\{X_{j+1}, \cdots X_k\} = X_k\} \\
&= \frac{1}{j}\frac{k-j}{k}\frac{1}{k-j} = \frac{1}{jk} = P\{I_j = 1\}P\{I_k = 1\} = \langle I_j \rangle \langle I_k \rangle.
\end{aligned} \tag{5.7}
$$

In other words the probability of the position of the records is a Bernoulli process, Ber$(1/j)$.

As the total number of records N_n in a sequence $\{X_1, X_2, \cdots X_n\}$ is $\sum_{j=1}^{n} I_j$, the expectation and variance can be easily calculated:

$$\begin{aligned} \langle N_n \rangle &= \sum_{j=1}^{n} \langle I_j \rangle = \sum_{j=1}^{n} \frac{1}{j} = H_n, \quad n^{\text{th}}\text{Harmonic number} \\ V(N_n) &= \sum_{j=1}^{n} V(I_j) = \sum_{j=1}^{n} \frac{1}{j} - \sum_{j=1}^{n} \frac{1}{j^2}. \end{aligned} \tag{5.8}$$

A remarkable, well-known fact from the theory of records is that for i.i.d. variables these quantities are distribution-free, that is independent of the particular underlying distribution $p(x)$ [Arnold 1998]. For example the average number of records $\langle N_n \rangle = H_n \sim \log(n) + \gamma$ is indeed very small compared to the length n of the data set; typically records are rare events. In next section onwards, we will change the notation from N_n to N_R.

5.3 δ-correlated variables

5.3.1 Upper records for complex random vectors

For a correlated sequence, let the probability density for a record variable R, at time t be $P(R,t)$. The average record is given by $\langle R \rangle = \int dRRP(R,t)$. Let $P(x_1, \ldots, x_N)$ be the JPDF of N random variables. The probability that the record at time t, R_t, is less than R is given by

$$Q(R,t) = \int_0^R \mathrm{d}x_1 \cdots \mathrm{d}x_t P_t(x_1, ...x_t) \tag{5.9}$$

where $P_t(x_1, \ldots, x_t) = \int P(x_1, \ldots, x_N)\, \mathrm{d}x_{t+1} \cdots \mathrm{d}x_N$ is the marginal JPDF of the first t random variables. It follows that $P(R,t) = \mathrm{d}Q(R,t)/\,\mathrm{d}R$.

Let's specialize in the δ correlated random variable *i.e.* sum of the random sequence entries are constant. Components of normalized complex random vectors $z_n = \langle n|\psi\rangle$, have the JPDF:

$$P(z_1, z_2, \ldots, z_N) = (\Gamma(N)/\pi^N)\delta\left(\sum_{j=1}^{N} |z_j|^2 - 1\right). \tag{5.10}$$

This is also the distribution of the components of the eigenvectors of the GUE or CUE (Gaussian or Circular unitary ensembles) random matrices. It is the invariant uniform distribution under an arbitrary unitary transformations on the $2N-1$ dimensional sphere. It is the unique (Haar) measure on S^{2N-1}. The normalization provides correlation among the components that becomes weak for large N. The intensities $x_i = |z_i|^2$ being the random variables of interest it is more useful to define the JPDF directly in terms of these:

$$P(x_1, \ldots, x_N; u) = \Gamma(N)\delta\left(\sum_{i=1}^{N} x_i - u\right), \tag{5.11}$$

where u is an auxiliary quantity, the actual JPDF corresponding to $u = 1$. Defining

$$Q(R, t; u) = \int_0^R \mathrm{d}x_1 \cdots \mathrm{d}x_t \int_0^\infty P(x_1, \ldots, x_N; u)\, \mathrm{d}x_{t+1} \cdots \mathrm{d}x_N \tag{5.12}$$

leads to

$$\int_0^\infty e^{-su} Q(R, t; u)\, \mathrm{d}u = \frac{\Gamma(N)}{s^N} \sum_{m=0}^{t} (-1)^m \binom{t}{m} e^{-smR}. \tag{5.13}$$

Using the convolution theorem, and then setting $u = 1$ in $Q(R, t; u)$ gives

$$Q(R, t) = \sum_{m=0}^{t} (-1)^m \binom{t}{m} (1 - mR)^{N-1} \Theta(1 - mR). \tag{5.14}$$

Hence

$$P(R,t) = \sum_{m=1}^{t} (-1)^{m+1} \binom{t}{m} m(N-1)(1-mR)^{N-2}\Theta(1-mR), \tag{5.15}$$

the probability density that the record is R at time t. Note that $P(R,N)$ is the probability density that the maximum value of the entire data set is R, which was calculated for the case of random GUE vectors in [Lakshminarayan 2008] and therefore $P(R,t)$ here is a generalization. The piecewise smooth probability distribution found there has a similar behaviour here.

It was shown in [Lakshminarayan 2008] that $P(R,N)$ is Gumbel distributed asymptotically. In fact the generalization presented in Eq. 5.14 is also Gumbel distributed for large N, as for large N and large $t \gg 1$

$$Q(R,t) \approx (1-\exp(-NR))^t \approx \exp\left(-t\exp(-NR)\right). \tag{5.16}$$

Since the Gumbel distribution is of the form $\exp[-\exp(-(x-a_N)/b_N]$ where a_N and b_N are the shift and scaling. It follows that for the record statistics the relevant parameters are $a_N = \log(t)/N$ and $b_N = 1/N$. The shift generalizes from $\log(N)/N$ for the maximum, while the scaling remains the same. The above form also appears in the limit when the correlations are ignored.

The average record as a function of time is

$$\langle R(t)\rangle = 1 - \int_0^1 Q(R,t)\, dR = \frac{1}{N}\sum_{m=1}^{t}(-1)^{m+1}\frac{1}{m}\binom{t}{m} = \frac{H_t}{N} = \frac{1}{N}\sum_{k=1}^{t}\frac{1}{k}, \tag{5.17}$$

where H_t is a Harmonic number as defined above. Known asymptotics of the Harmonic numbers implies that

$$\langle R(t)\rangle = \frac{1}{N}\left(\gamma + \ln(t) + \frac{1}{2t} - \sum_{k=1}^{\infty}\frac{B_{2k}}{2k\, t^{2k}}\right), \tag{5.18}$$

where B_{2k} are Bernoulli numbers, and γ is the Euler-Mascheroni constant. Again, this presents a generalization of the average maximum intensity found in [Lakshminarayan 2008] which corresponds to $t = N$.

It is not hard to prove that for intensities of random states too, the probability of the position of the records is a Bernoulli process although they are correlated by the normalization constraint. Let there be records at positions $(j_1 = 1 < j_2 < \cdots < j_m)$ and let $I_{J_k} = 1$ if there is a record at j_k or 0 otherwise. Then the JPDF

$$\text{Prob}(I_{j_1} = 1, I_{j_2} = 1, \ldots, I_{j_m} = 1) = \int_{\mathcal{C}} P(x_1, \ldots, x_N; u = 1) dx_1 \cdots dx_N = \prod_{k=1}^{m} \frac{1}{j_k}. \tag{5.19}$$

Here $\mathcal{C}$ is the set of constraints: $0 \leq x_k \leq x_{j_2}$, $j_1 \leq k \leq j_2 - 1$; $0 \leq x_k \leq x_{j_3}$, $j_2 \leq k \leq j_3 - 1$; $\cdots$, $0 \leq x_k \leq x_{j_m}$, $j_{m-1} \leq k \leq j_m - 1$; $0 \leq x_k \leq 1$, $j_m \leq k \leq N$. The above result follows on using the Laplace transform to free the constraint in Eq. 5.11. The details of the derivation is presented in Appendix A. However this is the result for i.i.d. random variables, and implies that the occurrence of a record at j_k is an independent process, as the above is valid for all arbitrary choices of the locations j_k. Hence $\text{Prob}(I_j = 1) = 1/j$ and $\text{Prob}(I_j = 0) = 1 - 1/j$, in other words the process is $\text{Ber}(1/j)$.

The average number of records is thus

$$\langle N_R \rangle = \left\langle \sum_{j=1}^{N} I_j \right\rangle = \sum_{j=1}^{N} \frac{1}{j} = H_N, \tag{5.20}$$

while as a random variable N_R has a distribution essentially given by the signless Stirling numbers of the first kind, some times called the Karamata-Stirling law [Nevzorov 1987]. Such laws hold for a variety of disparate processes including the number of cycles in a random permutation of N objects, number of

nodes in extreme side branch of random binary search trees etc. [Bai 1998]. Being distribution-free, the number of records is a statistics that directly detects correlations.

The probability that the final record, which is the maximum in the entire data sequence, lasts for time m can also be simply calculated: denoted $S_N(m) = P(I_N = 0, I_{N-1} = 0, \cdots, I_{N-m+2} = 0, I_{N-m+1} = 1) = 1/N$, it is (somewhat surprisingly) independent of m, and uniform. This implies that the *position* at which the maximum occurs is uniformly distributed. The implications of this for quantum chaotic wavefunctions where strong scarring effects of classical periodic orbits can affect the maxima of states is of natural interest [McDonald 1979, Heller 1984, Biswas 1990, Kudrolli 1995, Laurent 2007].

Let's move on to $T_N(m)$ which is "Probability" that life-time (length) of records is m in the string of length N. Records of exactly length m occurs as $\underbrace{RLL\ldots L}_{m}R$ except when last entry in the string is not R *i.e.* $\underbrace{RLL\ldots L}_{m}$.

Now if the first R is at position j the probability of $RL^{m-1}R$ is

$$\frac{1}{j}\left(1-\frac{1}{j+1}\right)\ldots\left(1-\frac{1}{j+m-1}\right)\frac{1}{j+m} = \frac{1}{(j+m-1)(j+m)}$$

$$= \frac{1}{j+m-1} - \frac{1}{j+m}$$

As the occurrence of $R_jL^{m-1}R$ at different j are exclusive events, and so is the event R_jL^{m-1}, so

$$T_N(m) = \sum_{j=1}^{N-m} \frac{1}{j+m-1} - \frac{1}{j+m} + \frac{1}{N} = \frac{1}{m}.$$

5.3.2 Lower records in complex random vectors

The question of a record minimum can be asked in a similar way, the cumulative density function for a record minimum, *i.e.* the probability that the record is

"greater" than R at a time t is given by

$$Q(R,t) = \int_R^\infty \mathrm{d}x_1 \cdots \mathrm{d}x_t P_t(x_1, \ldots, x_t) \tag{5.21}$$

where $P(x_1, \ldots, x_N)$ is JPDF of N random variables, and $P_t(x_1, \ldots, x_t)$ is the JPDF of t random variables given by $\int_{all\ range} P(x_1, \ldots, x_N)\, \mathrm{d}x_{t+1} \ldots \mathrm{d}x_N$.

From $Q(R,t)$ we can get $P(R,t)$ as

$$P(R,t) = -\frac{\mathrm{d}Q(R,t)}{\mathrm{d}R}. \tag{5.22}$$

It is not difficult to calculate the probability distribution of record minima in the case of a complex random vector, essentially following the same technique as in the case of maximum records,

$$\begin{aligned} Q(R,t;s) &= \Gamma(N) e^{-s\sum_{i=1}^t r_i} \left[\prod_{i=1}^t \int_R^\infty \mathrm{d}r_i e^{-sr_i}\right] \left[\prod_{i=t+1}^N \int_0^\infty \mathrm{d}r_i e^{-sr_i}\right] \\ &= \frac{\Gamma(N)}{s^{N-t}} \frac{e^{-sRt}}{s^t} \end{aligned}$$

Using identity 5.33 and then replacing u by 1, we get

$$Q(R,t) = (1-Rt)^{N-1}\Theta(1-Rt) \tag{5.23}$$

Density,

$$P(R,t) = -\frac{dQ(R,t)}{dR} = (N-1)t(1-Rt)^{N-2}\Theta(1-Rt) \tag{5.24}$$

and average record as a function of t can be easily found

$$\langle R(t)\rangle = \int RP(R,t)\, \mathrm{d}R$$

$$= \int_0^{1/t} R(N-1)t(1-Rt)^{N-2}\,\mathrm{d}R$$
$$= \frac{1}{Nt}. \tag{5.25}$$

Again this generalizes the results obtained in [Lakshminarayan 2008]. For large, N limit $Q(R,t)$ is again exponential and for $t = N$, it retrieves all the results obtained in [Lakshminarayan 2008]. It is easy to show (by just changing the conditions and hence the limits in appropriate integrations) that these are also Bernouli process, $Ber\,(1/n)$ and hence all the results for survival probability, lifetime distribution *etc.* remains same in this case too.

Attention is now turned from random vectors to eigenfunction of a quantum dynamical system that is chaotic in the classical limit. As the standard map is a simple dynamical system which has a well-studied transition to chaos through the usual route of smooth Hamiltonian systems it will be a good model to study. It also allows breaking parity and time-reversal symmetries through quantum phases and hence allows for studying GUE, GOE, (or CUE, COE), as well as intermediate statistics. Before discussing the record statistics for eigenvectors we are summarizing some aspects of the standard map pertaining to quantization and the intensity distribution of its eigenvectors.

5.4 Standard map

The Hamiltonian of δ-kicked rotor is given by

$$H(q,p,t) = \frac{p^2}{2} - \frac{g}{4\pi^2}\cos(2\pi q)\sum_{n=-\infty}^{\infty}\delta\left(t/T - n\right). \tag{5.26}$$

The Hamilton's equations of motion are

$$\begin{aligned} \dot{q} &= \frac{\partial H}{\partial p} = p, \\ \dot{p} &= -\frac{\partial H}{\partial q} = -\frac{g}{2\pi}\sin(2\pi q)\sum_{n=-\infty}^{\infty}\delta\left(t/T - n\right). \end{aligned} \tag{5.27}$$

To integrate the Eq. 5.27 over the one time period T, let's choose $t_0 = 0^+$ which will help to find out the *stroboscopic map* after each kick. In order to find the relation between (q_n^+, p_n^+) and (q_{n+1}^+, p_{n+1}^+), it is clear that momentum does not change after n^{th} and before $(n+1)^{th}$ kick, it changes abruptly at $(n+1)^{th}$ kick while position changes in between after n^{th} and before $(n+1)^{th}$ kick. After re-scaling $Tp \to p$ and $T^2 g \to K$, this gives the relation ,

$$\begin{aligned} q_{n+1} &= (q_n + p_n) \bmod 1, \\ p_{n+1} &= p_n - \frac{K}{2\pi}\sin(2\pi q_{n+1}). \end{aligned} \tag{5.28}$$

which is popularly known as *Chirikov-Taylor* map or *Standard map*. The fixed points of this map are $(0,0)$, $(1/2,0)$, stability analysis shows that $(0,0)$ is stable fixed point while $(1/2,0)$ is unstable. In addition, this is an area-preserving map. Cyclic property of q endows phase space with the topology of a cylinder. Let's give a boost of unity to momentum, and then we observe that due to mod 1, evolution of q is not affected and because of this and periodicity of the sinusoidal function, evolution of p also remains invariant. Hence translational boost by $n \in \mathbb{Z}$ is a symmetry of the Standard map. This allows one to take the modulo 1 for momentum as well and hence endows the topology of torus to the phase space. Similarly, it also enjoys a discrete symmetry of reflection about the centre of square *i.e.* $p \to (1-p)$, $q \to (1-q)$. In the limit $K = 0$, this map is completely integrable and with the increase in K, destruction and creation

of invariant surface (*i.e. KAM tori*) takes place. About $K \approx 1$, the last KAM torus breaks, allowing global diffusion in the momentum space. If the standard map is unfolded to a cylinder it displays normal diffusion in momentum for large enough K. When $K \gg 5$, the classical map is essentially fully chaotic. In Fig. 5.1, phase space of standard map for different K values are drawn. While for small $K(0.3)$, the phase space seems to constitute only invariant curves, $K = 10$ display phase space completely filled with points only (a hard chaos region) and $K = 1$ and 5 seems to represent the transition.

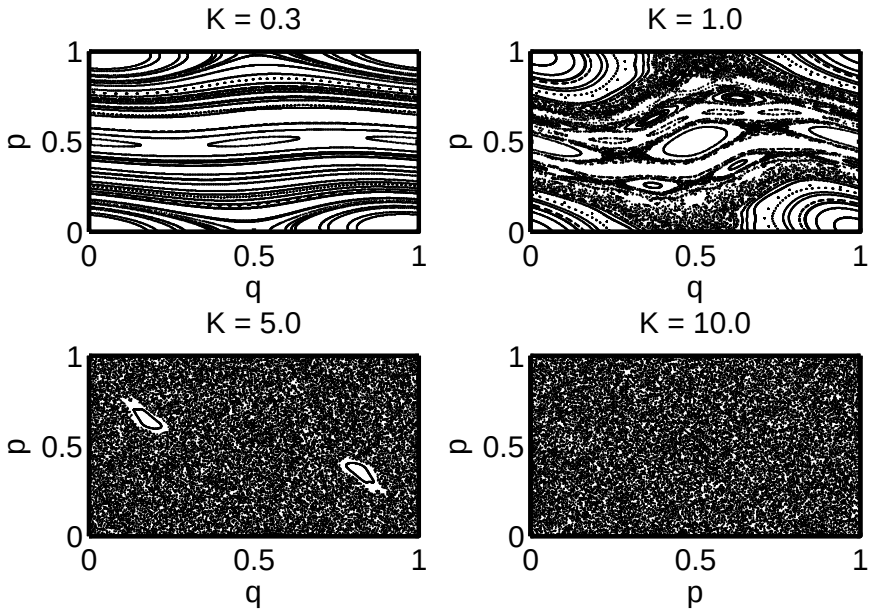

Figure 5.1: Phase space for different K values.

To study the quantum mechanics of such systems is what essentially defines the subject area of "Quantum Chaos" or "Quantum Chaology". Naturally quantization of such maps will be the first step. Analogous to (5.28), Heisenberg equations can be integrated to yield similar equation for the operators. Due to the δ-kicks, the duration of a kick is zero -this allows the integration of commutators between $\hat{q}$ and $\hat{p}$ to become zero. For standard map on the plane, it

is easy to see that corresponding unitary operator will be [Izrailev 1990],

$$\hat{U} = \exp\left(-\frac{igT}{2\pi^2\hbar}\cos(2\pi\hat{q})\right)\exp\left(-\frac{iT}{2\hbar}\hat{p}^2\right). \tag{5.29}$$

Due to periodicity in momentum and cyclic nature of position variable, the natural phase space will be $[0,1)\times[0,1)$ so this map needs to be quantized on torus. Due to periodicity of both the variables, quantum mechanics is to be done in finite dimension. A very illustrative description can be found in the notes [Lakshminarayan 2009]. The quantized standard map in position basis on torus takes the form,

$$\begin{aligned} U_{nn'} &= \frac{1}{N}\sum_{m=0}^{N-1}\exp\left[-i\pi\frac{(m+\beta)^2}{N}+2\pi i\frac{(m+\beta)}{N}(n-n')\right] \\ &\quad\times\exp\left[i\frac{KN}{2\pi}\cos\frac{2\pi(n'+\alpha)}{N}\right]. \end{aligned} \tag{5.30}$$

β and α are the phases which a state acquires along position and momentum directions respectively. For periodic boundary conditions, β is 0 while for anti-periodic, β is $1/2$. For all other β values, time-reversal symmetry is broken. A similar role is played by α for parity symmetry.

We will focus for the case, $\beta \neq 0$ and $\alpha \neq 0, 1/2$ when we can expect that both the time-reversal symmetry and parity symmetry are broken and the typical eigenstates would be like complex random states.

To develop more familiarity about the intensities in different eigenfunctions of Standard map, we have plotted them in Fig. 5.2 for $K = 0.3, 0.7$ and 5. It is clear that up to $K = 1$, intensities are (almost) symmetric about $p = 1/2$ despite α being 0.25. This will have an impact when different aspects of record statistics of intensity vectors are considered. Again, to develop the intuition in building up of various eigenfunctions on classical phase space structures, the

various eigenfunctions in coherent representation for $K = 0.3$ is shown in Fig. 5.3, alongside the classical phase space of standard map at the same parameter value. The various classical structure on which these states are built up can be clearly identified.

5.4.1 Intensity Distribution

Let's briefly recall the intensity distribution expected from random matrix theory for a complex random state. Constrained only by normalization, the joint probability distribution function is given by Eq. 5.10. Laplace transform of Eq. 5.11 is given by

$$\mathcal{L}(P) = P(x_1, \ldots, x_n; s) = \int_0^\infty e^{-us} P(x_1, \ldots, x_n; u) du. \tag{5.31}$$

To find the reduced JPDF depending only on first t variable, we need to integrate over $x_{t+1}, \cdots, x_N$,

$$\begin{aligned} P(x_1, \ldots x_t; s) &= \Gamma(N)\, e^{-s\sum_{i=1}^{t} x_i} \left[\prod_{i=t+1}^{N} \int_0^\infty dx_i e^{-sx_i} \right] \\ &= \frac{\Gamma(N)}{s^{N-t}} e^{-s\sum_{i=1}^{t} x_i}. \end{aligned}$$

For $t = 1$, reduced JPDF gives density distribution of the intensity of eigenvectors of the standard map,

$$\begin{aligned} \rho(x, s) &= \frac{\Gamma(N)}{s^{N-1}} e^{-sx}, \\ \rho(x) &= (N-1)(1-x)^{(N-2)} \Theta(1-x) \end{aligned} \tag{5.32}$$

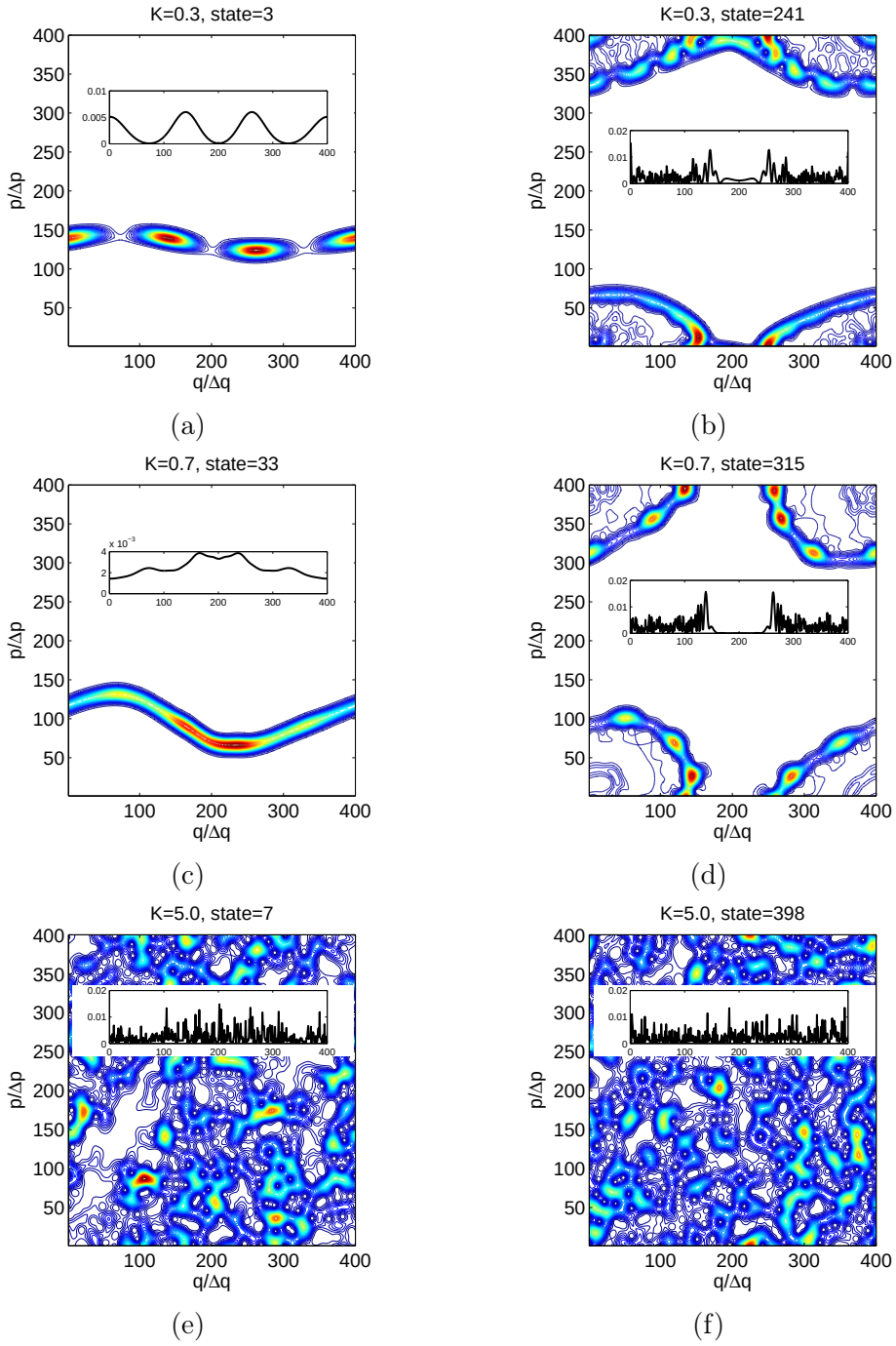

Figure 5.2: For different K value Husimi function, $|\langle q,p|\psi\rangle|^2$, of representative states and respective intensity plots are shown where $|q,p\rangle$ is coherent state which has been calculated following reference [Saraceno 1990]. Parity seems to be hold good for lower K values despite the value of α being 0.25 (*i.e. maximally broken parity*).

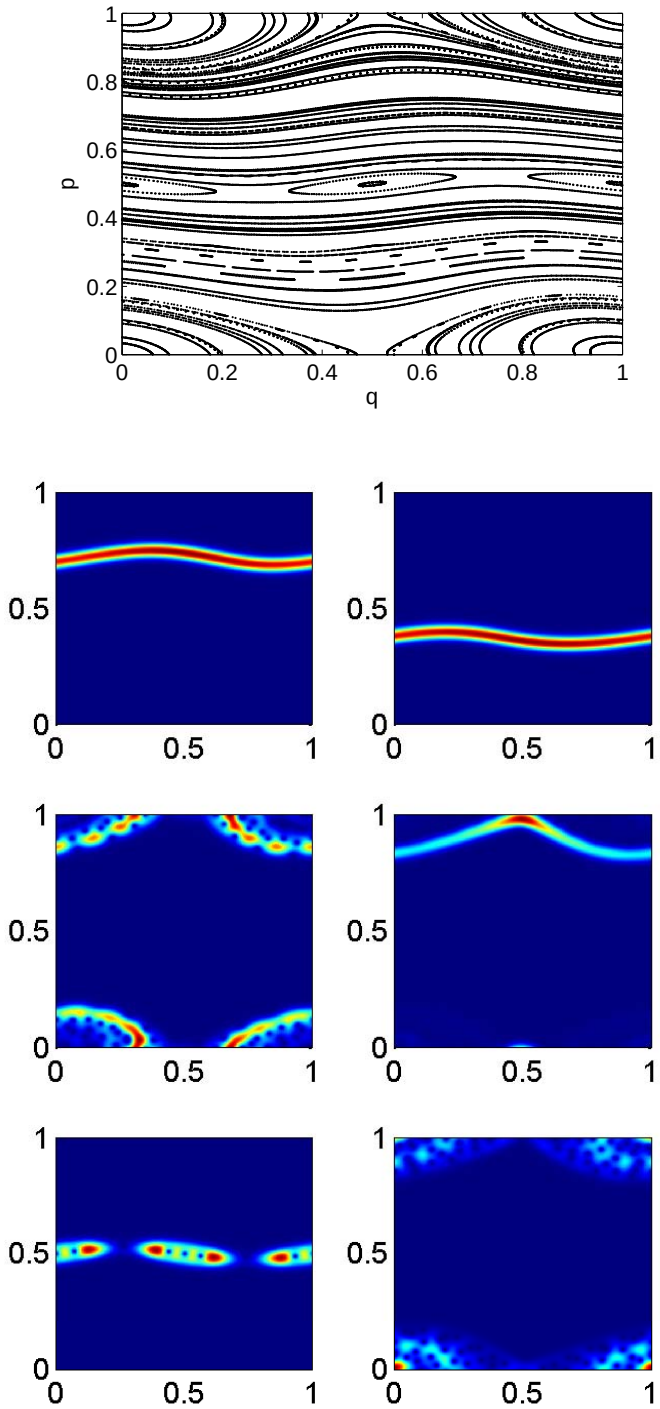

Figure 5.3: Phase space plot of standard map at $K = 0.3$ and Husimi function plot of various eigenfunctions of quantized standard map with same K.

where we have made use of the identity given in Eq. 5.33 for evaluating the inverse Laplace transform

$$\mathcal{L}^{-1}[e^{-as}G(s)] = \Theta(u-a)g(u-a) \quad \text{where} \quad G(s) = \mathcal{L}[g(u)]. \tag{5.33}$$

As the expected value of each intensity component is $1/N$, it will be convenient to transform to normalized variable $y = Nx$, and in the limit $N \to \infty$; this becomes the exponential distribution,

$$\rho(y) = e^{-y}. \tag{5.34}$$

For $N = 2048,\ 2050,\ 4096,\ 4098$, it is shown in Fig. 5.4. Except the tail region, it matches very well with the exponential distribution.

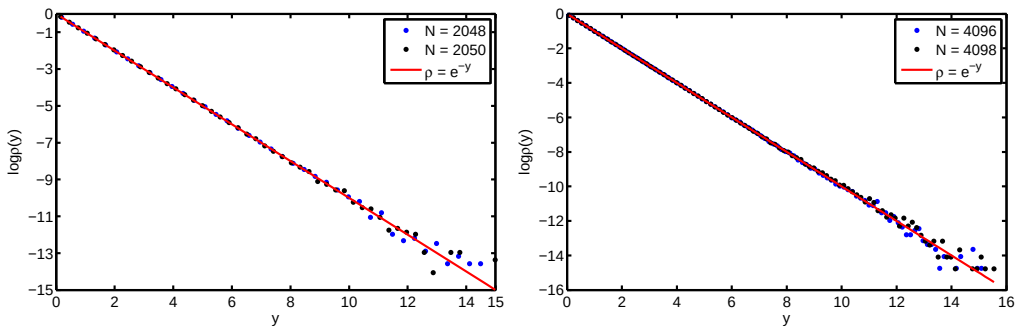

Figure 5.4: Intensity distribution for eigenvectors of standard map at $K = 10$, $\alpha = 0.25$, $\beta = 0.25$ for different $N = 2048,\ 2050,\ 4096,\ 4098$.

It is interesting to now talk about what is happening in the tail region, what is the distribution of these large intensities? Is there a pattern in observing the higher and higher intensities as we go along the index of eigenvectors? What is the probability of occurrence of maximum intensity in, say middle of the eigenfunction? These are some questions that we will be addressing in the remaining part of the chapter utilizing the results obtained in Section 5.3.

5.5 Record statistics for standard map eigenvectors

For large K quantum eigenstates of standard map follow the CUE/GUE or COE/GOE results depending on the value of the phases α and β. If $\beta \neq 0$ and $\alpha \neq 0, 1/2$ we can expect that both the time-reversal symmetry and parity symmetry is broken and the typical eigenstates would be like complex random states.

The dimensionality of the Hilbert space N is the inverse (scaled) Planck constant. Thus the "data" in this case are the various eigenfunctions and especially their intensities. The upper records, created in "time" are the peaks of the eigenfunctions that outdo all the intensities prior to it as we increase the index of the eigenfunction component. Clearly this can in general depend on the space in which the eigenfunctions are represented. Thus for small values of K we expect there to be many localized states in the momentum space while being nearly uniformly distributed in the position, and this will reflect in any studies of records or extremes. However for large K, position or momentum basis will be equivalent up to fluctuations.

The average upper record as a function of the index, normalized by the dimension of the Hilbert space (which acts as "time" for these vectors), for various values of K is plotted in Fig. 5.5a. While this agrees well with the random states result in the chaotic region, there are interesting deviations in the mixed phase space regime of $K < 5$. For example when K $(= 0.3)$, in the position space most of the records are set up by $t/N = 0.5$ originating in the very weakly broken parity symmetry. There are significant deviations from the random state even for $K = 5$, while for $K = 10$ these disappear. The momentum space average records are somewhat similar but mostly lie above

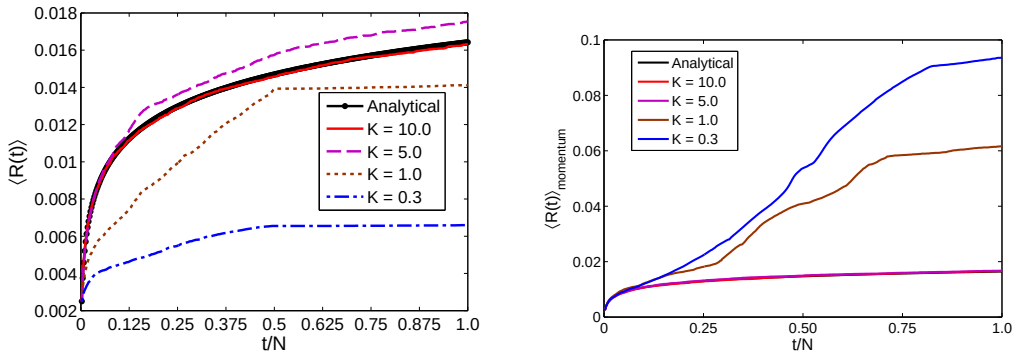

(a) position representation (b) momentum representation

Figure 5.5: The average upper record $\langle R(t)\rangle$, from the ensemble of eigenstates of the quantum standard map. The parameters used are $N = 400$ and $K = 10$ (highly chaotic), $K = 5$ (mostly chaotic), $K = 1$ (mixed phase space), and $K = 0.3$ (mostly regular). The analytical curve refers to the random state result in Eq. 5.18. In all cases $\alpha = \beta = 0.25$.

the random state result and are not affected as much by the weakly broken parity symmetry due to their localization (see Fig. 5.5b). A similar picture appears with lower records as well, the results of random vector is followed for large $K(= 10)$, while for smaller K the records themselves do not vary with t as compared to chaotic cases. (see Fig. 5.6). As is clear that upper record and lower record combined will give the variation of the values that function assumes, let's call it range, therefore in the case of standard map for smaller K values (close to integrable regime), say $K = 0.3$, average range of the intensities of eigenvectors is very small as compared to large K values (chaotic regime), say $K = 10$ (See Fig. 5.5a and Fig. 5.6). This is consistent with semiclassical analysis that for smaller value of K invariant rotation KAM tori are not broken and therefore support wavefunctions with smaller range.

As has been previously discussed, the distribution of the upper (lower) record at "time" t is Gumbel (exponential) for large N with appropriate shift and scaling. It is shown in Fig. 5.7a (Fig. 5.7b) that indeed the upper (lower) record for eigenfunctions of the quantum standard map in the classically chaotic

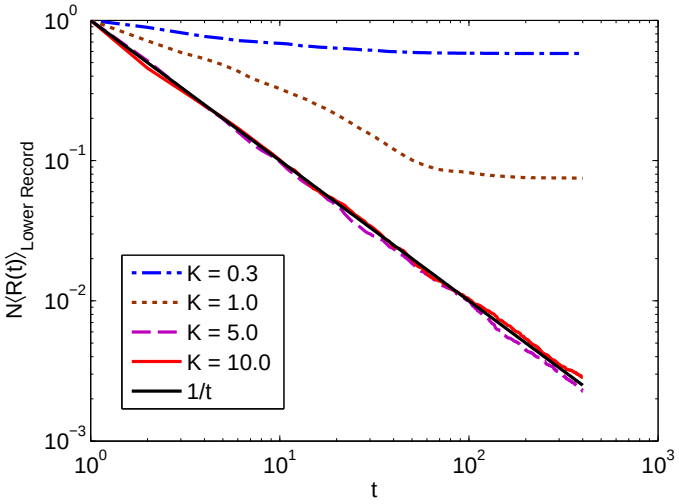

Figure 5.6: The average lower record $\langle R(t)\rangle_{\text{lower record}}$, from the ensemble of eigenstates of the quantum standard map in position representation. The parameters used are $N = 400$ and $K = 10$ (highly chaotic), $K = 5$ (mostly chaotic), $K = 1$ (mixed phase space), and $K = 0.3$ (mostly regular). The analytical curve refers to the random state result in Eq. 5.25. In all cases $\alpha = \beta = 0.25$.

regime is Gumbel (exponentially)-distributed; also plotted is the distribution for the "upper (lower) record" when $t = N$ which refers to the maximum (minimum) intensity, thus recovering the earlier results of [Lakshminarayan 2008]. For small N, deviations from Gumbel are seen when the exact result $P(R, t)$ derived above is to be used; this is illustrated in the inset of this figure.

The distribution of the position of the maximum in the position representation is shown in Fig. 5.8a, where one can see a transition to the uniform distribution along with the transition to classical chaos. The sharp peak at the center for small K (here $K = 0.3$) is interesting and deserves further comment. For small K, when there are many narrow classical resonances, a significant fraction of eigenfunctions that are localized on separatrices possess maximum intensity at or very close to $q = 1/2$. For instance, for $N = 400$ when $K = 0.1$ and 0.3, about 75% and 50% of states are peaked at $q = 1/2$. As we increase K, more islands start appearing with turning points away from $q = 1/2$, and

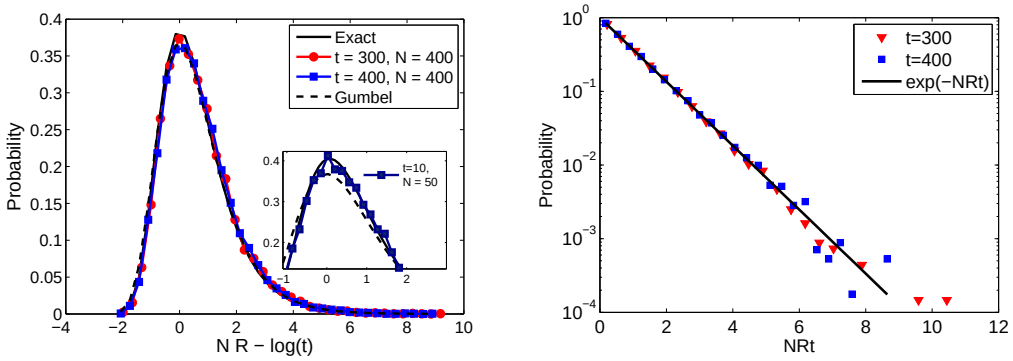

(a) upper record (b) lower record

Figure 5.7: The distribution of the upper (lower) records when the index is t for eigenfunctions of the quantum standard map with $K = 10$. After re-scaling and a shift, the distributions are of the Gumbel (exponential) type. In case of upper records for small N (see inset for upper record case) deviations are seen from Gumbel and the exact formula for $P(R, t)$ is to be used.

eigenstates localized in their interior, thereby the maximum intensity shifts away from $q = 1/2$. This provides a qualitative mechanism leading to uniform distribution for maximum intensity for large K. This qualitative explanation is also well supported by the distribution of the position of minimum in the position representation. As we expect and indeed observe that most of the states have their minimum around stable fixed point, *i.e.* $q = 0$ (see Fig. 5.8b. The transition in classical behavior from integrable ($K = 0$), to mixed phase space where islands of stability coexist within the stochastic sea (intermediate K), to fully-developed chaos is well captured by the quantity $S_N(m)$. In the inset of Fig. 5.8a is shown the maximum intensity of individual states (again $N = 400$) vs their actual position. For $K = 0.3$, there are a large number of states which have maximum intensity at $q = 1/2$ (index = 200). This manifests in the form of the observed sharp peak. These get gradually destroyed on increasing K; indeed such measures seem useful to pursue further in classifying states in the mixed phase-space regime.

It has been shown above that for random N-dimensional vectors there are

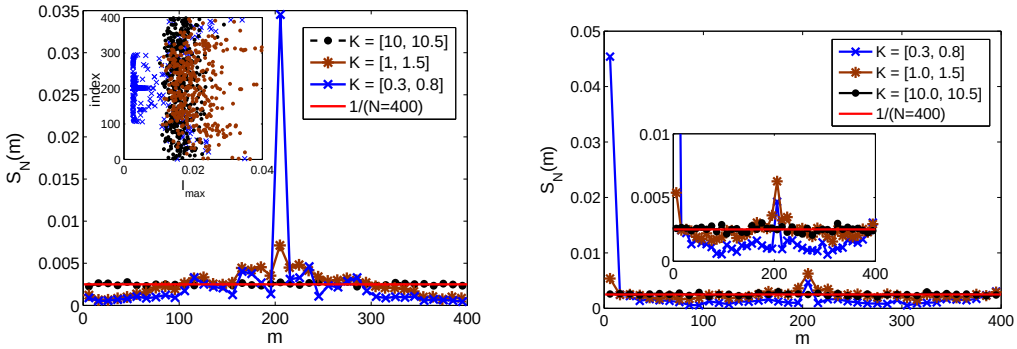

(a) upper record (b) lower record

Figure 5.8: The distribution of the position of the last record set, which is also the maximum in case of upper record and minimum in case of lower record, for eigenfunctions of the standard map with $N = 400$ and for various values of K. In Fig. 5.8b, inset shows a zoomed in view to clearly see the features of $S_N(m)$ as function of m for various K values.

on the average $\sim \log N + \gamma$ intensity records for both upper and lower. While we can expect to see this for the standard map in the chaotic regime, the mixed and near-integrable regimes show a marked departure. The correlations lead to results that are similar to those for the random walks, with a power-law scaling in N. The ratio of standard deviation of the number of records to the average is found to be of order one, indicating non-stationarity of the distribution. For very small K the number of records is simply $\mathcal{O}(N)$, as the eigenfunctions are describable by smooth functions. In the mixed-regime, and, when $K < 1$, a power-law along with a logarithmic dependance is clearly indicated. Intriguingly, *it is almost a pure power-law with exponent* 0.5 *at the critical value* $K = 0.98$. For moderate values such as $K = 2.3$ a clear separation of the phase space into chaotic and regular regions and a subsequent separation of the quantum spectra seems to make the numerical fits unstable. Further, for very large K (say 9.8), the result from the random vector case applies (Fig. 5.9a)and Fig. 5.9b. This reflects the changing nature of the wavefunction intensities, and indicates that at criticality it is close to some

kind of $1/f$ noise. Eigenvalue fluctuations in quantum chaotic systems are known to have $1/f^{\gamma}$ noise [Santhanam 2005a], and further work on the spectral properties of intensities is therefore called for. The average number of records

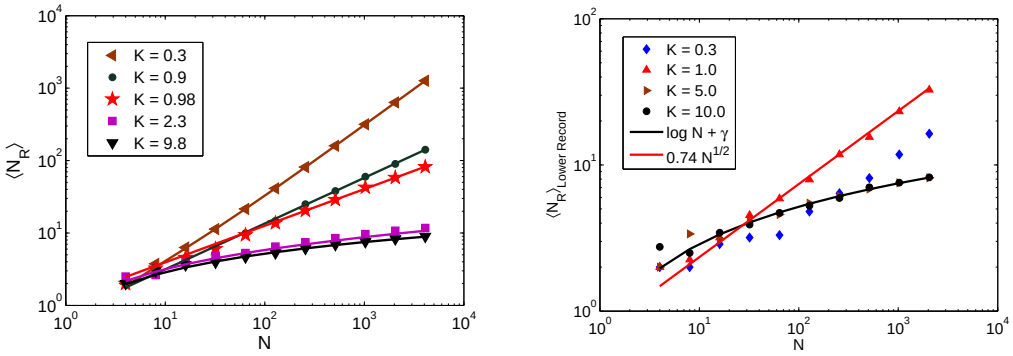

(a) upper record (b) lower record

Figure 5.9: (a) Average number of record in eigenfunction of the quantum standard map of length N vs N is plotted for various K values. Solid line (except $K = 9.8$) are fitted expression $a\log(N) + bN^c$, for $K = 9.8$ it is $\log(N) + \gamma$. a, b, c for different K values are,(I) $K = 0.3$, $a = 0.45 \pm 0.15$, $b = 0.306 \pm 0.007$, $c = 1.001 \pm 0.003$,(II) $K = 0.9$, $a \approx 0$, $b = 0.73 \pm 0.06$, $c = 0.63 \pm 0.01$, (III) $K = 0.98$, $a \approx 0$, $b = 1.2 \pm 0.2$, $c = 0.50 \pm 0.01$ and (IV) $K = 2.3$, $a = 0.9 \pm 0.3$, $b = 0.7 \pm 0.6$, $c = 0.21 \pm 0.04$. (b) For lower records representative fitted expressions are put in legend. Here too as in case of upper records, at $K \sim 1$ function $N^{1/2}$ provides good fit.

as a function of K is presented in Fig. 5.10, where the effects of the scaling in the mixed regime manifests. It is remarkable that while record numbers in both, the momentum and the position representation, approximately converge after $K \approx 2$, it is only when $K > 5$ when there may be tiny islands (if at all) that it returns to the result of the random vectors. These observations establish the connection between classical dynamics in all the regimes with the record statistics for the eigenvectors of the quantum standard map. Since the standard map is a paradigmatic model, we believe this connection to hold generally.

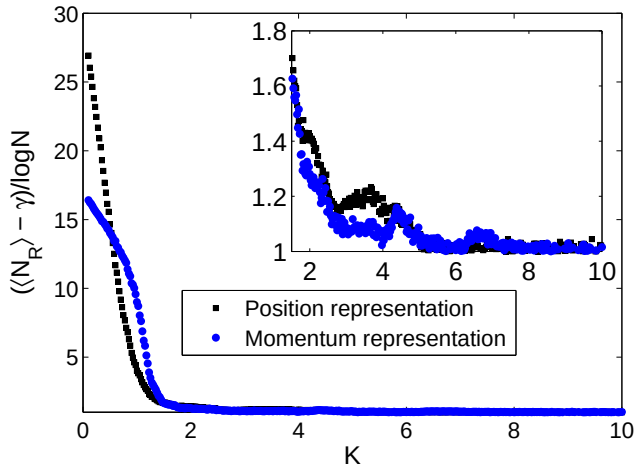

Figure 5.10: An appropriately scaled and shifted average number of records $\langle N_R \rangle$ *vs* K for the eigenfunctions of the quantum standard map with $N = 400$. In inset zooming up graph around $K > 1.5$ is plotted and a lot of structures can be seen. It is only after $K > 5$, both representations converge to the result obtained for random vector case.

5.6 Summary

In this chapter, we have derived results on upper (lower) records of intensities of correlated random vectors. Apart from deriving the average record, it has been shown that the probability that a record appears at an index j is a Bernoulli process, which is the same as for i.i.d. variables. The quantum standard map presents the scope of studying systems which possess increasingly complex spectrum with the system parameter, K. For a quantum system with random high-lying states, records' statistics found in the Section 5.3 applies. The study of position of the last record set in case of standard map, parameterized by K suggests that beyond a certain value of K, the eigenvectors become like random vectors insofar as the records of intensities is concerned. This is also consistent with the finding where the number of records vs N goes through a transition from linear to algebraic to logarithmic, as K increases. Remarkably, a signature of breaking of the last torus at $K \simeq 0.98$ is found to be in

the exponent one-half in the power-law obeyed by the number of records. It is very likely that the conclusions drawn on the quantum standard map would hold for other quasi-integrable and mixed systems.

Chapter 6

Kolmogorov stochasticity parameter as a measure of quantum chaos

Contents

6.1 Introduction

Quantum chaos presents an understanding of how classical dynamics of a system manifests in its quantal behaviour. In this pursuit, a detailed study of correlations among the energy levels has been undertaken and several universality classes have been identified. Based on the statistical correlations of fluctuations in the energy level sequences, a highly successful theory in terms of random matrices is already in place [Brack 2003, Mehta 2004, Reichl 2004, Haake 1991]. Semiclassically, these fluctuation properties are studied in terms of periodic orbits by employing trace formulae [Gutzwiller 1990,

Parab 1996, Heusler 2007]. Perhaps the most popular measure is the nearest-neighbour level-spacing statistics [Reichl 2004, Haake 1991], $P(S)$ giving the frequency of occurrence of a certain spacing, S for a given spectrum of levels. For generic integrable systems, it was argued by Berry and Tabor that the spacing amongst the nearest neighbours is distributed in a Poissonian manner [Berry 1977b]. It is observed that the fluctuation properties of energy levels of quantized time-reversal invariant chaotic systems, either possessing an additional continuous symmetry (like rotation) or with a broken rotational symmetry but possessing an integral spin, agree with those of the Orthogonal Ensemble of random matrices, exhibiting level repulsion as $P(S) \sim S$, for small S [Mehta 2004, Haake 1991, Bohigas 1984]. However, a linear level repulsion is observed for quantized polygonal billiards [Date 1995, Grémaud 1998, Bogomolny 1999, Richens 1981] also when these are non-integrable and non-chaotic (*e.g.*rhombus billiard) [Richens 1981, Eckhardt 1984, Jain 1995]. In addition, there are some recent works where a linear level repulsion is obtained when both parity and time-reversal invariance are broken where there exists a pseudo-unitary symmetry [Ahmed 2003b, Ahmed 2003a, Jain 2008b, Jain 2009]. In random matrix theory context, we have shown other examples of cyclic and reverse cyclic matrices in Chapters 2 and 3 producing linear level repulsion.

There are other instances when fluctuation properties of the level sequences are studied with quantities like fluctuations in average cumulative density of states [Aurich 1994] and the conjectures given have been verified in experimental data or numerically [Alt 1998]. In another work fluctuation in level sequences has been treated as time-series and spectrum has been shown to display a characteristic $f^{-\gamma}$ noise during order to chaos transition with γ related to classical chaos in the system [Santhanam 2005b, Relaño 2002]. Further self-similarity of the spectrum was studied and Hausdorff measure for the spectra of atoms

and Gaussian ensemble has been calculated [Santhanam 2006]. Inspired by the work of Arnold [Arnold 2008], in which he employed the stochasticity parameter of Kolmogorov [Kolmogorov 1933] to number sequences for discussing inherent randomness, we propose to study the fluctuation properties in cumulative level density of quantum systems. In this work, we have shown that the probability distribution function for the proposed measure falls in two different categories for most of the level sequences studied. It is interesting to observe that the sequences in one family originate from the integrable systems while the other from classically chaotic systems. We have mostly considered billiards as the models of our dynamical systems apart from studying the Standard map, the Riemann zeros and the Gaussian Unitary Ensemble (GUE) of random matrices. The statistic we propose has a long history for the independent, identically distributed random variables. The limiting distribution for such random variables is the well-known Kolmogorov distribution, a well-documented subject of study [Feller 1988, Kendall 1946]. It is well-known [Arnold 2008, Kendall 1946] that the stochastic probability for a shorter sequence can be given if the limiting distribution is known, an instance of this can be seen in [Arnold 2008] where a comparison is made for two number sequences with just fifteen numbers on the basis of the Kolmogorov distribution. We would like to derive the limiting distributions analytically also, but this remains open.

The plan of this chapter is as follows. In Section 6.2, we present the definition of Kolmogorov stochasticity parameter, λ. Using the semiclassical trace formulae for evaluating the oscillatory term, the stochasticity parameter is calculated and compared with the numerical calculations using the eigenvalue sequences for different systems. Putting all these expressions together, we show that λ scales with the length of the set of energy levels. In Section 6.3, we present probability distribution functions (PDF) of λ for energy level sequences

of different dynamical systems. We also present results for the zeros of the Riemann zeta function, and, for the Gaussian Unitary Ensemble (GUE) of random matrices. Finally, we conclude by showing that with these PDFs, we can distinguish the spectra from integrable and chaotic systems.

6.2 Kolmogorov stochasticity parameter

6.2.1 Definition

Consider a quantum system $\mathcal{S}_i$ which possesses energy levels corresponding to its bound states, $E_1 \leq E_2 \leq \ldots E_n$. The cumulative density of levels is defined as

$$N(E) = \sum_{i=1}^{n} g_i \Theta(E - E_i) \tag{6.1}$$

where g_i denotes the degree of degeneracy of the level, E_i, and the sum over the Heaviside step function represents the well-known staircase. The average cumulative density of levels can be obtained by various methods for quantum systems, be it the Thomas-Fermi method [Brack 2003] or via the Weyl formula [Baltes 1976]. To be specific, we take simple systems that are illustrative and popular in quantum chaos studies - the two-dimensional quantum billiards and quantized maps.

To motivate the analogy deriving from the work of Kolmogorov, let us first present the definition of this parameter, λ_n^K as given by Arnold for real numbers, $x_1 \leq x_2 \leq ... \leq x_n$. Let the number of elements x_i which are $\leq X$ be given by an empirical counting function, $C_n(X)$. Let us assume that there is a theoretical counting function, $C_0(X) = n\times$(probability that an event $x \leq X$) [Arnold 2008]. The parameter is defined as

$$\lambda_n^K = \sup_X |C_n(X) - C_0(X)|/\sqrt{n}. \tag{6.2}$$

In analogy with the definition given by Kolmogorov [Kolmogorov 1933], let us now introduce the stochasticity parameter in quantum mechanics,

$$\lambda_n = \sup_E \frac{|N(E) - \overline{N}(E)|}{\sqrt{n}}, \tag{6.3}$$

with $\overline{N}(E)$ denoting the average, smoothed cumulative density of energy levels [Baltes 1976, Balian 1970, Balian 1971]. In the large number of eigenvalue limit, the difference $N(E) - \overline{N}(E)$ will be just the oscillating part of the density of levels for which we can employ the trace formulae [Gutzwiller 1990] whenever possible.

For completeness, we would like to recall that statistical investigations of $N(E) - \overline{N}(E)$ have been carried out in the past, albeit with a different normalization, as a measure of quantum chaos in spectra [Aurich 1994]. In these studies, the measure was taken as

$$W(x) = \frac{N(x) - \overline{N}(x)}{\sqrt{\Delta_\infty(x)}} \tag{6.4}$$

where $\Delta_\infty(x)$ is the limit of the spectral rigidity, $\Delta_3(L; E)$ as $L \to \infty$. Let us recall that spectral rigidity , $\Delta_3(L)$ measures the mean square deviation of the cumulative density $N(E)$ from a straight line in an interval $[E - L/2, E + L/2]$. In [Aurich 1994], the discrete spectrum of a system $\{E_n\}$ was studied in terms of a variable x such that

$$x_n = (E_n)^\alpha, \quad \text{with } \alpha = \frac{1}{2} \text{ for billiards} \tag{6.5}$$

It is important to note here that here too the studies are performed with unfolded sequence of energy levels. It was shown that $W(x)$ possesses a limit distribution with zero mean and unit variance for bound, conservative and scal-

ing systems. For classically (integrable) chaotic systems, the distribution was expected to be (non-)Gaussian. These predictions were verified in a statistical analysis of eigenmodes of a superconducting microwave billiards [Alt 1998]. For a Bunimovich stadium, the three-dimensional Sinai billiard, and for Limacon billiards, a Gaussian distribution was found. In contrast, for a two-dimensional circular billiard, a non-Gaussian distribution was obtained.

Practically, to calculate λ_n for a given sequence of length n, the procedure followed is sketched as follows:

1. sort the given sequence and calculate $N(E_k) - \overline{N}(E_k)$ for various E_k, $k = 1, \ldots n$, where $N(E_k)$ is number of eigenvalues less than or equal to energy E_k and $\overline{N}(E_k)$ is the expected value of the same (calculated from Weyl's formula);

2. choose the maximum of the numbers calculated in step 1, and divide it by $\sqrt{n}$ where n being the length of the sequence. This is desired λ_n.

Our first task is to estimate the length of the sequence for systems which would allow statistical errors that wouldn't alter our main conclusions. To accomplish this, we have compared calculations of Eq. 6.3 from exact (analytically or numerically obtained) density with the calculations based on the trace formulae. The details of calculating eigenvalues for various systems considered here and calculation of λ_n using trace formulae are presented in the Appendix B. In this work, we have used Gutzwiller's trace formula for billiard systems while a Maclaurin series expansion (Selberg trace formula [Terras 1985]) for the Riemann zeros. We see that even a finite sequence length of size 5000 reproduces the behaviour obtained from trace formulae Fig. 6.1 quite well.

An important feature to note in the Fig. 6.1 are the prominence of discontinuities in λ_n as a function of n for integrable cases as compared to chaotic ones.

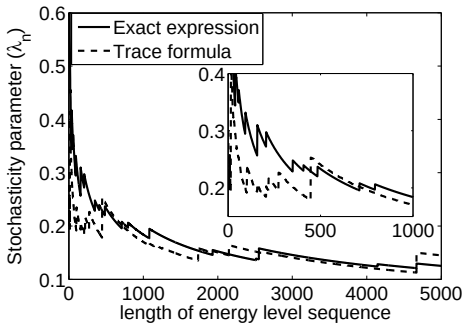

(a) rectangular billiard

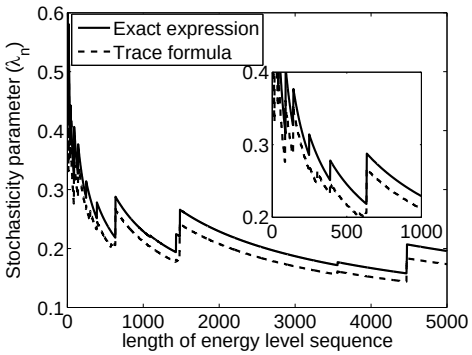

(b) circular billiard of unit radius

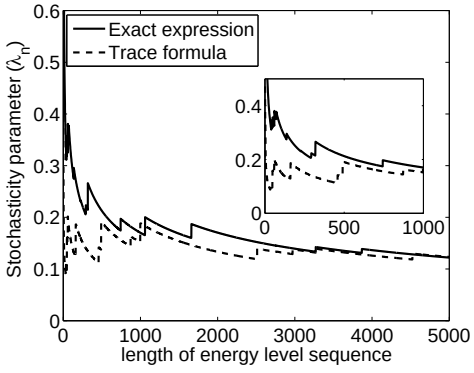

(c) triangular billiard of side length $\frac{4}{3}$

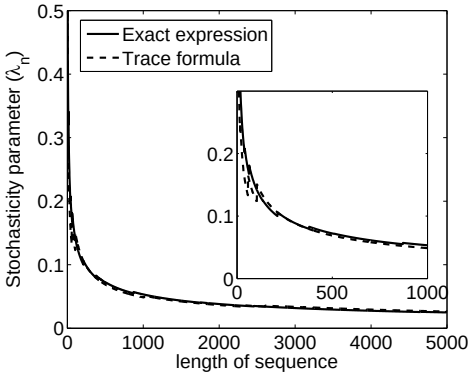

(d) zeros of Riemann zeta function,the values of σ is taken as $\frac{1}{2}$

Figure 6.1: Stochasticity parameter calculated using the exact expression and trace formula.

To understand this feature let's take a re-look on the definition of λ_n itself. It is clear that $\sqrt{n}$ is providing the correct scaling to make λ_n bounded in large sequence limit. The numerator as we have already discussed is $\sup_E |N_{\rm osc}(E)|$ is max of $|N_{\rm osc}(E_k)|$ for $k = 1, \ldots, n$, but this is definition of record as we have seen in Chapter 5. Hence, an irregularity occurs exactly at the point where a new record is setup and in between two such instances the last record set is being scaled by scaling factor $\sqrt{n}$. Number of discontinuities directly give the number of records set. As we have seen in Chapter 5 that for integrable system the number of records are given by power law in length of the sequence while in chaotic case it is much weaker logarithmic dependance. This explains

the comparatively smoother dependance of λ_n on n in case of Riemann zeros (which behaves like chaotic system) as seen in Fig. 6.1.

6.2.2 Scaling

For the Riemann zeros, λ_n versus n (a log-log plot will be straight line, as shown in Fig.6.2) suggests a power law behaviour. Surprisingly, we find a similar behaviour for various systems. Moreover, on comparing each of them with $\sim n^{-\alpha}$, we extract a monotonically changing index, α varying from 0.15 for circular billiard to 0.44 for Riemann zeros with a value 0.34 for the chaotic standard map. The values of this index are listed in Table 6.3. These show an increasing trend as the system becomes classically chaotic.

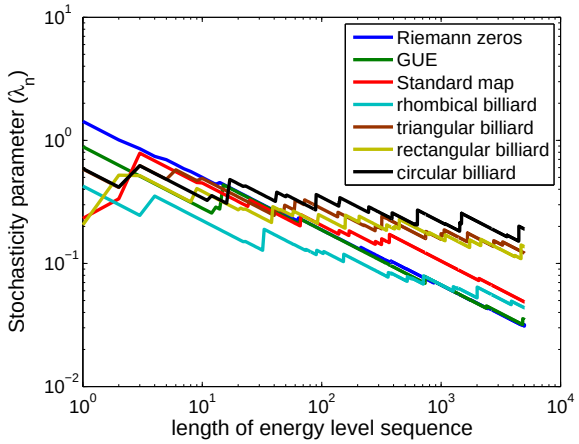

Figure 6.2: Stochasticity parameter for all the systems considered are displayed here as a function of logarithm of the length of the sequence, n. This brings out an interesting observation, λ scales as $n^{-\alpha}$ and leads us to finding the best fitted values for the index, α (R^2 (goodness of fit parameter) varies from 0.80 for circular billiard to 0.95 for Riemann zeros). As the systems become increasingly stochastic, the value of the index increases.

To understand the scaling behaviour of λ_n with n, let's take an extreme case where $|N_{\rm osc}(E)|$ is such that largest fluctuation occurs for the first eigenvalue itself, then in that case only one record is set and that is the λ_1 then all the λ_n will be given by $\lambda_1/\sqrt{n}$ and the scaling coefficient α will be 0.5. Due to

setting up of more records α will come down from value half. As there are more records in case of integrable system than chaotic cases or Riemann zeros, α will be smaller in former case than latter. This provides the qualitative understanding of ordering of α.

6.3 Probability distribution functions

For an ordered eigenvalue sequence of length n, for which we have n values of λ which themselves are random, the probability distribution function of these λ_ns has been studied. The numerical evaluation of a probability distribution function is summarized in the following steps:

- for an ordered sequence of length n, we can have n-subsequences of length $1, 2, \ldots n$, always starting from the lowest element and increasing by one element;
- for each subsequence we calculate λ;
- this way, we end-up with n, λs and a histogram of these λs gives the probability distribution function (PDF) of λ for the sequence denoted by $\Phi'(\lambda)$. The cumulative distribution function, $\Phi(\Lambda)$, is defined as, $\int_0^\Lambda \Phi'(\lambda)\,\mathrm{d}\lambda$.

For all the systems studied in this work, sequence length is kept fixed to 5000.

6.3.1 Integrable billiards

For the integrable billiards like circle, rectangle, and equilateral triangle, the values of the stochasticity parameter, λ evaluated for $n = 5000$ are respectively 0.19, 0.13, and 0.12, all comparable; these values are stable with the length of the sequence. Probability distribution functions of λ for the integrable systems are very close to each other (Fig. 6.3). The function, $\Phi'_{integrable}(\lambda) \sim$

Table 6.1: A form $c_1 \exp(-\lambda^\beta)$ is fitted for the probability distribution function $\Phi'(\lambda)$ for the class of integrable and almost integrable systems. The fitting co-efficient, goodness of fit parameters and value of $\Phi'(\Lambda)$ at $\Lambda = \lambda_{5000}$ is tabulated here.

System	Co-efficients	Goodness of fit	$\Lambda = \lambda_{5000}$	$\Phi'(\Lambda)$
Rectangle	c_1=4.163 (3.575,4.75), β=3.196 (2.202,4.19)	SSE: 2.33, R^2: 0.8721	0.1365	1.1146
Circle	c_1=4.344 (3.907,4.781), β=2.927(2.304,3.551)	SSE: 1.509, R^2: 0.9227	0.1900	1.1124
Triangle	c_1=4.703 (4.101,5.305), β=3.826 (2.719,4.933)	SSE: 1.84, R^2: 0.9023	0.1212	1.1057
Rhombus	c_1=3.626 (3.534,3.718), β=4.367(4.092,4.642)	SSE: 0.025, R^2: 0.9972	0.0436	1.0977

$c_1 \exp(-\lambda^\beta)$ fits the data reasonable well (for details, see the Table. 6.1)[1]. The value of Φ at λ gives the stochastic probability of the level sequence and is listed in Table 6.3 (It should be noted that the values quoted for the parameters are the fitted values in the given range, but finally we have to normalize the fitted function over zero to infinity and this normalized distribution will be used to calculate $\Phi'(\Lambda)$. The numbers given in the text or Tables are obtained in this manner).

6.3.2 Non-integrable systems

For the quantized standard map, $\Lambda_{standard}$ for 5000 levels is 0.0486. The function that fits the probability distribution of Λ for standard map, Riemann zeros, and eigenvalues of GUE are all close to each other, represented by $(c + \lambda)^{-\gamma}$ where γ is about 3.6 - 4.4 (see Table6.2). We find the measure of stochasticity, $\Phi(\Lambda_{standard}) = 0.4862$. Further, on considering zeros of Riemann zeta function,

[1]SSE is sum of squared error which measures the total deviation from fit value, while R^2 measures the success of the fit in explaining the variation of the data.

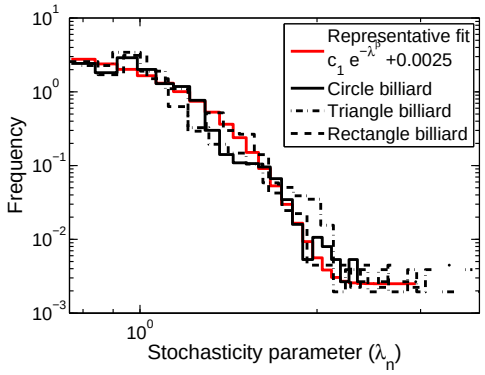

Figure 6.3: The probability distribution functions of the stochasticity parameter are shown for three integrable billiards, viz. circle (solid), rectangle (dashed), and equilateral triangle (dot-dashed). For these billiards, the distributions have been fitted to a functional form, $c_1 \exp(-\lambda^\beta)$), with (c_1, β) taking values (4.344, 2.927), (4.163, 3.196), and (4.703, 3.826) for circle, rectangle, and equilateral triangle respectively.

$\Lambda_\zeta = 0.0315$ and $\Phi(\Lambda_\zeta) = 0.3775$. These are more than twice compared to the values for integrable case (see Table 6.3). Since it is very well-known that the fluctuation properties of Riemann zeros agree with those of the eigenvalues of unitary ensemble of random matrices, we have also calculated the stochasticity parameter and its distribution for them. We find $\Lambda_{GUE} = 0.035$, fitting function is identical and $\Phi(\Lambda_{GUE}) = 0.4028$. For the $\pi/3$-rhombus billiard, classical phase space surface is topologically equivalent to a sphere with two handles

Table 6.2: A form $(c + \lambda)^{-\gamma}$ is fitted for the probability distribution function $\Phi'(\lambda)$ for the class of chaotic system. The fitting co-efficient, goodness of fit parameters and value of $\Phi'(\Lambda)$ at $\Lambda = \lambda_{5000}$ is tabulated here.

System	Co-efficients	Goodness of fit	$\Lambda = \lambda_{5000}$	$\Phi'(\Lambda)$
Standard map	c=0.1688(0.1606,0.1771), γ=3.632(3.463,3.8)	SSE: 0.014, R^2: 0.9972	0.0486	6.2202
GUE	c=0.1932(0.1907,0.1958), γ=4.097(4.02,4.173)	SSE: 0.001, R^2: 0.9997	0.035	8.1038
Riemann zeros	c=0.2103(0.2091,0.2115), γ=4.397(4.336,4.459)	SSE: 0.0002, R^2: 0.9999	0.0315	8.7443

Table 6.3: α, Φ and Φ' for different systems.

System	α	Φ	Φ'
Circle	0.15	0.21	1.11
Rectangle	0.18	0.15	1.11
Triangle	0.18	0.13	1.10
Rhombus	0.25	0.05	1.09
Standard Map	0.34	0.49	6.22
GUE	0.39	0.40	8.10
Riemann zeros	0.44	0.38	8.74

[Eckhardt 1984, Jain 2008a], Lyapunov exponent is zero. The energy levels of this almost integrable system entails an intermediate value for the stochasticity parameter. The probability distribution function also shows a concurrence with the family of integrable billiards (see Table 6.1).

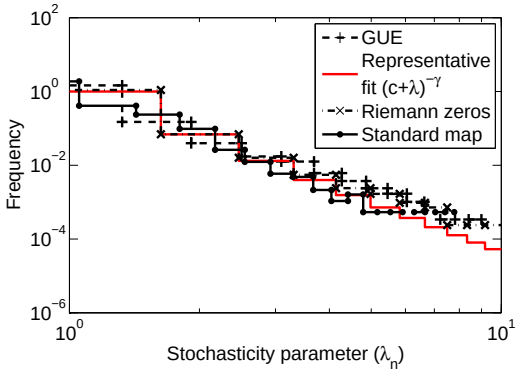

Figure 6.4: The probability distributions of the stochasticity parameter are shown for standard map, Gaussian Unitary Ensemble (GUE), and Riemann zeros. For these systems, the distributions can be fitted to a functional form, $(c+\lambda)^{-\gamma}$, with (c, γ) taking values (0.1688, 3.632), (0.1932, 4.097), and (0.2103, 4.397) for standard map, GUE, and Riemann zeros respectively.

These results point at certain interesting conclusions: (i) stochasticity parameter can characterize the level sequences coming from random matrices, quantum systems, and number theory, (ii) probability density distributions are distinctly different for integrable and chaotic quantum systems, (iii) we observe the confluence of the statistical behaviour of Riemann zeros and unitary ensem-

ble in terms of λ as in random matrix theory. In a nutshell, we show Fig.6.5 which depicts how with changing α PDF values for all systems varies.[2]

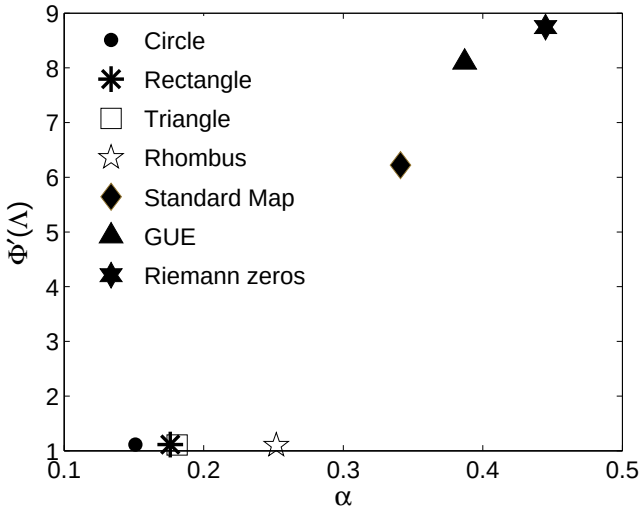

Figure 6.5: Two measures of stochasticity, α and $\Phi'(\Lambda)$, are being plotted here against each other. For calculating the PDF at stochasticity parameter for a specific system, we have normalized the distributions. As the index α increases, we see that the $\Phi'(\Lambda)$ undergoes a jump by an order of magnitude.

6.3.3 Connections with number theory

Finally, we would like to present the precise connection of our ideas with a well-known number-theoretic problem of counting the lattice points in a circle of radius, R, first studied by Gauss [Hardy 1979]. The difference of this number with the area of the circle, known as the error term with proper normalization, has been investigated extensively [Iwaniec 1988]. A connection of this problem with quantized integrable systems in two dimensions which have

[2]However as a side note, we remark that for 1000 levels, the values for rectangle and circle billiard do not change much from 1.10 value for (Φ') while the values for zeta function turns out to be 4.81, and for GUE the stochastic probability comes down to 3.46. We do not know the invariant distribution beforehand so we require considerable data (length of sequence) to reduce statistical errors for finding the distribution; we have utilized the trace formulae to fix the length sufficient to produce the same λ_n. This enables us to see the differences among different dynamical systems in α vs Φ' graph by considering only 5000 levels. It is noteworthy to mention that once we have got the distribution (still numerical!) then even 1000 levels were sufficient to see the differences.

two quantum numbers has been studied in the past [Bleher 1993], however a measure of stochasticity was not discussed. For the rectangle billiard, if the fundamental domain is extended over the two-dimensional plane, a trajectory will also straighten out as a line on this plane. The vertices of the rectangular fundamental domain make a lattice where periodic orbits correspond to lines connecting equivalent lattice points. The trace formula giving the energy spectrum involves a sum over periodic orbits. The first Weyl term corresponds to counting the points inside a circle, and the corrections are provided by fluctuations. Including the normalization, this is precisely the Gauss circle problem. For cases that cannot be cast in terms of a problem with lattice points, our discussion opens up an enormous mathematical challenge to develop arguments which would probably result from a generalization of the classic work of Heath-Brown [Heath-Brown 1992].

6.4 Summary

In Fig. 6.5, we have compiled the values of α and $\Phi'(\Lambda)$ for different systems. As the nature of the classical behaviour of a system becomes more complicated, we have discovered the existence of a scaling exponent α of stochasticity parameter with the number of levels. A qualitative explanation for increase in α as from integrable to chaotic dynamical system is provided in terms of number of records. Our studies are based on a number of systems displaying a variety of dynamical behaviours which have been shown to belong to distinct classes, not only in terms of this exponent but also in terms of the probability density distribution functions, Φ' of the stochasticity parameter. The values of Φ' show a jump by a factor of six to eight as we go from integrable system to chaotic one. In a future work, we would like to understand the details of this "jump" analytically. The cumulative distribution function $\Phi(\lambda)$ for chaotic systems

rises more sharply for smaller λ than the one for the integrable systems. The Kolmogorov distribution lies in an intermediate to these distributions.

Chapter 7

Summary and outlook

Random matrix theory has been developed for both Hermitian and pseudo-Hermitian systems with varying degree of success. In modern days, it has found applications in a variety of areas from basic sciences (Nuclear physics, Quantum Chaos, Number theory) to more applied areas like RNA folding in biology, wireless communication theory and financial analysis. In this thesis, we have developed RMT for pseudo-Hermitian systems and structured matrices, alongwith developing new measures like Stochasticity parameter and record statistics for classifying and characterizing dynamical systems quantum mechanically.

In the second chapter, our focus has been to extend the random matrix theory to the case of cyclic matrices which happen to be pseudo-Hermitian. We have shown that due to the special structure of these class of matrices, the joint probability distribution function and hence all the correlation functions for general $N \times N$ matrices can be analytically obtained. As cyclic matrices are not symmetric, one would expect the results to be in accord with the random matrix theory of Ginibre orthogonal ensemble. The situation however is quite different, the deviation in JPDF and spacing distribution from general results are fully displayed. We also saw that being asymmetric matrices and having very small number of independent elements makes them attractive to study [Jain 2008b]. The results for the block extension of these class of matrices have been obtained in full generality.

The distribution functions obtained for random cyclic matrices in Chapter 2 have been applied to a problem of random walks in Chapter 4. We generalized the biased random walk in a straightforward way as an eigenvalue problem and have shown that the transfer matrix is a cyclic. Once we demand that jump probabilities are random in nature, this has been cast as a biased random walk on disordered lattices. The evolution of entropy with time has been calculated and saturates as expected to $\log N$. Importantly, the rate of approach to equilibrium for ensemble averaged jump probabilities has been shown to follow a $1/t$ law. The point to note is that any other form of randomness or bias can be modeled using the general scheme here by a suitable modification of the distribution of matrix elements. The main advantage is the simplicity of the treatment given here [Manikandan 2011]. We may recall the usual process where one sets up a master equation with a non-Hermitian Hamiltonian [Mallick 2009] and solves for the steady state solution to study the approach to equilibrium.

In Chapter 3, the reverse-cyclic matrices, a subset of symmetric matrices, are shown to have an unusual density and spacing distribution. In contrast to the semi-circle density, this ensemble admits a density with a hole at the origin. Again, the spacing distribution has a variety, ranging from Gaussian-looking distributions to Wigner type distributions. Along with bulk properties like density, we have also obtained the record statistics of eigenvalues and shown that the upper records, when properly shifted and scaled, follow Gumbel distribution while lower records follow Wigner like distribution. As the last upper record is also the largest eigenvalue of the sequence, we have re-derived the largest eigenvalue distribution to be Gumbel. Let's recall that the largest eigenvalue of general Gaussian orthogonal ensemble follow the Tracy-Widom distribution. Similarly the last lower record is the smallest eigenvalue of the given sequence of positive non-trivial eigenvalues. We have shown that, when properly shifted

and scaled, they follow Wigner distribution. This complements the information about eigenvalues from the point of view of extreme value. We also observed that the JPDF is just the square of the modulus of the ground-state eigenfunction of an exactly solvable many-body Hamiltonian in one dimension - the screened harmonic oscillator potential. Hence the correlations between the different particles in the potential will be the same as that derived from the JPDF for the random matrix theory [Srivastava 2012]. This concludes the first part of thesis.

In the rest of the chapters, we have focused on new measures for characterizing quantum chaos.

The quantum signatures of chaos in wavefunctions has also been studied for long old. Among others, signatures of periodic orbits in wavefunctions *i.e.* scarring has been studied for a long time, theoretically and experimentally [Heller 1984, Kudrolli 1995, Laurent 2007]. The extremum of intensities in wavefunctions and electromagnetic modes motivates us to look for a measure using them which can capture integrable to chaotic transitions. For the same, we have proposed the record statistics to be such a measure. We have derived results on upper (lower) records of intensities of correlated random vectors. In addition to the derivation of the average record, it has been shown that the probability that a record appears at an index j is a Bernoulli process that is the same as that for i.i.d. variables. The quantum standard map presents the scope of studying systems which possess increasingly complex spectrum with the system parameter, K. For a quantum system with random high-lying states, records' statistics found in the Section 5.3 applies. The study of position of the last record set in case of the standard map, parameterized by K suggests that beyond a certain value of K, the eigenvectors become like random vectors insofar as the records of intensities is concerned. This is also consistent with the

finding where the number of records vs N goes through a transition from linear to algebraic to logarithmic, as K increases. At the point where classical golden mean torus breaks namely at $K \simeq 0.98$, the exponent in power law is found to be one-half. It is very likely that the conclusions drawn on the quantum standard map would hold for other quasi-integrable and mixed systems.

Random matrix theory has been very successful in describing the fluctuation properties and correlation in eigenvalue sequences. However, there are other situations known when fluctuation properties of the energy level sequences differ from the corresponding random matrix ensemble [Ahmed 2003b, Ahmed 2003a, Jain 2008b, Jain 2009]. These have motivated us to study new statistical quantities which can characterize the dynamical systems emphasizing their classical nature. There are instances when fluctuation properties of the level sequences are studied with quantities like fluctuations in average cumulative density of states [Aurich 1994] and the conjectures given have been verified in experimental data or numerically [Alt 1998]. However, a large number of levels are needed before dynamical systems can be distinguished if they are integrable or chaotic on classical level.

Inspired by the work of Arnold [Arnold 2008], in which he employed the stochasticity parameter of Kolmogorov [Kolmogorov 1933] to number sequences for discussing inherent randomness, we have studied the fluctuation properties in the cumulative level densities of quantum systems. In Chapter 6, we have shown that the probability distribution function for the proposed measure falls in two different categories for most of the level sequences studied. It is interesting to observe that the sequences in one family originate from the integrable systems while the other from classically chaotic systems. We have mostly considered billiards as models of our dynamical systems besides studying the standard map, the Riemann zeros and the Gaussian Unitary Ensemble (GUE) of

random matrices. As the nature of the classical behaviour of a system becomes more complicated, we have discovered the existence of a scaling exponent α of the stochasticity parameter with the number of levels. In Fig. 6.5, we have compiled the values of the scaling exponent of level sequences, α and the probability of having the stochasticity parameter λ taking values between λ and $\lambda + d\lambda$, $\Phi'(\lambda)$ for different systems. Based on a number of systems displaying a variety of dynamical behaviour which have been shown to belong to distinct classes, we have shown that the values of Φ' jump by a factor of six to eight as we go from integrable systems to chaotic ones in α-$\Phi'(\lambda)$ plot.

Some future directions could be (i) looking for the random matrix theory for the sparse cyclic, reverse cyclic matrices, (ii) record statistics for the other KAM systems and generalization of records for billiard systems, (iii) understanding the details of the "jump" in α-$\Phi'(\lambda)$ plot.

Appendix A

Record Statistics

A.1 JPDF of positions of records

Let $X_1, X_2, \ldots X_N$ be drawn from JPDF $P(X_1, X_2, \ldots X_N)$. Let there be records at positions $(1 = j_1, < j_2, \ldots, < j_m = N)$. Define Indicator function

$$I_j = \begin{cases} 1 & \text{if there is a record at } j \\ 0 & \text{otherwise} \end{cases} \tag{A.1}$$

Now we calculate, the probability of occurance of records at positions $(1 = j_1, < j_2, \ldots, < (j_m < N))$, $Prob(I_{j_1} = 1, \ldots I_{j_m} = 1)$.

$$Prob(I_{j_1} = 1, \ldots I_{j_m} = 1) = \int_C P(X_1, X_2, \ldots X_N) dX_1 \ldots dX_N \tag{A.2}$$

where C=set of conditions in the $\{X_i\}$ space.

$$\begin{aligned} j_1 = 1, \quad X_{j_1} = X_1; \quad & 0 < X_k < X_{j_2} && k = j_1, j_1 + 1, \ldots, j_2 - 1 \\ & 0 < X_k < X_{j_3} && k = j_2, j_2 + 1, \ldots, j_3 - 1 \\ & \vdots && \vdots \\ & 0 < X_k < X_{j_m} && k = j_{m-1}, j_{m-1} + 1, \ldots, j_m - 1 \\ & 0 < X_k < 1 && k = j_m, j_m + 1, \ldots, N \end{aligned}$$

To derive the jpdf for positions of records in case of random variables drawn from GUE distribution with a fictitious parameter u as in all previous cases,

$$P(X_1, \ldots, X_n; u) = \Gamma(N)\delta\left(\sum_{i=1}^{N} X_i - u\right) \tag{A.3}$$

Let's calculate Eq. A.2 for this distribution, and let's calculate with first row of conditions in Laplace transformed space

$$\begin{aligned}
Prob(I_{j_1} = 1, \ldots, I_{j_m} = 1; s) &= \Gamma(N) \int_C e^{-s\sum_{i=1}^{N} X_i} dX_1 \ldots dX_N \\
Prob(I_{j_1} = 1, \ldots, I_{j_m} = 1; s) &= \Gamma(N) \int_{C'} \left[\prod_{i=1}^{j_2-1} \int_0^{X_{j_2}} dX_i e^{-sX_i}\right] \\
&\quad \times e^{-s\sum_{i=j_2}^{N} X_i} dX_{j_2} \ldots dX_N \\
&= \Gamma(N) \int_{C''} \int_0^{X_{j_3}} \left(\frac{1 - e^{-sX_{j_2}}}{s}\right)^{j_2-1} e^{-sX_{j_2}} dX_{j_2} \\
&\quad \times \left[\prod_{i=j_2+1}^{j_3-1} \int_0^{X_{j_3}} dX_i e^{-sX_i}\right] \\
&\quad \times e^{-s\sum_{i=j_2}^{N} X_i} dX_{j_3} \ldots dX_N \\
&= \Gamma(N) \int_{C''} \frac{1}{j_2 s^{j_2}} \left(1 - e^{-sX_{j_3}}\right)^{j_2} \\
&\quad \times \int_0^{X_{j_4}} \underbrace{\left(\frac{1 - e^{-sX_{j_3}}}{s}\right)^{j_3-j_2-1}}_{from 0 < X_k < X_{j_3}, k = j_2+1 \ldots j_3-1} e^{-sX_{j_3}} dX_{j_3} \ldots \\
&= \vdots \\
&= \frac{1}{j_m j_{m-1} \ldots j_1} \frac{1}{s^N} \left(\text{ in last iteration } \int_0^{\infty} \right)
\end{aligned}$$

Finally after taking inverse Laplace transform, and setting $u = 1$ we get

$$Prob(I_{j_1} = 1, \ldots, I_{j_m} = 1) = \frac{1}{j_m j_{m-1} \ldots j_1} \tag{A.4}$$

Appendix B

Stochasticity Parameter

Here we collect the trace formulae [Brack 2003] for different classes of dynamical systems and present the calculations of the stochasticity parameter based on them. The point is to make a comparison with the numerical results and we shall see that with 5000 energy levels, we have a good agreement (Fig. 1). We have chosen the following examples to guide us to the length of the sequence of levels required to arrive at reliable conclusions: (i) rectangle billiard - a separable, integrable system where the quantization condition is an algebraic relation; (ii) circular billiard - a separable, integrable system where the quantization condition is a transcendental equation; (iii) equilateral triangle billiard - a non-separable, integrable system where the quantization condition is an algebraic relation; (iv) Riemann zeta function - nontrivial Riemann zeros are being considered here, the interest being due to their possible connection with unitary ensemble of random matrices which, in turn, share spectral fluctuations with some well-known quantum systems which are classically chaotic. [1]

B.1 Rectangle billiard

Let us consider a rectangle billiard where the sides of the rectangle are a_1 and a_2 for which the density of energy levels (derivative of the cumulative density)

[1] The eigenvalues in case of rectangular, equilateral triangle and circle billiards are obtained from the formulae. Standard map eigenvalues are calculated by numerical diagonalization of corresponding unitary matrix. Numerical eigenvalues for rhombus billiards have been kindly provided by Prof. Benoît Grémaud. We acknowledge here his help. The Riemann zeros are taken from the website of Prof. Odlyzko (www.dtc.umn.edu/∼odlyzko/zeta_tables/).

is given by the trace formula [Brack 2003]:

$$\begin{aligned} d(E) &= \sum_{i=1}^{\infty} g_i \delta(E - E_i) \\ &= \frac{m a_1 a_2}{2\pi\hbar^2} \sum_{(M_1,M_2)=(-\infty,-\infty)}^{(\infty,\infty)} J_0\left(\frac{S_{M_1M_2}}{\hbar}\right) \\ &\quad - \sum_{i=1,2} \frac{a_i}{4\pi\hbar}\sqrt{\frac{2m}{E}} \sum_{M=-\infty}^{\infty} \cos\left(2Ma_i\sqrt{2mE}/\hbar\right). \end{aligned} \tag{B.1}$$

where $J_0(x)$ is the cylindrical Bessel function [Edwards 1974] and action, $S_{M_1M_2}$ is given by

$$S_{M_1M_2} = \sqrt{2mE} L_{M_1M_2}, \;\; L_{M_1M_2} = \sqrt{M_1^2 a_1^2 + M_2^2 a_2^2}. \tag{B.2}$$

With this, putting $\frac{\hbar^2}{2m} = 1$ (for all the systems),

$$\begin{aligned} N(E) - \overline{N}(E) &= \frac{a_1 a_2}{4\pi} \sum_{(M_1,M_2)}^{(n_1,n_2)} \frac{8\sqrt{E}}{L_{M_1,M_2}} J_1[\sqrt{E} L_{M_1,M_2}] \\ &\quad + \frac{a_1 a_2}{4\pi} \sum_{M_1=1}^{\infty} \frac{4\sqrt{E}}{L_{M_1,0}} J_1[\sqrt{E} L_{M_1,0}] \\ &\quad + \frac{a_1 a_2}{4\pi} \sum_{M_2=1}^{\infty} \frac{4\sqrt{E}}{L_{0,M_2}} J_1[\sqrt{E} L_{0,M_2}] \\ &\quad - \frac{1}{4\pi} \sum_{M=1}^{\infty} \frac{2}{M} \left(\sin(2Ma_1\sqrt{E}) + \sin(2Ma_2\sqrt{E})\right) \end{aligned} \tag{B.3}$$

where $J_1(x)$ is cylindrical Bessel function of order one.

For the denominator of (6.3), we will use Weyl's staircase function for the energy levels of rectangle. With the corner corrections included, this is read as

$$\overline{N}(E \le E_0) = \frac{E_0}{4} - \frac{(1+\pi)\sqrt{E_0}}{2\pi} + \frac{1}{4}. \tag{B.4}$$

where area and perimeter is taken π, $2(1+\pi)$ respectively.

Using first 5000 energy levels of rectangle, we calculated Kolmogorov's stochasticity parameter (6.3) as a function of length of energy level sequence and compared the same when (6.3) is calculated using (B.3) and (B.4). The agreement is shown in Fig.6.1a.

B.2 Circular billiard

For a circular billiard of radius R, the treatment in terms of periodic orbits can be seen in the work of Balian and Bloch [Balian 1972]. However, the trace formula was given by Bogachek and Gogadze [Bogachek 1973]. The oscillatory part of the density of eigenvalues is

$$g_{osc}(E) = \frac{1}{E_o}\sqrt{\frac{\hbar}{\pi pR}}\sum_{w=1}^{\infty}\sum_{v=2w}^{\infty} f_{vw}\frac{\sin^{\frac{3}{2}}\phi_{vw}}{\sqrt{v}}\sin\Phi_{vw}, \tag{B.5}$$

where

$$\begin{aligned} E_o &= \frac{\hbar^2}{2mR^2}, \quad \phi_{vw} = \frac{\pi w}{v}, \quad L_{vw} = 2vR\sin\phi_{vw}, \\ p &= \sqrt{2mE}, \quad \Phi_{vw} = \frac{pL_{vw}}{\hbar} - 3v\frac{\pi}{2} + \frac{3\pi}{4}, \\ f_{vw} &= 1 \quad \text{for} \quad v = 2w \\ &= 2 \quad \text{for} \quad v > 2w. \end{aligned} \tag{B.6}$$

L_{vw} is the length of the classical periodic orbits characterized by two integers (v, w) denoting number of vertices and winding number around the center.

The average cumulative density of energy, E_0 for a circle of area σ, circumference, γ is given by [Baltes 1976]

$$\overline{N}(E \leq E_0) = \frac{\sigma E_0}{4\pi} - \frac{\gamma\sqrt{E_0}}{4\pi} + \frac{1}{6}. \tag{B.7}$$

$$
\begin{aligned}
N(E) - \overline{N}(E) &= \frac{2mR^2}{\sqrt{\pi R}} \sum_{w=1}^{\infty} \int_0^E dE' \frac{\sin\left[4wR\sqrt{2mE'} - 3\pi w + \frac{3\pi}{4}\right]}{(2mE')^{\frac{1}{4}}} \\
&\quad + \frac{4mR^2}{\sqrt{\pi R}} \sum_{w=1}^{\infty} \sum_{v>2w} \frac{1}{\sqrt{v}} \sin^{\frac{3}{2}}\left(\frac{\pi w}{v}\right) \\
&\quad \int_0^E dE' \frac{\sin\left[2vR\sin\frac{\pi w}{v}\sqrt{2mE'} - 3v\frac{\pi}{2} + \frac{3\pi}{4}\right]}{(2mE')^{\frac{1}{4}}}. \qquad \text{(B.8)}
\end{aligned}
$$

The integral involved in this expression is

$$
I(E) = \int_0^E dx x^{-\frac{1}{4}} \sin(\gamma\sqrt{x} + \delta). \qquad \text{(B.9)}
$$

Let $\sqrt{x} = (y - \delta)/\gamma$, so $dx/(2\sqrt{x}) = dy/\gamma$. Then, $I(E)$ becomes

$$
\begin{aligned}
I(E) &= \int_{\delta}^{\gamma\sqrt{E}+\delta} dy \frac{2}{\gamma^{3/2}} \sin y (y - \delta)^{1/2} \\
&= \int_0^{\gamma\sqrt{E}} \frac{2}{\gamma^{3/2}} \sin(z + \delta) z^{1/2} \quad (z = y - \delta) \\
&= -\frac{2E^{1/4}}{\gamma} \cos(\gamma\sqrt{E} + \delta) + \sqrt{\frac{2\pi}{\gamma^3}} \left(\cos\delta \ \text{FresnelC}\left[\sqrt{\frac{2\gamma\sqrt{E}}{\pi}}\right] \right. \\
&\qquad \left. - \text{FresnelS}\left[\sqrt{\frac{2\gamma\sqrt{E}}{\pi}}\right] \sin\delta \right) \qquad \text{(B.10)}
\end{aligned}
$$

In (B.10), the terms containing FresnelC and FresnelS terms contributes at the third decimal place which for all the numerical comparison purposes we can ignore. The agreement is good and given in Fig.6.1b.

B.3 Equilateral triangular billiard

Equilateral triangular billiard represents a class of dynamical systems which are integrable but not separable. For equilateral triangular billiard, the eigenvalue spectrum is given by

$$\begin{aligned} E(m,n) &= E_\Delta \left(m^2+n^2-mn\right) \\ & E_\Delta = \frac{16}{9}\frac{\hbar^2\pi^2}{2\mu L^2} \quad m=1,2,3,... \\ & n=1,2,3,...(m\geq 2n). \end{aligned} \tag{B.11}$$

All the eigenvalues are doubly degenerate except $(m = 2n)$ which is singly degenerate. Taking these in consideration the level density is given by

$$\begin{aligned} g(E) &= \frac{\pi}{3\sqrt{3}E_\Delta}\sum_{M_1,M_2=-\infty}^{\infty} J_0(kL_{M_1,M_2}) - \frac{1}{2\sqrt{EE_\Delta}}\sum_{M=-\infty}^{\infty}\cos(kL_{M_1,M_2}) + \frac{1}{3}\delta(E) \\ & \text{where } L_{M_1,M_2} = \sqrt{3(M_1^2+M_2^2+M_1M_2)}L. \end{aligned} \tag{B.12}$$

The analogue of (B.3) and (B.4) for equilateral triangular billiards are

$$\begin{aligned} N(E)-\overline{N}(E) &= \frac{\pi}{3\sqrt{3}E_\Delta}\sum_{(M_1=0,M_2=1)}^{\infty}\frac{8\sqrt{E}}{L_{0,M_2}}J_1[\sqrt{E}L_{0,M_2}] \\ &+\frac{\pi}{3\sqrt{3}E_\Delta}\sum_{M_1,M_2=1}^{\infty}\frac{4\sqrt{E}}{L_{M_1,M_2}}J_1[\sqrt{E}L_{M_1,M_2}] \\ &+\frac{\pi}{3\sqrt{3}E_\Delta}\sum_{M_1=1}^{\infty}\sum_{M_1=-\infty}^{-1}\frac{4\sqrt{E}}{L_{M_1,M_2}}J_1[\sqrt{E}L_{M_1,M_2}] \\ &-\frac{2}{E_\Delta}\sum_{M=1}^{\infty}\frac{1}{L_M}\sin(\sqrt{E}L_M) \end{aligned} \tag{B.13}$$

$$\overline{N}(E \leq E_0) = \frac{\pi E_0}{3\sqrt{3}E_\Delta} - \sqrt{\frac{E_0}{E_\Delta}} + \frac{1}{3}. \tag{B.14}$$

In our calculation of stochasticity parameter for this system $E_\Delta = \pi^2$. A comparison similar to rectangular billiard between the stochasticity parameter calculated exactly using 5000 energy levels of equilateral triangular billiard and using trace formula is presented in Fig.6.1c.

B.4 Zeros of Riemann zeta function

Riemann zeta function is a very important special function [Edwards 1974] with many interesting connections with number theory. It is defined in terms of a Dirichlet series or a product form as follows:

$$\begin{aligned} \zeta(s) &= \sum_{n=1}^{\infty} \frac{1}{n^s} \\ &= \prod_{\text{primes, } p} \left(1 - \frac{1}{p^{\sigma+it}}\right)^{-1}. \end{aligned} \tag{B.15}$$

According to the Riemann hypothesis, all the nontrivial zeros lie on the critical line, given by $s_n = \frac{1}{2} + it_n$. The product formula is convergent only for $\sigma > 1$, but we employ it to write an analogue of Gutzwiller trace formula [Gutzwiller 1990]. Taking logarithm of the product form above and using $\log(1-x) = -\sum_{k=1}^{\infty} x^k/k$,

$$\log \zeta(s) = \sum_p \sum_k \frac{\exp(-ikt \log p)}{k p^{k\sigma}}. \tag{B.16}$$

Taking imaginary part of both sides, and differentiating with respect to t, we obtain for fixed $\sigma > 1$:

$$d^{\sigma}_{osc} = -\frac{1}{\pi}\sum_{p}\sum_{k}\frac{\log p}{p^{k\sigma}}\cos(kt\log p). \tag{B.17}$$

The oscillating part of the cumulative density will be

$$N^{\sigma}_{osc} = -\frac{1}{\pi}\sum_{p}\sum_{k}\frac{1}{kp^{k\sigma}}\sin(kt\log p). \tag{B.18}$$

For the denominator of (6.3),

$$\overline{N}(t) \;=\; \mathrm{Int}\left[\frac{t}{2\pi}\log\frac{t}{2\pi} - \frac{t}{2\pi}\right]. \tag{B.19}$$

Finally, for the zeros of Riemann zeta functions on the critical line,

$$\lambda \;=\; \sup_{t}\frac{|N^{\sigma}_{osc}|}{\sqrt{n}} = -\sup_{t}\sqrt{\frac{2}{\pi}}\left|\sum_{p}\sum_{k=1}^{\infty}\frac{\sin[(k\log p)t]}{k(p)^{k\sigma}\sqrt{t\log(t/2\pi)-t}}\right|. \tag{B.20}$$

This expression should be doomed as its convergence is in the domain where there are no nontrivial zeros. However, as noted in [Brack 2003], trace formula contains information about the zeros on the critical line, with the shortest orbits (corresponding to the smallest primes) contributing the most (In a private communication to Dr Sudhir Jain, dated January 20, 2000, Dr Arul Lakshminarayan has noted that $|\sum_{\text{zeros, }j}\exp(it_j x)|^2$ shows dominant contributions at $\log 5$, $\log 47$, $\log 51$, the reason is not known to the author). We have compared the values of stochasticity parameter using numerical values of the zeros (www.dtc.umn.edu/∼odlyzko/zeta_tables/) and the expression (B.20) in Fig.6.1d. For calculation we have utilized first 5000 only. This is done to compare the results from various systems for same sequence length.

Bibliography

[Adler 1998] S. L. Adler. *Model for particle masses, flavor mixing, and CP violation, based on spontaneously broken discrete chiral symmetry as the origin of families.* Phys. Rev. D **59** (1998) 015012. (Cited on page 52.)

[Ahmed 2003a] Z. Ahmed and S. R. Jain. *Gaussian ensemble of 2 by 2 pseudo-Hermitian random matrices.* J. Phys. A: Math. Gen. **36** (2003) 3349. (Cited on pages 30, 34, 68, 116 and 134.)

[Ahmed 2003b] Z. Ahmed and S. R. Jain. *Pseudounitary symmetry and the Gaussian pseudounitary ensemble of random matrices.* Phys. Rev. E **67** (2003) 045106 (R). (Cited on pages xvi, 2, 28, 29, 34, 68, 116 and 134.)

[Ahmed 2006] Z. Ahmed and S. R. Jain. *A pseudo-unitary ensemble of random matrices, PT-symmetry and the riemann hypothesis.* Mod. Phys. lett. A **21** (2006) 331 . (Cited on page 39.)

[Aitken 1962] A. C. Aitken. *Two Notes on Matrices.* Proceedings of the Glasgow Mathematical Association **5** (1962) 109 . (Cited on page 55.)

[Akemann 2007] G. Akemann and E. Kanzieper. *Integrable Structure of Ginibreś Ensemble of Real Random Matrices and a Pfaffian Integration Theorem.* J. Stat. Phys. **129** (2007) 1159. (Cited on pages xv, 2 and 21.)

[Alt 1998] H. Alt, A. Bäcker, C. Dembowski, H.-D. Gräf, R. Hofferbert, H. Rehfeld and A. Richter. *Mode fluctuation distribution for spectra of superconducting microwave billiards.* Physical Review E **58** (1998) 1737. (Cited on pages 3, 116, 120 and 134.)

[Arnold 1998] B. C. Arnold, N. Balakrishnan and H. N. Nagaraja. Records. John Wiley & Sons, New York (1998). (Cited on pages xxvi, 86, 90 and 92.)

[Arnold 2008] V. I. Arnold. *Orbits statistics in chaotic dynamical systems.* Nonlinearity **21** (2008) T109. (Cited on pages 117, 118 and 134.)

[Auberson 2001] G. Auberson, S. R. Jain and A. Khare. *A class of N-body problems with nearest- and next-to-nearest-neighbour interactions.* J. Phys. A **34** (2001) 695. (Cited on page 68.)

[Aurich 1993] R. Aurich and F. Steiner. *Statistical properties of highly excited quantum eigenstates of a strongly chaotic system.* Physica D: Nonlinear Phenomena **64** (1993) 185. (Cited on page 14.)

[Aurich 1994] R. Aurich, J. Bolte and F. Steiner. *Universal signatures of quantum chaos.* Phys. Rev. Lett. **73** (1994) 1356. (Cited on pages 3, 116, 119 and 134.)

[b. Gong 2012] J. b. Gong and Q. h. Wang. 2×2 *random matrix ensembles with reduced symmetry: from Hermitian to* $\mathcal{PT}$ *-symmetric matrices.* Journal of Physics A: Mathematical and Theoretical **45** (2012) 444014. (Cited on page 34.)

[Bai 1998] Z.-D. Bai, H.-K. Hwang and W.-Q. Liang. *Normal approximations of the number of records in geometrically distributed random variables.* Random Structures and Algorithms **13** (1998) 319. (Cited on page 96.)

[Balian 1970] R. Balian and C. Bloch. *Distribution of eigenfrequencies for the wave equation in a finite domain: I. Three-dimensional problem with smooth boundary surface.* Ann. Phys. **60** (1970) 401. (Cited on page 119.)

[Balian 1971] R. Balian and C. Bloch. *Asymptotic evaluation of the Green's function for large quantum numbers* . Ann. Phys. **63** (1971) 592. (Cited on page 119.)

[Balian 1972] R. Balian and C. Bloch. *Distribution of eigenfrequencies for the wave equation in a finite domain: III. Eigenfrequency density oscillations.* Annals of Physics **69** (1972) 76 . (Cited on page 141.)

[Baltes 1976] H. P. Baltes and E. R. Hilf. Spectra of finite systems. B. I. Wissenschaftsverlag Bibliographisches Institut, Mannheim 1976 édition (1976). (Cited on pages 118, 119 and 141.)

[Bazant 2000] M. Z. Bazant. *Largest cluster in subcritical percolation.* Phys. Rev. E **62** (2000) 1660. (Cited on page 88.)

[Bender 2002] C. M. Bender, D. C. Brody and H. F. Jones. *Complex Extension of Quantum Mechanics.* Phys. Rev. Lett. **89** (2002) 270401. (Cited on pages xv, 2, 9 and 39.)

[Berg 1993] H. C. Berg. Random walks in biology. Princeton University Press 1993 édition (1993). (Cited on page 73.)

[Berg 2003] H. C. Berg. E. Coli in motion. Springer 2003 édition (2003). (Cited on page 73.)

[Berry 1977a] M. V. Berry. *Regular and irregular semiclassical wavefunctions.* Journal of Physics A: Mathematical and General **10** (1977) 2083. (Cited on page 14.)

[Berry 1977b] M. V. Berry and M. Tabor. *Level clustering in the regular spectrum.* Proc. Roy. Soc. London A **356** (1977) 375. (Cited on pages 2, 13 and 116.)

[Berry 1989] M. V. Berry. *Quantum Chaology, Not Quantum Chaos.* Physica Scripta **40** (1989) 335. (Cited on page 12.)

[Bhosale 2012] U. T. Bhosale, S. Tomsovic and A. Lakshminarayan. *Entanglement between two subsystems, the Wigner semicircle and extreme-value statistics.* Phys. Rev. A **85** (2012) 062331. (Cited on page 3.)

[Biswas 1990] D. Biswas and S. R. Jain. *Quantum description of a pseudointegrable system: The $\pi/3$-rhombus billiard.* Phys. Rev. A **42** (1990) 3170. (Cited on page 96.)

[Bleher 1993] P. M. Bleher. *Distribution of the error term in the Weyl asymptotics for the Laplace operator on a two-dimensional torus and related lattice problems.* Duke Math. J. **70** (1993) 655. (Cited on page 128.)

[Bogachek 1973] E.N. Bogachek and G.A. Gogadze. *Oscillation Effects of the "Flux Quantization" Type in Normal Metals .* Sov. Phys. JETP **36** (1973) 973. (Cited on page 141.)

[Bogomolny 1999] E. B. Bogomolny, U. Gerland and C. Schmit. *Models of intermediate spectral statistics.* Phys. Rev. E **59** (1999) R1315. (Cited on pages 31 and 116.)

[Bogomolny 2001] E. B. Bogomolny, U. Gerland and C. Schmit. *Short-range plasma model for intermediate spectral statistics .* Eur. Phys. J. B **19** (2001) 121. (Cited on page 68.)

[Bohigas 1984] O. Bohigas, M.-J. Giannoni and C. Schmit. *Characterization of Chaotic Quantum Spectra and Universality of Level Fluctuation Laws.* Phys. Rev. Lett. **52** (1984) 1. (Cited on pages 2, 13, 88 and 116.)

[Bolte 1992] J. Bolte, G. Steil and F. Steiner. *Arithmetical chaos and violation of universality in energy level statistics.* Phys. Rev. Lett. **69** (1992) 2188 . (Cited on pages xxiii and 3.)

[Bose 2002] A. Bose and J. Mitra. *Limiting spectral distribution of a special circulant.* Statistics & Probability Letters, **60** (2002) 111. (Cited on pages 51 and 58.)

[Bose 2009] A. Bose, R. S. Hazra and K. Saha. *Limiting spectral distribution of circulant type matrices withdependent inputs.* Electronic Journal of Probability **14** (2009) 2463 . (Cited on pages xxii and 52.)

[Bose 2011] A. Bose, R. S. Hazra and K. Saha. *Spectral Norm of Circulant-Type Matrices.* Journal of Theoretical Probability **24** (2011) 479. (Cited on page 65.)

[Brack 2003] M. Brack and R. K. Bhaduri. Semiclassical Physics. Westview Press, Oxford 2003 édition (2003). (Cited on pages 115, 118, 139, 140 and 145.)

[Brézin 1978] E. Brézin, C. Itzykson, G. Parisi and J. B. Zuber. *Planar diagrams.* Comm. Math. Phys. **59** (1978) 35. (Cited on page 7.)

[Brody 1981] T. A. Brody, J. Flores, J. B. French, P. A. Mello, A. Pandey and S. S. M. Wong. *Random-matrix physics: Spectrum and strength fluctuations.* Rev. Mod. Phys. **53** (1981) 385 . (Cited on page 88.)

[Bronk 1964] B. V. Bronk. *Accuracy of the Semicircle Approximation for the Density of Eigenvalues of Random Matrices.* Journal of Mathematical Physics **5** (1964) 215. (Cited on page 3.)

[Calogero 1969] F. Calogero. *Solution of a three-body problem in one dimension.* J. Math. Phys. **10** (1969) 2191. (Cited on page 68.)

[Cartarius 2007] H. Cartarius, J. Main and G. Wunner. *Exceptional Points in Atomic Spectra.* Phys. Rev. Lett. **99** (2007) 173003. (Cited on page 10.)

[Chaudhury 2009] S. Chaudhury, A. Smith, B.E. Anderson, S. Ghose and P.S. Jessen. *Quantum signatures of chaos in a kicked top.* Nature **461** (2009) 768. (Cited on page 12.)

[Chirikov 1979] B. V. Chirikov. *A universal instability of many dimensional oscillator systems.* Phys. Rep. **52** (1979) 263. (Cited on page 13.)

[Date 1995] G. Date, S. R. Jain and M. V. N. Murthy. *Rectangular billiard in the presence of a flux line.* Phys. Rev. E **51** (1995) 198 . (Cited on page 116.)

[Davidson 1932] P. M. Davidson. *Eigenfunctions for Calculating Electronic Vibrational Intensities.* Proc. R. Soc. London A **135** (1932) 459. (Cited on page 8.)

[de Gennes 1979] P. G. de Gennes. Scaling concepts in polymer physics. Cornell University Press 1979 édition (1979). (Cited on page 73.)

[Dev 2011] S. Dev, Shivani Gupta and Radha Raman Gautam. *Broken symmetry in the neutrino mass matrix.* Physics Letters B **702** (2011) 28 . (Cited on page 52.)

[DLMF 2010] DLMF. *Digital Library of Mathematical Functions. National Institute of Standards and Technology from.* `http://dlmf.nist.gov/8.11.ii.` (2010). (Cited on page 80.)

[Dorfman 1999] J. R. Dorfman. An introduction to chaos in nonequilibrium statistical mechanics. Cambridge University Press 1999 édition (1999). (Cited on page 74.)

[Dyson 1962a] F. J. Dyson. *Statistical theory of the energy levels of complex systems, I.* J. Math. Phys. **3** (1962) 140. (Cited on pages xv and 1.)

[Dyson 1962b] F. J. Dyson. *Statistical theory of the energy levels of complex systems, II.* J. Math. Phys. **3** (1962) 157. (Cited on pages xv and 1.)

[Dyson 1962c] F. J. Dyson. *Statistical theory of the energy levels of complex systems, III.* J. Math. Phys. **3** (1962) 166. (Cited on pages xv and 1.)

[Dyson 1962d] F. J. Dyson. *The threefold way. Algebraic structure of symmetry groups and ensembles in quantum mechanics.* J. Math. Phys. **3** (1962) 1200. (Cited on pages xv, 1 and 6.)

[Eckhardt 1984] B. Eckhardt, J. Ford and F. Vivaldi. *Analytically solvable systems which are not integrable.* Physica D **13** (1984) 339. (Cited on pages 116 and 126.)

[Edelman 1997] A. Edelman. *The Probability that a Random Real Gaussian Matrix Has k Real Eigenvalues, Related Distributions, and the Circular Law.* J. Multivariate Anal. **60** (1997) 203. (Cited on pages xv and 24.)

[Edwards 1974] H.M. Edwards. RiemannŠs Zeta Function. Academic Press, New York - London 1974 édition (1974). (Cited on pages 140 and 144.)

[Einstein 1956] A. Einstein. Investigations on the theory of Brownian movement. Dover 1956 édition (1956). (Cited on page 73.)

[Feller 1968] W. Feller. An introduction to probability theory and its applications. Wiley third ed. édition (1968). (Cited on page 74.)

[Feller 1988] W. Feller. An introduction to probability theory and its applications Vol. II. Wiley Eastern Ltd, New Delhi 1988 édition (1988). (Cited on page 117.)

[Fishman 1982] S. Fishman, D. R.Grempel and R. E. Prange. *Chaos, Quantum Recurrences, and Anderson Localization.* Phys. Rev. Lett. **49** (1982) 509. (Cited on page 13.)

[Ford 1991] J. Ford, G. Mantica and G. H. Ristow. *The Arnol'd cat: Failure of the correspondence principle.* Physica D: Nonlinear Phenomena (1991) 493. (Cited on page 12.)

[Forrester 2010] P. J. Forrester. Log-Gases and Random Matrices. Princeton University Press 2010 édition (2010). (Cited on page 63.)

[Franceschetti 1993] D. R. Franceschetti, E. C. Hunke, X. Zhang and J. R. Haddock. *The random walk as an eigenvalue problem.* Am. J. Phys. **61** (1993) 1111. (Cited on pages 73 and 74.)

[Friedman 1961] B. Friedman. *Eigenvalues of composite matrices.* Mathematical Proceedings of the Cambridge Philosophical Society **57** (1961) 37. (Cited on page 41.)

[Frobenius 1906] F. G. Frobenius and I. Schur. *Über die reellen Darstellungen der endlichen Gruppen.* Sitzungsber. Akad. Preuss. Wiss. (1906) 186Ũ208. (Cited on page 6.)

[Gembris 2002] D. Gembris, J. G. Taylor and D. Suter. *Sports statistics: Trends and random fluctuations in athletics.* Nature **417** (2002) 506. (Cited on page 86.)

[Ginibre 1965] J. Ginibre. *Statistical ensembles of complex, quaternion, and real matrices.* J. Math. Phys. **6** (1965) 440. (Cited on pages xv, 1 and 19.)

[Glick 1978] N. Glick. *Breaking records and breaking boards.* American Mathematical Monthly **85** (1978) 2. (Cited on pages 86 and 91.)

[Grémaud 1998] B. Grémaud and S. R. Jain. *Spacing distributions for rhombus billiards.* J. Phys. A **31** (1998) L637. (Cited on pages 13, 31, 68 and 116.)

[Guo 2009] A. Guo, G. J. Salamo, D. Duchesne, R. Morandotti, M. Volatier-Ravat, V. Aimez, G. A. Siviloglou and D. N. Christodoulides. *Observation of $\mathcal{PT}$-Symmetry Breaking in Complex Optical Potentials.* Phys. Rev. Lett. **103** (2009) 093902. (Cited on page 10.)

[Gutzwiller 1990] M. C. Gutzwiller. Chaos in classical and quantum mechanics. Springer Verlag, Berlin 1990 édition (1990). (Cited on pages 115, 119 and 144.)

[Haake 1991] F. Haake. Quantum Signatures of Chaos. Springer-Verlag, New York (1991). (Cited on pages 31, 115 and 116.)

[Hardy 1979] G. H. Hardy and E. M. Wright. An introduction to the theory of numbers. Oxford University Press, New York 1979 édition (1979). (Cited on page 127.)

[Hatano 1996] N. Hatano and D. R. Nelson. *Localization Transitions in Non-Hermitian Quantum Mechanics.* Phys. Rev. Lett. **77** (1996) 570. (Cited on page 9.)

[Hatano 1997] N. Hatano and D. R. Nelson. *Vortex pinning and non-Hermitian quantum mechanics.* Phys. Rev. B **56** (1997) 8651. (Cited on page 9.)

[Heath-Brown 1992] D. R. Heath-Brown. *The distribution and the moments of error term in the Dirichlet divisor problem.* Acta Arithmetica **60** (1992) 389. (Cited on page 128.)

[Heiss 1991] W. D. Heiss and A. L. Sannino. *Transitional regions of finite Fermi systems and quantum chaos.* Phys. Rev. A **43** (1991) 4159. (Cited on page 10.)

[Heller 1984] E. J. Heller. *Bound-State Eigenfunctions of Classically Chaotic Hamiltonian Systems: Scars of Periodic Orbits.* Physical Review Letters **53** (1984) 1515. (Cited on pages 15, 96 and 133.)

[Heusler 2007] S. Heusler, S. Muller, A.Altland, P. Braun and F. Haake. *Periodic-Orbit Theory of Level Correlations.* Phys. Rev. Lett. **98** (2007) 044103. (Cited on page 115.)

[Hoppe 1992] J. Hoppe. Lectures on integrable systems. Springer 1992 édition (1992). (Cited on page 69.)

[Iwaniec 1988] H. Iwaniec and C. J. Mozzochi. *On the divisor and circle problem.* J. Number Th. **29** (1988) 60. (Cited on page 127.)

[Izrailev 1990] F. M. Izrailev. *Simple Models of Quantum Chaos: Spectrum and Eigenfunctions.* Phys. Rep. **196** (1990) 299. (Cited on page 101.)

[Jain 1993] S. R. Jain. *Fractal-like quasienergy spectrum in the Fermi-Ulam model.* Phys. Rev. Lett. **70** (1993) 3553. (Cited on page 13.)

[Jain 1995] S. R. Jain and S. V. Lawande. *Almost integrable billiards.* Proc. Indian Natl. Sci. Acad. A **61** (1995) 275. (Cited on page 116.)

[Jain 1999] S. R. Jain and A. Khare. *An exactly solvable many-body problem in one dimension and the short-range Dyson model.* Phys. Lett. A **262** (1999) 35. (Cited on page 68.)

[Jain 2002] S. R. Jain, B. Grémaud and A. Khare. *Quantum modes on chaotic motion: Analytically exact results.* Phys. Rev. E **66** (2002) 016216. (Cited on page 68.)

[Jain 2006] S. R. Jain. *Random matrix theories and exactly solvable models.* Czech. J. Phys **56** (2006) 1021. (Cited on page 68.)

[Jain 2008a] S. R. Jain. *Exact solution of the SchrÃűdinger equation for a particle in a regular N-simplex.* Physics Letters A **372** (2008) 1978 . (Cited on page 126.)

[Jain 2008b] S. R. Jain and S. C. L. Srivastava. *Random cyclic matrices.* Phys. Rev. E **78** (2008) 036213. (Cited on pages xvi, xxx, 45, 50, 63, 73, 78, 116, 131 and 134.)

[Jain 2009] S. R. Jain and S. C. L. Srivastava. *Random matrix theory for pseudo-Hermitian systems: Cyclic blocks.* Pramana-J. Phys. **73** (2009) 989. (Cited on pages 116 and 134.)

[Kalish 2012] S. Kalish, Z. Lin and T. Kottos. *Light transport in random media with $\mathcal{PT}$ symmetry.* Phys. Rev. A **85** (2012) 055802. (Cited on page 11.)

[Kanzieper 2005] E. Kanzieper and G. Akemann. *Statistics of Real Eigenvalues in GinibreŠs Ensemble of Random Real Matrices.* Phys. Rev. Lett. **95** (2005) 230201. (Cited on pages xv, 21 and 24.)

[Karner 2003] H. Karner, J. Schneid and C. W. Ueberhuber. *Spectral decomposition of real circulant matrices*. Linear Algebra Appl. **367** (2003) 301. (Cited on pages 53 and 61.)

[Kendall 1946] M. G. Kendall and A. Stuart. The advanced theory of statistics Vol. 2. Charles Griffin and Co. Ltd, London 1946 édition (1946). (Cited on page 117.)

[Klaiman 2008] S. Klaiman, U. Günther and N. Moiseyev. *Visualization of Branch Points in $\mathcal{PT}$-Symmetric Waveguides*. Phys. Rev. Lett. **101** (2008) 080402. (Cited on page 10.)

[Kolmogorov 1933] A. Kolmogorov. G. Ist. Ital. Attuari **4** (1933) 83. (Cited on pages 117, 119 and 134.)

[Kowaleski 1948] G. Kowaleski. Determinantentheorie. Chelsea, New York 3rd ed édition (1948). (Cited on pages 34, 63 and 75.)

[Kudrolli 1995] A. Kudrolli, V. Kidambi and S. Sridhar. *Experimental Studies of Chaos and Localization in Quantum Wave Functions*. Phys. Rev. Lett. **75** (1995) 822. (Cited on pages 96 and 133.)

[Lakshminarayan 2008] A. Lakshminarayan, S. Tomsovic, O. Bohigas and S. N. Majumdar. *Extreme Statistics of Complex Random and Quantum Chaotic States*. Phys. Rev. Lett. **100** (2008) 044103. (Cited on pages 3, 15, 94, 95, 98 and 108.)

[Lakshminarayan 2009] A. Lakshminarayan. *SERC School-2009, Delhi University: Lecture Notes*. `www.physics.iitm.ac.in/~arul/serc/serc1.html` (2009). (Cited on page 101.)

[Landau 1955] L. Landau and Ya. Smorodinsky. Lectures on the theory of the atomic nucleus. State Technical-Theoretical Literature Press, Moscow 1955 édition (1955). (Cited on pages xv and 1.)

[Laurent 2007] D. Laurent, O. Legrand, P. Sebbah, C. Vanneste and F. Mortessagne. *Localized Modes in a Finite-Size Open Disordered Microwave Cavity*. Phys. Rev. Lett. **99** (2007) 253902. (Cited on pages 96 and 133.)

[Lehmann 1991] N. Lehmann and H.-J. Sommers. *Eigenvalue statistics of random real matrices*. Phys. Rev. Lett. **67** (1991) 941. (Cited on page 24.)

[Liboff 1979] R. L. Liboff. *On the potential x^{2N} and the correspondence principle*. International Journal of Theoretical Physics (1979) 185. (Cited on page 12.)

[Majumdar 2008] S. N. Majumdar and R. M. Ziff. *Universal Record Statistics of Random Walks and Lévy Flights*. Phys. Rev. Lett. **101** (2008) 050601. (Cited on pages xxvii and 86.)

[Makris 2008] K. G. Makris, R. El-Ganainy, D. N. Christodoulides and Z. H. Musslimani. *Beam Dynamics in $\mathcal{PT}$ Symmetric Optical Lattices*. Phys. Rev. Lett. **100** (2008) 103904. (Cited on page 10.)

[Mallick 2009] K. Mallick. *Some recent developments in non-equilibrium statistical physics*. Pramana-J. Phys. **73** (2009) 417. (Cited on pages 73, 83 and 132.)

[Manikandan 2011] K. Manikandan, S. C. L. Srivastava and S. R. Jain. *Biased random walks on a disordered one-dimensional lattice*. Phys. Lett. A **375** (2011) 368. (Cited on pages xxi and 132.)

[McDonald 1979] S. W. McDonald and A. N. Kaufman. *Spectrum and Eigenfunctions for a Hamiltonian with Stochastic Trajectories.* Phys. Rev. Lett. **42** (1979) 1189. (Cited on page 96.)

[McDonald 1988] S. W. McDonald and A. N. Kaufman. *Wave chaos in the stadium: Statistical properties of short-wave solutions of the Helmholtz equation.* Phys. Rev. A **37** (1988) 3067. (Cited on page 14.)

[Meckes 2009] M. W. Meckes. *Some results on random circulant matrices.* IMS Collections High Dimensional Probability V: The Luminy Volume **5** (2009) 213. (Cited on page 52.)

[Mehta 1967] M. L. Mehta. Random matrices and the statistical theory of energy levels. Academic Press, New York (1967). (Cited on page 20.)

[Mehta 1991] M. L. Mehta. Random matrices. Academic Press, Boston 2nd édition (1991). (Cited on pages 20, 31 and 34.)

[Mehta 2004] M. L. Mehta. Random Matrices. Elsevier Academic Press, London (2004). (Cited on pages xv, 1, 22, 88, 115 and 116.)

[Moser 1975] J. K. Moser. *Three integrable Hamiltonian systems connected with isospectral deformations* . Adv. Math. **16** (1975) 197. (Cited on page 68.)

[Nevzorov 1987] V. B. Nevzorov. *Records.* Theory of Probability and its Applications **32** (1987) 201. (Cited on page 95.)

[Oliveira 2005] L. P. Oliveira, H. J. Jensen, M. Nicodemi and P. Sibani. *Record dynamics and the observed temperature plateau in the magnetic creep-rate of type-II superconductors.* Phys. Rev. B **71** (2005) 104526. (Cited on page 88.)

[Parab 1996] H. D. Parab and S. R. Jain. *Non-universal spectral rigidity of quantum pseudo-integrable billiards.* Journal of Physics A: Mathematical and General **29** (1996) 3903. (Cited on pages 31 and 115.)

[Patil 2007] S. H. Patil and K. D. Sen. *Uncertainty relations for modified isotropic harmonic oscillator and Coulomb potentials.* Phys. Lett. A **362** (2007) 109. (Cited on page 8.)

[Perelomov 1971] A. Perelomov. *Algebraic approach to the solution of a one-dimensional model of N interacting particles.* Theor. Math. Phys. **6** (1971) 263. (Cited on pages 8 and 69.)

[Raposo 1991] E. P. Raposo, S. M. de Oliviera, A. M. Nemirovsky, and M. D. Countinho-Filho. *Random walks: A pedestrian approach to polymers, critical phenomena, and field theory.* Am. J. Phys. **59** (1991) 633. (Cited on page 73.)

[Redner 2006] S. Redner and M. R. Petersen. *Role of global warming on the statistics of record-breaking temperatures.* Phys. Rev. E **74** (2006) 061114. (Cited on page 86.)

[Reichl 2004] L. E. Reichl. The transition to chaos: conservative classical systems and quantum manifestations. Springer, Heidelberg 2004 édition (2004). (Cited on pages 115 and 116.)

[Relaño 2002] A. Relaño, J. M. G. Gómez, R. A. Molina, J. Retamosa and E. Faleiro. *Quantum Chaos and* $1/f$ *Noise.* Phys. Rev. Lett. **89** (2002) 244102. (Cited on page 116.)

[Renyi 1962] A. Renyi. Theorie des elements saillants dúne suite dóbservations, Selected Papers of Alfred Renyi volume 2. Academic Press, New York (1962). (Cited on pages xxvi, 86 and 90.)

[Rey 1997] S. Rey and P. Choquard. *The Calogero - Sutherland - Moser (CSM) model as a quantum billiard.* Eur. J. Phys. **18** (1997) 94. (Cited on page 68.)

[Richens 1981] P. J. Richens and M. V. Berry. *Pseudointegrable systems in classical and quantum mechanics.* Physica D **2** (1981) 495. (Cited on page 116.)

[Rotter 2001] I. Rotter. *Correlations in quantum systems and branch points in the complex plane.* Phys. Rev. C **64** (2001) 034301. (Cited on page 10.)

[Rowe 2005] D. J. Rowe. *An algebraic approach to problems with polynomial Hamiltonians on Euclidean spaces.* J. Phys. A **38** (2005) 10181. (Cited on page 8.)

[Ruter 2010] C. E. Ruter, K. G. Makris, R. El-Ganainy, D. N. Christodoulides, M. Segev and D. Kip. *Observation of parity-time symmetry in optics.* Nat Phys **6** (2010) 192. (Cited on page 10.)

[Sabhapandit 2011] S. Sabhapandit. *Record statistics of continuous time random walk.* EPL (Europhysics Letters) **94** (2011) 20003. (Cited on page 87.)

[Santhanam 2005a] M. S. Santhanam and J. N. Bandyopadhyay. *Spectral Fluctuations and $1/f$ Noise in the Order-Chaos Transition Regime.* Phys. Rev. Lett. **95** (2005) 114101. (Cited on page 111.)

[Santhanam 2005b] M. S. Santhanam and J. N. Bandyopadhyay. *Spectral Fluctuations and $1/f$ Noise in the Order-Chaos Transition Regime.* Phys. Rev. Lett. **95** (2005) 114101. (Cited on page 116.)

[Santhanam 2006] M. S. Santhanam, J. N. Bandyopadhyay and D. Angom. *Quantum spectrum as a time series: Fluctuation measures*. Phys. Rev. E **73** (2006) 015201. (Cited on page 117.)

[Saraceno 1990] M Saraceno. *Classical structures in the quantized baker transformation*. Annals of Physics **199** (1990) 37 . (Cited on pages xxxi and 103.)

[Schindler 2011] J. Schindler, A. Li, M. C. Zheng, F. M. Ellis and T. Kottos. *Experimental study of active LRC circuits with $\mathcal{PT}$ symmetries*. Phys. Rev. A **84** (2011) 040101. (Cited on page 10.)

[Sommers 1988] H. J. Sommers, A. Crisanti, H. Sompolinsky and Y. Stein. *Spectrum of Large Random Asymmetric Matrices*. Phys. Rev. Lett. **60** (1988) 1895. (Cited on page 23.)

[Sommers 2008] H.-J. Sommers and W. Wieczorek. *General eigenvalue correlations for the real Ginibre ensemble*. J. Phys. A: Math. Theor. **41** (2008) 405003. (Cited on pages xv, 2 and 24.)

[Spohn 1991] H. Spohn. Large scale dynamics of interacting particles. Springer 1991 édition (1991). (Cited on page 73.)

[Srivastava 2011] S. C. L. Srivastava and S. R. Jain. *Kolmogorov stochasticity parameter as a measure of quantum chaos*. ArXiv e-prints (2011). (Cited on page xxiii.)

[Srivastava 2012] S. C. L. Srivastava and S. R. Jain. *Random reverse-cyclic matrices and screened harmonic oscillator*. Phys. Rev. E **85** (2012) 041143. (Cited on pages xxi and 133.)

[Srivastava 2013] S. C. L. Srivastava, A. Lakshminarayan and S. R. jain. *Record statistics in random vectors and quantum chaos*. EPL **101** (2013) 10003. (Cited on pages xxvii and 88.)

[Sutherland 1971] B. Sutherland. *Exact Results for a Quantum Many-Body Problem in One Dimension*. Phys. Rev. A **4** (1971) 2019. (Cited on page 68.)

[Sutherland 1972] B. Sutherland. *Exact Results for a Quantum Many-Body Problem in One Dimension. II*. Phys. Rev. A **5** (1972) 1372. (Cited on page 68.)

[Sutherland 2005] B. Sutherland. Beautiful models. World Scientific, Chennai, 2005 édition (2005). (Cited on page 68.)

[Terras 1985] A. Terras. Harmonic analysis in symmetric spaces vols I and II. Springer Verlag, Berlin 1985 édition (1985). (Cited on page 120.)

[Tracy 1994] C. A. Tracy and H. Widom. *Level-spacing distributions and the Airy kernel*. Communications in Mathematical Physics **159** (1994) 151. (Cited on page 3.)

[Tracy 1996] C. A. Tracy and H. Widom. *On orthogonal and symplectic matrix ensembles*. Communications in Mathematical Physics **177** (1996) 727 . (Cited on page 3.)

[Verbaarschot 2005] J. J.M. Verbaarschot. *The Supersymmetric method in random matrix theory and applications to QCD*. AIP Conf.Proc. **744** (2005) 277. (Cited on page 6.)

[Vivo 2011] P. Vivo. *Largest Schmidt eigenvalue of random pure states and conductance distribution in chaotic cavities.* Journal of Statistical Mechanics: Theory and Experiment **2011** (2011) P01022. (Cited on page 3.)

[Vogel 2001] R. M. Vogel, A. Zafirakou-Koulouris and N. C. Matalas. *Frequency of record-breaking floods in the United States.* Water Res. Research **37** (2001) 1723. (Cited on page 86.)

[Wergen 2011] G. Wergen, M. Bogner and J. Krug. *Record statistics for biased random walks, with an application to financial data.* Phys. Rev. E **83** (2011) 051109. (Cited on page 87.)

[Wigner 1957] E. P. Wigner. *Statistical properties of real symmetric matrices with many dimensions.* Can. Math. Congr. Proc. (1957) 174. (Cited on pages xv and 1.)

[Wu 2000] Z.-B. Wu and J.-Y. Zeng. *Dynamical symmetry of screened Coulomb potential and isotropic harmonic oscillator.* Phys Rev A **62** (2000) 032509. (Cited on page 8.)

[Zelevinsky 1996] V. Zelevinsky. *Quantum chaos and complexity in nuclei.* Annu. Rev. Nucl. Part. Sci. **46** (1996) 237. (Cited on page 31.)